Title
Genetics and Mechanisms of Host Resistance against Mycobacterium tuberculosis: a Study in Mice

Author
Ji, Daisy Xiaoxi

Publication Date
2019

Peer reviewed|Thesis/dissertation

Genetics and Mechanisms of Host Resistance against *Mycobacterium tuberculosis*: a Study in Mice

By

Daisy Xiaoxi Ji

A dissertation submitted in partial satisfaction of the

requirement for the degree of

Doctor of Philosophy

in

Molecular and Cell Biology

in the

Graduate Division

of the

University of California, Berkeley

Committee in charge:

Professor Russell E. Vance, Chair
Professor Jeffery S. Cox
Professor Kaoru Saijo
Professor Shauna Somerville

Spring 2019

Genetics and Mechanisms of Host Resistance against *Mycobacterium tuberculosis*: a Study in Mice

By Daisy Xiaoxi Ji

Abstract

Genetics and Mechanisms of Host Resistance against *Mycobacterium tuberculosis*: a Study in Mice

By

Daisy Xiaoxi Ji

Doctor of Philosophy in Molecular and Cell Biology

University of California, Berkeley

Professor Russell E. Vance, Chair

Mycobacterium tuberculosis (*Mtb*) is the etiological agent of the disease tuberculosis (TB), and is the leading cause of death worldwide from a single pathogen[1]. Exposure to *Mtb* in immunocompetent humans results in diverse outcomes, varying from active, transmissible disease to asymptomatic infection that cannot spread to others. Host genetics, amongst other factors, are thought to contribute to the divergent outcomes upon *Mtb* infection. Improved understanding of the host immune responses against *Mtb*—how is the pathogen detected, what immune responses are induced, and which responses are protective—would better inform future development of vaccines, therapeutics and diagnostics.

To study the effect of host genetics on susceptibility to *Mtb* infection, I used a previously published congenic mouse (B6.*Sst1*^{S}) that carries the susceptible allele of the *Super susceptibility to tuberculosis 1* (*Sst1*) locus on the C57BL/6 (B6) background [2,3]. Compared to B6 mice, B6.*Sst1*^{S} mice are significantly more susceptible to *Mtb* infection, though the mechanisms of this susceptibility are not well understood. A previous study proposed *Ipr1* (also known as *Sp110*) as the causative gene within the *Sst1* locus[2], though this has never been thoroughly verified. In this dissertation I first investigate the mechanisms of susceptibility in the B6.*Sst1*^{S} mice, and demonstrate that the susceptibility is driven by type I interferon (IFN) signaling (Chapter 2). I further show that type I IFN signaling upregulates interleukin-1 receptor antagonist (IL-1Ra), which blocks signaling of interleukin-1 (IL-1), a vital antibacterial cytokine. Inhibition of IL-1Ra by genetic deletion or neutralization with a blocking antibody protected B6.*Sst1*^{S} mice, suggesting that IL-1Ra is a potential target for host-directed therapy.

I then examine the genetic determinants of the *Sst1* locus, where I observe that contradictory to previous report[2], *Sp110*$^{-/-}$ mice were not susceptible to *Mtb* infections (Chapter 3). I demonstrate that a homolog of *Sp110, Sp140* is also a possible candidate gene, and generated *Sp140*$^{-/-}$ mice that were similarly susceptible to infections by *Mtb* and other intracellular bacteria as B6.*Sst1*^{S} mice. My work suggests that *Sp140* is the dominant causal gene within the *Sst1* locus, and is a novel negative regulator of type I IFN signaling during bacterial infections.

The findings presented in this dissertation highlight the complexities of immune regulation during *Mtb* infection *in vivo*, as well as the many questions that remain open.

In Chapter 4, I discuss some ideas on future directions and potential experiments that may help illuminate some of these outstanding questions.

To my love,

who taught me that the darkness is always temporary,
and keeps me warm in the cold, cold summers.

To my parents,

“For you have chosen to travel far, then let neither rain nor wind slow you.”

Acknowledgement

I decided to enroll in the Graduate Program at the University of California, Berkeley because of Russell, and there are no regrets. Russell towers in my mind, and will always remain so, as an example of rigorous science mixed with endless curiosity and genuine enjoyment of the process. This dissertation would not have existed without his support and mentoring.

All the Vance lab members, past and present, have all been incredibly kind and supportive throughout my time there. Andrew "Bubbles" Sandstrom, my eternal bay-mate, who guided me through everything, both scientific and not: my first heartbreak, the seemingly endless periods when no experiments work, first paper submission and reviews... to name only a few. Bella Rauch is someone I wish I could be like someday. She is an amazing scientist, generous mentor, and somehow always composed and unflappable. My fellow labmates not only provided an intellectually stimulating environment, they made coming into work every day so enjoyable, and filled the space with happiness. The road of science is often lonely and difficult; I am fortunate to have had labmates who have been the rays of sunshine in my life.

Greg Barton and the Barton lab have been a second home, an additional repository of knowledge and ideas. The IMP division has been incredibly supportive in not just the science, but also fostering my growth as a scientist. The members of the BSL3 community, Sarah and Jeff and their respective labs, have been so welcoming and generous in helping us at every step. In particular Erik van Dis, Robyn Jong and Teresa Repasy have been incredibly generous with their time and expertise. Laura Flores, the extraordinary director of the high containment labs, is the goddess that keeps the world of the BSL3 labs turning.

We would not be walking down the road of *Mycobacterium tuberculosis*, this difficult yet rewarding road, without Heran Darwin. Her enthusiasm for science is boundless, and her rigorous approach is inspirational.

Last but not least, the findings described in the following chapters would not exist without the contributions of many, many collaborators. Igor Kramnik, the original creator of the B6.*Sst1*^{S} mice (also known as the "Kramnik" mice); Katherine Chen, former technician who helped with the initial BSL3 experiments; Peter Dietzen, our lab manager extraordinaire/fixer of all things; Roberto Chavez, mouse colony manager, without whom I would be buried in mouse feces; Angus Y. Lee and Harman Dhaliwal, who performed all the CRISPR gene-targeting; Dario Zamboni, Gustavo Quirino and Shally Margolis, who developed the protocol for *in vivo* infection with *Legionella*; Alexander Louie, who performed the *Listeria* infections described; and Naofumi Mukaida, who generated the anti-IL-1Ra hybridoma used to generate the antibodies.

I am deeply grateful for all the support I have received.

Table of Contents

Chapter 1: TB pathogenesis and Type I IFNs (and Sp140)

Mycobacterium tuberculosis—the etiological agent of the disease tuberculosis (TB)—is responsible for the greatest number of deaths from a single pathogen worldwide, claiming 1.6 million lives in 2017 alone[1]. *Mtb* is an obligate human pathogen: humans are its only natural reservoir[4]. Consequently, it is highly adapted to surviving and manipulating the host immune responses. Exposure to *Mtb* results in a diverse set of outcomes, from apparent resistance to asymptomatic infection to active disease[5]. While asymptomatic infection is not transmissible, an estimated 10% of asymptomatic cases will progress to active disease at some point, posing a significant public health risk[6]. Host/bacterial genetics and environmental factors likely all contribute to progression to active disease or resistance. Many of the contributing host genetic factors have been discovered through patients who have Mendelian susceptibility to mycobacterial disease (MSMD)[7]. However, mutations associated with MSMD are often associated with general susceptibility to infections, and cannot explain why disease outcomes differ between otherwise immunocompetent individuals. Better understanding of the protective immune responses would benefit vaccine and therapy development, and the ability to predict who with latent TB infection (LTBI) will progress to active disease would better focus public health efforts in controlling TB transmission. My dissertation examines the role of host cytokines, including type I interferons (IFNs), in the progression to active TB disease. Here I will discuss type I IFNs and their role in mediating TB disease. In the following two chapters I will describe my experimental investigations on the role of type I IFNs during TB, and in the final chapter I will discuss some experiments and ideas for future studies.

1.1 What are type I IFNs

Type I IFNs were first described in 1957 in chick embryo cells infected with viruses that were able to produce a protein that led to resistance against subsequent viral infections[8]. Type I IFNs are composed of 13 *Ifn*α (14 in mice), 1 *Ifn*β and 6 poorly defined gene products (ε, τ, κ, ω, δ, ζ)[9]. Most of the research has been focused on *Ifnα* and *Ifnβ*[9,10]. All type I IFNs signal through the type I IFN receptor, IFNAR, which induces expression of hundreds of downstream genes collectively known as interferon stimulated genes (ISGs)[10]. Signaling downstream of type I IFNs can also repress the expression of many genes. Many ISGs can also be regulated by IFNγ (also called type II IFN) that signals through the IFNγ receptor (IFNGR). Despite considerable overlap in genes induced by type I IFN and IFNγ, IFNγ is particularly vital in protection against intracellular bacteria, including *Mtb,* whereas Type I IFNs are best known for their role in antiviral responses: many of the ISGs restrict viral replication, and can be induced in both infected and uninfected bystander cells[9,10]. All type I IFNs can bind IFNAR, but do so with different kinetics and affinity to IFNAR and have distinct activities downstream[11]. Type I IFNs can also be induced by a variety of bacterial pathogens, where it can be both detrimental and beneficial to the host (reviewed in [9,10,12]). In the following sections we will discuss some of the evidence surrounding the role of type I IFNs during *Mtb* infections in both humans and mice.

1.1.1 Evidence for the role of type I IFNs in TB from human studies

To date, there have been over a dozen studies demonstrating a correlation between elevated type I IFN expression signature in the peripheral blood and active TB disease or progression to active disease (reviewed in [13–15]). Several more studies found similar associations in previously published data sets[13,14]. These studies cover a range of host genetics and *Mtb* strains, suggesting that increased level of type I IFN transcriptional profile is broadly associated with active TB disease or greater likelihood of progressing to active TB disease. Because of this strong correlation, there has been interest in using type I IFN expression signatures as biomarkers for diagnostics or treatment monitoring[13–15]. However, based on these correlative data alone, it is unclear whether the type I IFN signature is an effect of increased *Mtb* replication (which cannot be measured in asymptomatic infections) or an actual driver of the disease.

Direct evidence for a detrimental role of type I IFN signaling in human TB is more limited. Bogunovic *et al* described several patients with null mutations in ISG15 that all suffered from MSMD[16]. ISG15 is thought to be a negative regulator of type I IFN signaling, and patients with ISG15 deficiency had elevated circulating type I IFNs, increased expression of other ISGs in the peripheral blood, and symptoms resembling known interferonopathies[17]. However, loss of ISG15 also led to a defect in IFNγ production which is known to cause MSMDs[16]. It is currently unclear whether the phenotypes associated with loss of ISG15 are all dependent on type I IFN signaling. Recently Zhang *et al* reported that a rare SNP in IFNAR led to reduced signaling and correlated with decreased TB infection and less pathology when infected compared to the control population[18]. Interestingly, those carrying this SNP had an increased rate of hepatitis C virus (HCV) infection as compared to the control population, illustrating the tradeoff between the antiviral and antibacterial activities of type I IFNs. This is mirrored by reports of TB reactivation in patients who received IFNα therapy for chronic viral infections (such as HCV)[19–23]. While intriguing, these case studies are extremely limited in scope, and cannot account for other potential underlying immunodeficiencies that may contribute to TB disease. Interestingly, IFNβ is a major component of multiple sclerosis treatment, yet it is not associated with significant increase in infections (tuberculosis or otherwise)[24]. IFNα has also been used in combination with antimicrobials to treat mycobacterial infections including TB (summarized in [15]). Many of these cases had already failed conventional anti-TB treatments or had other immunodeficiencies (such as lack of IFNγ receptor)[25,26] that may have altered their response to type I IFNs.

Collectively these results suggest that the relationship between type I IFN signaling and TB disease in humans is complex. When, where, and which of the type I IFNs are administered or induced and a wealth of other host factors will all influence whether type I IFNs augment or ameliorate the risk of TB disease. Improved understanding of the spatiotemporal effects of various type I IFNs in the presence of active *Mtb* providing immune stimuli is required to better parse these human results.

1.1.2 Mechanisms of type I IFNs during *Mycobacterium tuberculosis* infection from mice and *in vitro* models

Mouse and macrophage cultures (mouse or human) are used to dissect the role of type I IFNs in *Mtb* infections. Below, I summarize studies on how type I IFNs are induced during *Mtb* infections, and whether type I IFNs play a detrimental, or a

protective role for the host.

1.1.2.1 How is type I IFNs induced during Mycobacterium tuberculosis infections?

Mtb can induce type I IFNs during *in vivo* and *in vitro* experiments[27–30]. More virulent, clinical strains of *Mtb* are associated with increased *Ifnb* production, though the mechanism or biological relevance of this is unclear[31–34]. *Mtb* is detected by a variety of cytosolic and cell surface pathogen recognition receptors (PRRs), and many of these induce type I IFNs (reviewed in [35]). Interestingly while *Mtb* can upregulate *Ifnb* transcription through a particular PRR *in vitro*, the biological relevance *in vivo* is often unclear. This may be because *Mtb* is able to induce type I IFN signaling through multiple pathways, such that others compensate loss of one *in vivo*. Different strains of *Mtb* also differentially induce type I IFN signaling through different PRRs, which may contribute to the different results[33]. Furthermore, any *in vivo* phenotype is often not verified by inhibiting type I IFN signaling by blocking antibody or genetic deletion of IFNAR. PRR signaling induces a wide variety of signals downstream and cross-regulate an overlapping set of genes; therefore it is often difficult to convincingly ascribe the effects of the knockout to type I IFNs without *Ifnar*$^{-/-}$ controls. Below we discuss some of the best candidates for inducing type I IFN responses *in vivo*: TLR4, C-type lectins, and cGAS/STING.

1. Surface receptors

Of the surface receptors, *Mtb* or *Mtb*-secreted products have been suggested to signal through TLR2, 4, 9 and mincle, a c-type lectin. While TLR4 is predominantly associated with recognition of LPS from Gram-negative bacteria, it has also been proposed to detect lipomannans and various secreted proteins from *Mtb*[36–43]. While these reports attempt to control for LPS contamination by proteinase K or polymyxin B treatment, there is currently no evidence of direct interaction between any of these molecules and TLR4. Therefore these results should be considered with caution. Activation of TLR4 can induce expression of type I IFNs through a TRIF- and IRF3-dependent pathway[10], though this has not been specifically shown for any of the proposed TLR4-stimuli in *Mtb*. The virulent Beijing strain BTB02-171 and Euro-American strain Harlingen strongly both appeared to induce *Ifnb* expression *in vitro* through TLR4[33,44]. BTB02-171 also appeared to induce *Ifnb* expression *in vivo* through TLR4, whereas for H37Rv, the induction was TLR4-indepndent[33]. *Tlr4*$^{-/-}$ mice on the B6 background are more susceptible to the virulent BTB02-171 strain of *Mtb*, but not to H37Rv[33]. Other groups used C3H/HeJ mice carrying a natural null mutation in TLR4, though the results were contradictory: two reported no difference between *Tlr4*^{null} and control when infected with H37Rv, one observed increased bacterial burden and decreased survival in *Tlr4*^{null}[45–47]. However, it appears that the authors of these studies did not co-house or use littermate controls in their experiments; therefore these differences may be simply due to divergent microbiota composition. Together, these results lead to an inconclusive picture of the role of *Tlr4* during *Mtb* infection.

C-type lectins recognize carbohydrate moieties on various pathogens[35]. Mincle binds to trehalose-6',6 dimycolate (TDM, also known as cord factor)[35]. *Mincle*$^{-/-}$ splenic B cells are less able to induce *Ifnb* expression compared to wildtype cells when stimulated with *Mtb* or culture filtrate[48]. However, infection of *Mincle*$^{-/-}$ mice with low-dose *Mtb* by aerosol or BCG intratrecheally showed no significant difference from the

control mice[49,50]. Collectively these limited evidence do not demonstrate a conclusive role for surface receptors in inducing type I IFN production in response to *Mtb.*

2. Cytosolic receptors

Cytosolic nucleotide sensors strongly induce type I IFNs when activated by their cognate ligands: RIG-I detects dsRNA and signals via the adaptor MAVS, whereas cGAS detects dsDNA and signals via the adaptor STING. A series of elegant studies [see footnote[1]] demonstrated that recognition of *Mtb* by the cGAS/STING-mediated cytosolic DNA-sensing pathway led to upregulation of *Ifnb* and anti-bacterial autophagy in macrophages[51–55]. This requires the ESX-1 secretion system[27,30,51,55]. cGAS detects cytosolic DNA[56] released by *Mtb*[51,53] to produce the secondary messenger cGAMP[57] that binds to STING, resulting in TBK1 phosphorylation of IRF3 that mediates expression of *Ifnb*[58]. These results suggest that the majority of the *Ifnb* expression observed is dependent on *Mtb* DNA and not bacterial cyclic-di-AMP that also activates STING[51,52]. However, overexpression of the *Mtb* diadenylate cyclase can induce some cGAS-independent and STING-dependent type I IFN expression in certain *Mtb* strains[59]. Despite a robust phenotype *in vitro*, STING and cGAS knockout mice have no difference in bacterial burden and very little difference in survival compared to wildtype mice[52,54]. Because cGAS/STING can activate autophagy and inflammatory cytokines, one hypothesis was that these host-protective pathways balance out any detrimental effects of type I IFNs. In support of this, a recent study reported that a STING-agonist improved immunogenicity of a protein vaccine through an IFNAR-independent pathway[60]. However Wilson, Yamashiro and colleagues in the Vance Lab generated mice with STING that cannot interact with TBK1 but can still induce autophagy and inflammatory cytokines, yet found no difference compared to the control mice (unpublished work). Another possibility is that the C57BL/6 background produces relatively little type I IFNs during infection by laboratory strains of *Mtb*[29], and the protective effect of $Sting^{-/-}$ was not apparent. We crossed mice carrying the null mutation $Sting^{gt/gt}$ [61] on to the B6.$Sst1^{S}$ mice with a strong type I IFN-driven susceptibility but again found limited protection (see Chapter 2). These results suggest that though cGAS/STING pathway is essential for inducing type I IFN responses in bone marrow-derived macrophages *in vitro*, its purpose *in vivo* (if any) remains elusive.

A recent report has shown that *Mtb* secretes bacterial RNA into the host cytosol via the sec2A secretion pathway and activates RIG-I/MAVS[62]. *In vitro* this phenotype requires cGAS/STING to upregulate IRF7; but at late time points, a significant amount of *Ifnb* expression is dependent on RIG-I[62]. Interestingly $Mavs^{-/-}$ mice are more resistant to high dose aerosol *Mtb* infection with the CDC1551 strain than the wildtype mice, which correlated to less *Ifnb* transcripts in the lung[62]. This result suggests that RIG-I/MAVS-dependent signaling may compensate for the loss of cGAS or STING in mice, and that both pathways are required to induce robust type I IFN responses *in vivo.*

1.1.2.2 Detrimental roles of type I IFNs

Mouse models of *Mtb,* like the human studies described above, suggest a complex role for type I IFN signaling[13,15]. Some of the results are confounded in part by the

[1] I read the 2012 Watson and Manzanillo papers in my senior year in college, and I was so impressed that I applied to UCSF. They rejected me, probably for the best.

different inbred strains of mice as well as *Mtb* strains used by different groups (summarized in [13,15]). C57BL/6 (B6) mice used by many groups naturally produce very little type I IFNs during low-dose, laboratory strain (H37Rv or Erdman) *Mtb* infections by aerosol[29]. Therefore the majority of experiments using *Ifnar*$^{-/-}$ mice on the B6 background show little difference in lung bacterial burden or survival from the wildtype control[28,30,63–67]. However, treatment with recombinant IFNα/β or induction of type I IFNs via polyICLC injection or viral infections enhanced susceptibility in IFNAR-dependent manner[29,31,65,66]. IFNAR-deletion also rescues the more susceptible 129 mice, resulting in reduced lung bacterial burden and enhanced survival in two studies[32,68][Footnote[2]]. Taking into consideration some of these caveats about methods, collectively the mouse model suggests type I IFN signaling is detrimental to the host during *Mtb* infections.

A better understanding of how type I IFN drives disease will open new avenues of research for host-directed therapies, diagnostics and treatment monitoring. However, it bears repeating here that type I IFN signaling induces hundreds of ISGs downstream[9,10,12]. The functions of most are not understood, though we can speculate the many might overlap in activity. Therefore apparent genetic redundancy is an inherent hurdle to demonstrating the importance of individual downstream effectors.

1. Suppression of IL-1 and its downstream effectors

IL-1 signaling is vital for the host during *Mtb* infection. Mice deficient in IL-1 receptor (IL-1R) or in both IL-1α/β are extremely susceptible to *Mtb* infection, succumbing rapidly with high bacterial burdens[69–72]. Conversion of pro-IL-1β to mature IL-1β usually requires inflammasome formation and caspase-1 activation[73]. Curiously, during *Mtb* infection, processing of mature IL-1β is not completely dependent on caspase-1 activity[72] or GSDMD (unpublished results). Clearly there are alternate ways of processing IL-1β during *Mtb* infections *in vivo*[73]. *Il1a*$^{-/-}$ and *Il1b*$^{-/-}$ are both less susceptible than *Il1r1*$^{-/-}$ which has no IL-1 signaling, but more susceptible than wildtype mice[64,74]

Type I IFNs induced by *Mtb* infection *in vitro* suppress IL-1β expression in both mouse BMDMs and human monocyte-derived macrophages[27,28,64]. Use of *Ifnar*$^{-/-}$ macrophages or anti-IFNAR blocking antibody led to increased IL-1β expression[27,28,64]. Conversely, addition of recombinant IFNβ or polyICLC to induce IFNβ expression strongly inhibits IL-1α and IL-1β secretion in response to *Mtb* infection[27,28,64]. This suppression is partly IL-10-dependent, though blocking IL-10R in the presence IFNβ does not completely restore IL-1 levels[28,64]. During *in vivo* infection, IL-1 protein is expressed in CD68^{+}Ly6C^{hi} (macrophage/monocyte) and CD11c^{+} (dendritic cell) populations[64], though non-hematopoietic cells were not examined in this study. Similar to *in vitro* experiments, loss of IFNAR specifically in these cells increases IL-1 expression[64]. Interestingly, regulation of type I IFNs and IL-1 is reciprocal. Addition of recombinant IL-1α or β during *in vitro Mtb* infection significantly reduces IFNβ levels, and this is thought to be partially-dependent on lipid mediators such as prostaglandi-E2

[2] Ordway *et al* 2007 was omitted from this discussion as the authors used *Ifnar*$^{-/-}$ on the more susceptible 129 background but B6 as wildtype control, which I do not consider an appropriate comparison. There are other interesting results from this paper that will be cited elsewhere.

(PGE2)[65]. PGE2 reduces expression of IFNβ in infected BMDMs, and when supplemented *in vivo* rescues the susceptibility of polyICLC-treated mice[65]. Conversely, susceptibility of the *Il1r1*$^{-/-}$ mice is partially rescued by concurrent deletion of *Ifnar*, suggesting that part of the IL-1 signaling-dependent protection is suppressing type I IFN responses[65].

A recent report using reciprocal and competitive mixed bone marrow-chimeras of *Il1r1*$^{-/-}$ and wildtype mice have shown that IL-1-mediated protection occurs in *trans*[75]. In other words, the animal is protected as long as there is IL-1R expression on either the non-hematopoietic or the hematopoietic cells[75]. Interestingly, a separate study reports that IL-1R signaling on non-hematopoietic cells is required for alveolar macrophages to migrate from airway spaces into the interstitium of the lung, facilitating dissemination to other cell types[76]. However based on Bohrer *et al*, loss of IL-1R on non-hematopoietic cells does not affect overall bacterial burden[75]. It remains to be seen whether the control of bacterial growth is unaffected by altered alveolar macrophage migration or due to compensatory mechanisms. These results highlight the complexity of IL-1 signaling in the lung, which is clearly not just limited to hematopoietic cells. As both IL-1R and IFNAR are ubiquitously expressed[10,77], the role of type I IFN signaling in non-hematopoietic cells should be examined in future studies.

2. IL-10 induction

IL-10 is a major immunosuppressive cytokine induced by type I IFN as well as by a myriad of stimuli such as IL-27, TLR, and C-type lectin signaling[10,78]. During *Mtb* infection many cell types can produce IL-10: interstitial macrophages, recruited monocytes (Ly6C^{+} and Ly6C^{-}), NK cells, T cells and B cells[79]. IL-10 is a pleiotropic cytokine, capable of suppressing IL-12 production, DC maturation and trafficking to the lymph nodes, T_H1 differentiation and production of inflammatory cytokines[78]. IL-10 induction during *Mtb* infection is amplified by type I IFN signaling both *in vivo* and *in vitro*[28,64,65,79], though this does not occur during infection with clinical strain BTB02-171[44]. In a mixed bone marrow-chimera, fewer *Ifnar*$^{-/-}$ cells produce IL-10, and this correlates with increased IL-1α/β expression in the same cells[64]. *Il10*$^{-/-}$ mice or anti-IL-10 treatment on a variety of backgrounds are more resistant to various strains of *Mtb*, though the effect is only apparent during the chronic phase of infection (past 50 days post-infection)[29,65,68,79–82]. T cells secrete a significant amount of IL-10, which may explain why IL-10-dependent effects are delayed[79]. Overexpression of IL-10 enhances susceptibility[83]. Type I IFN-driven susceptibility in polyICLC-treated B6 mice can be reversed by anti-IL-10 antibody treatment[65], suggesting that IL-10 is a major mechanism downstream of type I IFNs. Of note, not all *Mtb* strains induce elevated IL-10, suggesting that anti-IL-10 treatment would not work in all models[84].

3. Inhibition of IL12 and TNFα production, and IFNγ signaling

Previous studies have also shown that type I IFN suppresses macrophage response to IFNγ, a major component of anti-bacterial response[28,85–87]. Type I IFNs can reduce IFNγR expression on macrophages *in vitro*[85–87], though this effect is not consistently observed *in vivo* during *Mtb* infection and is not correlated with cell intrinsic control of bacteria replication[29,64]. Addition of IFNβ can block IFNγ-dependent upregulation of IL-12p40 and TNFα in infected macrophages[28,87]. However, *Ifnar*$^{-/-}$ mice have similar TNFα levels as wildtype control during infection, suggesting suppression of TNFα may not be a major pathway *in vivo*[29,44]. Infection with the virulent HN878 that induces more type I

IFNs led to decreased IL-12 in the lung and less cell proliferation in draining lymph nodes and spleen, but this was not specifically shown to be *Ifnar* dependent[31]. Moreover, mice treated with polyICLC had similar ratio of activated CD4+ T cells in the lung, and these cells were similarly able to produce IFNγ and TNFα[29]. These data do not suggest that type I IFNs strongly affect TNFα or IL-12 levels *in vivo,* though their functions may be altered in other ways no yet examined.

1.1.2.3 Protective roles of type I IFNs

Cytokines are just like "the Force: there is a light side and a dark side, and they hold" the immune system together [footnote[3]]. Type I IFNs can have protective effects during a variety of bacterial infections[9,12]. And as discussed, data from human studies suggest that exogenous IFNα can compensate for loss of IFNγ signaling during mycobacterial diseases[25,26]. Studies in *Ifngr*$^{-/-}$ mice is consistent with this conclusion: *Ifnar*$^{-/-}$*Ifngr*$^{-/-}$ mice are more susceptible to both H37Rv and the more virulent BTB02-171 compared to wildtype, *Ifnar*$^{-/-}$, or the already susceptible *Ifngr*$^{-/-}$ mice[44,88]. Infected *Ifnar*$^{-/-}$ macrophages also have higher bacterial burden than wildtype cells in the absence of exogenous IFNγ, mirroring the results *in vivo*[28]. It appears that type I IFN signaling can mediate protective effects, but this effect is not apparent in the presence of intact IFNγ signaling and is otherwise overshadowed by its detrimental effects *in vivo.* It is not surprising that type I IFNs can compensate for IFNγ at some levels: ISGs induced by either cytokine overlap greatly[10]. Both recombinant IFNβ and IFNγ can induce iNOS and nitrite production[44] as well as suppress IL-1 production *in vitro*[44,64]. Interestingly, tonic signaling of IFNβ also appear to be important for expression of IL-12p40 and TNFα in macrophages *in vitro*, as *Ifnar*$^{-/-}$ secrete less cytokines when infected with *Mtb* than wildtype cells[28,89]. Pre-treating the cells with IFNβ led to increased production of IL-12p40 and TNFα upon *Mtb* infection[28].

Other mycobacteria are more sensitive to type I IFN-mediated control. Both opportunistic pathogen *M. smegmatis* and attenuated *M. bovis* BCG are cleared rapidly from wildtype mice but replicate significantly better in *Ifnar*$^{-/-}$ mice[90,91]. Exogenous IFNβ (either recombinant or through polyICLC induction) improved control of *M. avium* in wildtype mice[90,91].

Collectively the results from mouse model studies suggest that type I IFNs can contribute to control of mycobacterial infections *in vitro* and under limited contexts. But with *Mtb* the host-detrimental type I IFN-dependent response (described in the previous section) mediated by suppression of IL-1 and upregulation of IL-10 is more dominant.

1.2 Sp110, Sp140 and the regulation of innate signaling by epigenetics

Different inbred mice exhibit differential susceptibility to *Mtb* infection: 129, CBA/J and C3H/HeJ are more sensitive than B6 mice[3,68,82]. To understand the host determinants of susceptibility, Kramnik and colleagues made a series of congenic mice and identified the *Super susceptibility to tuberculosis 1* (*Sst1*) locus on chromosome 1[2,3,92]. Congenic B6 mice carrying the susceptible allele (B6.*Sst1*^{S}) are extremely susceptible to *Mtb* and *L. monocytogenes*[2,92]. Within this locus, the authors identified the

[3] Quote adapted from Adam Savage[177]. Original quote was "Duct tape is just like the Force: it has a dark side and a light side, and it holds the universe together."

gene *Sp110* (*Ipr1*) as the candidate gene[2]. *Sp110* is a member of the speckled protein family composed of *Sp100, Sp140* and *Sp110.* They are all putative transcriptional regulators composed of an Sp100 domain (formerly known as HSR), a DNA binding domain SAND, plant homeobox domain PHD (only in *Sp100* and *Sp140*) and a bromodomain (only in *Sp140*). Interestingly the Sp100 domain and SAND are also found in *Aire*, a well-known transcriptional regulator involved in expression of tissue specific antigens during T cell development[93]. All three SP100-family proteins can colocalize with the PML nuclear body (PML-NB) in the nucleus[94,95]. However, very little is known about the functions of these genes. Sp100 restricts viral replication in the nucleus, and is targeted by viral proteins[94]. Several studies have suggested that in human cells Sp110 and Sp140 may have similar functions (see Chapter 3 for more detailed discussion).

1.3 Summary

Type I IFNs were first discovered for their ability to interfere with viral infections[8]. Our knowledge about their pleiotropic functions has greatly expanded in the sixty years since their discovery. Type I IFN signaling pathways are closely intertwined with both innate and adaptive immune responses[10]. They can be induced by both viral and bacterial pathogens through a similar set of sensors, and can be both beneficial to the pathogen and the host[9,12]. Overall, *Mtb* seems to benefit from type I IFN signaling, as demonstrated by both human studies and numerous previous works using the mouse model. In the next two chapters, I describe my work showing that susceptible B6.*Sst1*^{S} mice exhibit type I IFN-driven susceptibility to *Mtb*. I further demonstrate that this susceptibility is mediated by overexpression of IL-1 receptor antagonist, a competitive inhibitor of IL-1R signaling. Consequently B6.*Sst1*^{S} mice have low IL-1 signaling despite of increased IL-1 proteins. I further demonstrate that the loss of *Sp140* but not *Sp110* is sufficient to replicate the susceptibility associated with the *Sst1*^{S} allele, suggesting that *Sp140* may be a novel suppressor of type I IFN signaling. My work highlights the complexities of immune regulation during *Mtb* infection, both upstream and downstream of type I IFNs.

Chapter 2. Interleukin-1 receptor antagonist mediates type I interferon-driven susceptibility to *Mycobacterium tuberculosis*

[Footnote 4]

2.1 Summary

The bacterium *Mycobacterium tuberculosis* (*Mtb*) causes tuberculosis (TB) and is responsible for more human mortality than any other single pathogen[1]. Progression to active disease occurs in ~10% of infected individuals and is predicted by an elevated type I interferon (IFN) response[13,15,96–99]. Type I IFNs are vital for antiviral immunity, but whether or how they mediate susceptibility to *Mtb* has been difficult to study, in part because the standard C57BL/6 (B6) mouse model does not robustly recapitulate the type I IFN signature associated with human active TB disease[96–99]. Here we examined B6.*Sst1*^{S} congenic mice that carry the C3H "sensitive" allele of the *Sst1* locus that renders them highly susceptible to *Mtb* infections[2,3,92]. We found that B6.*Sst1*^{S} mice exhibit markedly increased type I IFN signaling, and that type I IFNs were required for the enhanced susceptibility of B6.*Sst1*^{S} mice to *Mtb*. Type I IFNs affect the expression of hundreds of genes, several of which have previously been implicated in susceptibility to bacterial infections[9,12]. Nevertheless, we found that heterozygous deficiency in just a single IFN target gene, IL-1 receptor antagonist (IL-1Ra), is sufficient to reverse IFN-driven susceptibility to *Mtb.* As even a partial reduction in IL-1Ra levels led to significant protection, we hypothesized that IL-1Ra may be a plausible target for host-directed anti-TB therapy. Indeed, antibody-mediated neutralization of IL-1Ra provided therapeutic benefit to *Mtb*-infected B6.*Sst1*^{S} mice. Our results provide an example of how the diversity of inbred mouse strains can be exploited to better model human TB, and demonstrate that IL-1Ra is an important mediator of type I IFN-driven susceptibility to *Mtb* infections *in vivo*.

2.2 Introduction

Mycobacterium tuberculosis (*Mtb*) infections in humans result in highly diverse outcomes ranging from asymptomatic lung granulomas to lethal disseminated disease. Active TB disease is characterized by the uncontrolled replication of bacteria and pathological inflammation in the lungs and other organs, and arises in an estimated ~10% of Mtb-infected HIV-negative individuals. There is no vaccine that reliably protects against pulmonary TB, and although antibiotics can be curative, the long (≥6-month) course of treatment and increasing prevalence of multi-drug resistant *Mtb* infections has spurred a search for alternative therapeutic approaches[100,101]. Since only individuals with active TB readily transmit infection, and as humans are the only natural reservoir of *Mtb*, a favored strategy to contain the TB epidemic is to identify and treat those individuals likely to progress to active disease[1,96,97]. Identification of such individuals is challenging, but recent studies have demonstrated that an enhanced type I interferon (IFN) signature correlates with active TB[98,99] and can predict progression to active TB up to 18 months prior to diagnosis[13,15,96,97]. A partial loss-of-function polymorphism in the type I IFN receptor (IFNAR1) is associated with resistance to TB in humans, suggesting that

[4] An earlier form of this chapter is currently available on bioRxiv under the same name, doi: https://doi.org/10.1101/389288

elevated levels of type I IFNs not only predict but may even be causally linked to TB progression[18]. A small number of cases also link IFN treatment during chronic viral infections with increased susceptibility to TB[13,19,21,22]. In addition, numerous animal studies have demonstrated causal roles for type I IFNs in susceptibility to Mtb[13,15,29,31,65,68,102] and other bacterial infections[9,12].

Given the strong association between type I IFNs and susceptibility to human TB, two major remaining challenges are: (1) to determine the mechanisms by which type I IFNs mediate susceptibility to active TB, and (2) to exploit this knowledge to develop interventions that can reverse the susceptibility. Mechanistic studies and initial trials of possible therapeutic interventions require a robust animal model. However, the most commonly used animal model, the C57BL/6 (B6) mouse, does not robustly recapitulate the interferon-driven TB susceptibility seen in humans. B6 *Ifnar*$^{-/-}$ mice show mild resistance to *Mtb* in the spleen and variable but modest effects in the lungs[30,44,88]. To better model IFN-driven susceptibility, some investigators treat *Mtb*-infected B6 mice with poly-IC, a potent inducer of type I IFNs[29,65]. Such treatment dramatically increases susceptibility to *Mtb* in an *Ifnar*-dependent manner[29,65], but because the IFN is induced artificially and not by *Mtb* itself, it is unclear if poly-IC mimics the course of IFN-driven disease in humans.

2.3 Results

As an alternative approach, we sought to exploit the natural diversity of available inbred mouse strains. The 129 mouse strain shows clear IFN-driven susceptibility to *Mtb*[68], but there are limited tools on this genetic background. We therefore turned to a previously described congenic mouse strain, B6.*Sst1*^{S}, that carries the 10.7Mb *Super susceptibility to tuberculosis 1* (*Sst1*) region of mouse chromosome 1 from C3H on an otherwise B6 genetic background[2,92]. The B6.*Sst1*^{S} mice exhibit marked susceptibility to aerosol TB infection[2,92], however the mechanism by which the *Sst1*^{S} locus confers susceptibility remains incompletely understood. The previously published candidate gene for the *Sst1* locus is *Ipr1* (also known as *Sp110* in both mouse and human)[2]. Because *Ipr1* is in a highly repetitive region of the mouse genome no *Ipr1*$^{-/-}$ has been published. Therefore, it has not been fully confirmed that *Ipr1* is in fact the gene responsible for the

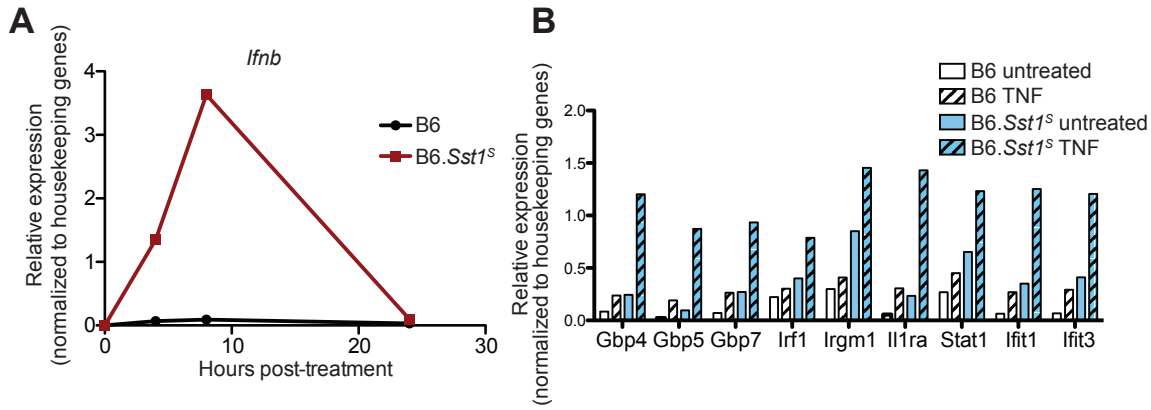

Figure 2.1 | B6.*Sst1*^{S} BMMs overexpress *Ifnb* and ISGs when stimulated with TNFα. A-B, Expression of *Ifnb* (A) or selected ISGs (B) in BMMs measured by RT-qPCR. Results normalized to housekeeping genes. Representative data of at least two independent experiments.

phenotypes associated with the *Sst1* locus. Recent work has established that macrophages from B6.*Sst1*^{S} mice exhibit an enhanced type I IFN response[103,104]. In agreement with this work, we found that bone marrow-derived macrophages (BMMs) from B6.*Sst1*^{S} mice expressed higher levels of interferon-beta (*Ifnb*) and interferon-stimulated genes (ISGs) upon stimulation with TNF (Figure 2.1).

To determine if B6.*Sst1*^{S} mice also exhibit an enhanced type I IFN signature *in vivo*, we measured *Ifnb* transcripts in the lungs of *M. tuberculosis*-infected mice. Indeed, B6.*Sst1*^{S} mice exhibited higher levels of *Ifnb* transcripts as compared to B6 mice (Figure 2.2A). To investigate whet her this enhanced type I IFN signaling causes the susceptibility of B6.*Sst1*^{S} mice to *Mtb*, we infected mice with *Mtb* and then treated with an IFNAR1-blocking antibody[105] to inhibit type I IFN signaling. B6.*Sst1*^{S} mice treated

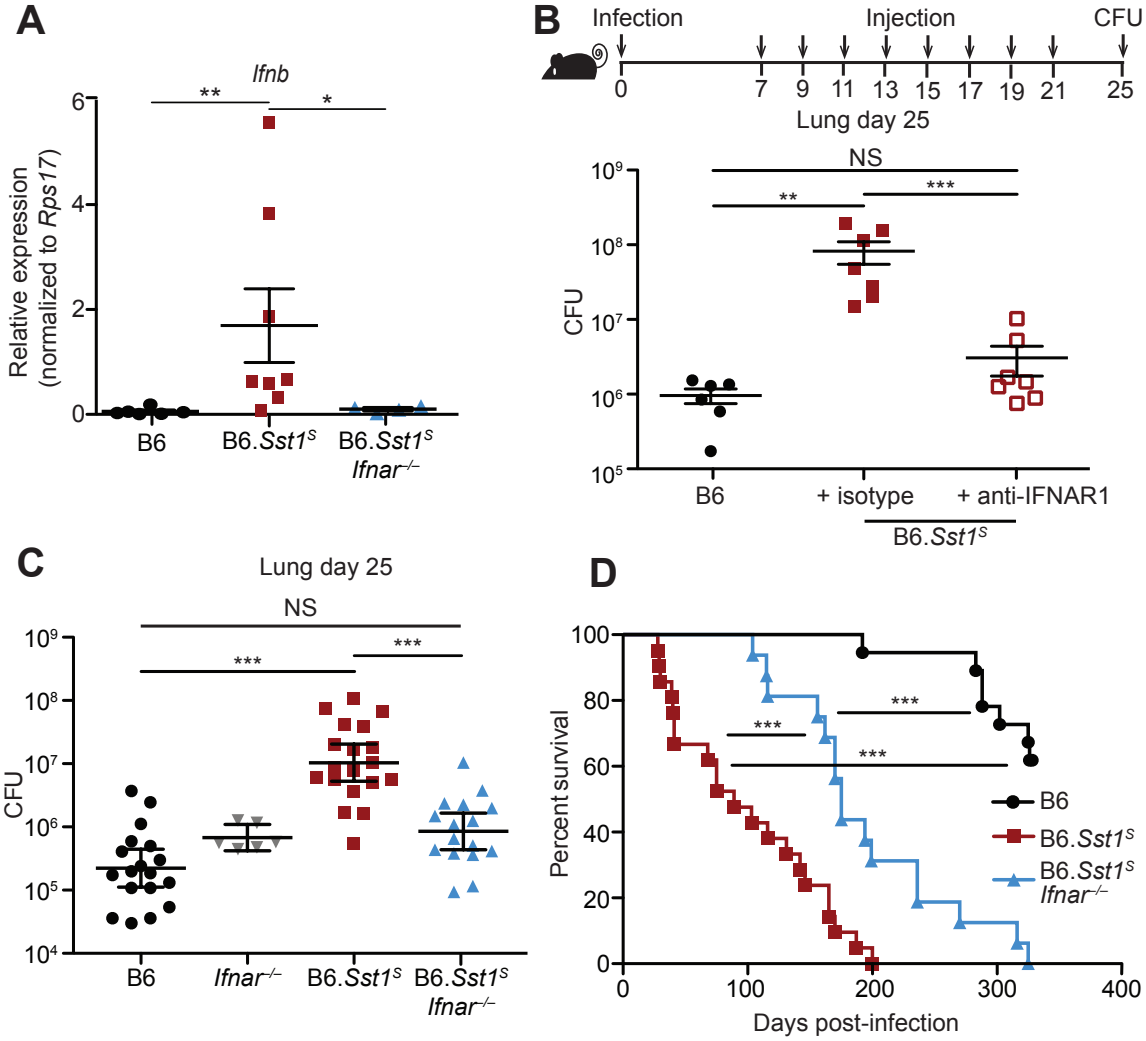

Figure 2.2 | Type I IFN drives enhanced susceptibility of B6.*Sst1*^{S} mice. A, Expression of *Ifnb* measured by qRTPCR relative to *Rps17* in *Mtb*-infected lungs at day 25. B, Lung bacterial burdens at day 25 from *Mtb*-infected mice treated with anti-IFNAR1 or isotype control antibody. C, Lung bacterial burdens at day 25, or D, survival, of *Mtb*-infected mice. For A-C, genotypes indicated on the x-axis. C-D, Combined results from three independent infections. For D, B6, n = 18; B6.*Sst1*^{S}, n = 21; B6.*Sst1*^{S}*Ifnar*$^{-/-}$, n = 16. All except B6 mice were bred in-house (B-D). Error bars are SEM. Analyzed with two-ended Mann-Whitney test (B, C) or Log-rank (Mantel-Cox) Test (D). Asterisk, $p \leq 0.05$; two asterisks, $p \leq 0.01$; three asterisks, $p \leq 0.001$.

with the IFNAR1-blocking antibody showed significantly decreased bacterial burdens compared to those that only received an isotype control antibody (Figure 2.2B). To provide genetic confirmation of this result, we crossed B6.*Sst1*^{S} mice to B6.*Ifnar*$^{-/-}$ mice. *Ifnar* deficiency largely reversed the enhanced susceptibility of B6.*Sst1*^{S} mice to *Mtb* infection. At 25 days post-infection, the bacterial burdens in the lungs of the B6.*Sst1*^{S}*Ifnar*$^{-/-}$ mice were significantly lower than in the lungs of B6.*Sst1*^{S} mice, and

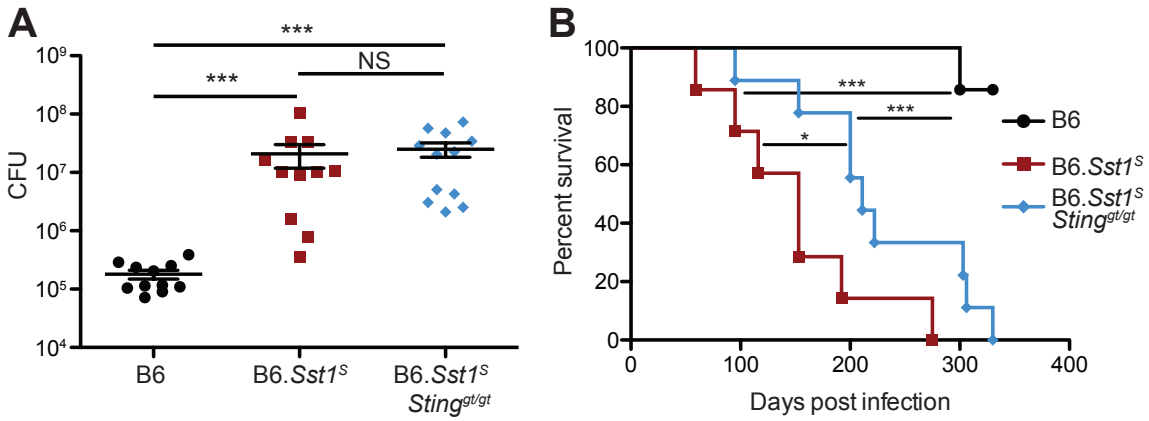

Figure 2.3 | B6.*Sst1*^{S}*Sting*$^{gt/gt}$ partially rescues the enhance susceptibility of B6.*Sst1*^{S} mice to *Mtb*. A, Lung bacterial burdens at day 25 (combined results of 2 independent infections) or B, survival of mice infected with *Mtb*. B6, n = 11; B6.*Sst1*^{S}, n = 11; B6.*Sst1*^{S}*Sting*$^{gt/gt}$, n = 11. All animals except 5 of the B6 were bred in-house (A) and all except B6 were bred in-house (B). Error bars are SEM. Analyzed with two-ended Mann-Whitney test (A) or Log-rank (Mantel-Cox) Test (B). Asterisk, $p \leq 0.05$; two asterisks, $p \leq 0.01$; three asterisks, $p \leq 0.001$.

were similar to B6 mice (Figure 2.2C). Infected B6.*Sst1*^{S}*Ifnar*$^{-/-}$ mice also survived significantly longer than B6.*Sst1*^{S} mice (Figure 2.2D), though there are also clearly *Ifnar*-independent effects of the *Sst1*^{S} locus that act at later time points. By contrast, and consistent with prior reports[30,44,88], *Ifnar* deficiency had little or no effect on *Mtb* disease in wild-type B6 (*Sst1*^{R}) mice. Recent data have suggested that the host protein STING is required for interferon induction to *Mtb*[52,54,55,59,106]. However, crossing B6.*Sst1*^{S} mice to STING-deficient *Sting*$^{gt/gt}$ mice did not significantly reduce bacterial burdens at day 25 compared to B6.*Sst1*^{S} mice (Figure 2.3A). However, the B6.*Sst1*^{S}*Sting*$^{gt/gt}$ mice did show a slight improvement in survival not seen in the B6 genetic background[54] (Figure 2.3B). Overall our data demonstrate that the *Sst1*^{S} locus acts directly or indirectly to increase type I IFN signaling *in vivo* and thereby exacerbate *Mtb* infection, particularly during the early phases of infection.

Type I IFN negatively regulates anti-bacterial immune responses via multiple mechanisms[13,15], including through increased IL-10 levels[28,65], decreased IFNγ signaling[85,86], induction of cholesterol 25-hydroxylase (*Ch25h*)[107], and/or decreased IL-1 levels[27,64,65]. We did not observe significant differences in IL-10 or IFNγ levels in the lung during *in vivo Mtb* infection (Figure 2.4A-B). In addition, crossing B6.*Sst1*^{S} mice to B6.*Ch25h*$^{-/-}$ mice did not alter day 25 lung bacterial burdens (Figure 2.4C). Moreover, despite clear evidence that type I IFN and IL-1 counter-regulate each other[108], the *Sst1*^{S} locus did not appear to act to decrease the levels of IL-1 *in vivo*; in fact, we unexpectedly observed higher levels of both IL-1α and IL-1β in the lungs of B6.*Sst1*^{S}mice at 25 days

post-infection as compared to B6 mice (Figure 2.5A-B). Other inflammatory mediators, including TNF, CXCL1 and prostaglandin E2 (PGE_2) were similarly elevated in the B6.*Sst1*^{S} mice (Figure 2.4D-F) as was the frequency of $CD11b^+Ly6G^+$ cells (neutrophils) in the lungs (Figure 2.4G). The elevated inflammation in B6.*Sst1*^{S} mice was a consequence of elevated type I IFNs, as inflammatory cytokines and neutrophils were reduced in B6.*Sst1*^{S}*Ifnar*$^{-/-}$ mice, but the underlying mechanism was not apparent.

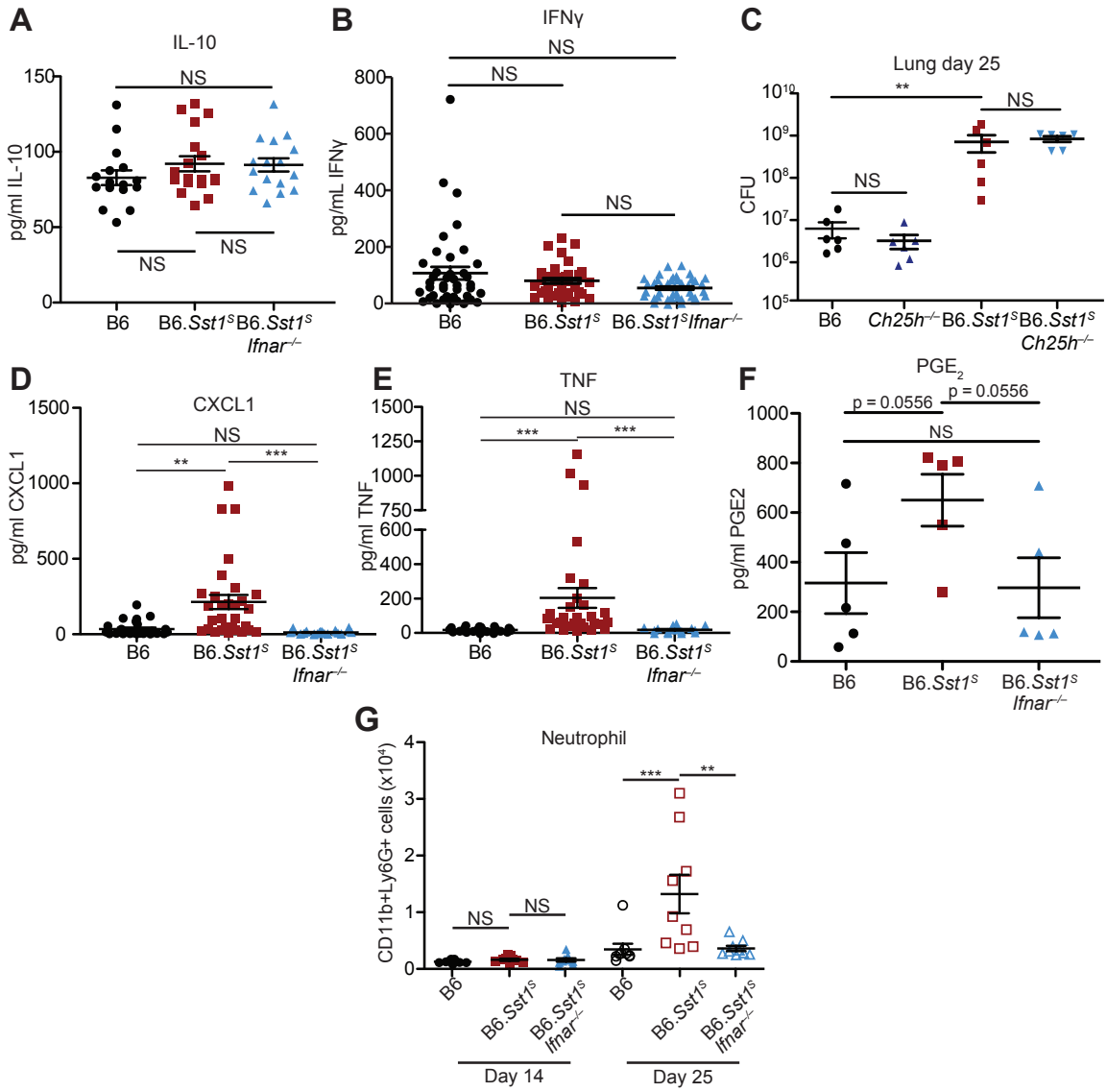

Figure 2.4 | Enhanced inflammation in B6.*Sst1*^{S} mice requires type I IFN but is not due to altered IL-10 or IFNγ levels or *Ch25h* or PGE_2. A, B, D, E, Protein levels of IL-10 (A), IFNγ (B), CXCL1 (D) and TNF (E) were measured in lungs of *Mtb*-infected mice at day 25. Combined results of three independent infections. C, Lung bacterial burden of *Mtb*-infected mice at day 25 (representative of two independent infections). F, Lungs of *Mtb*-infected mice were collected at 25 days post-infection and lipids were purified using C18 columns. PGE_2 levels were measured by ELISA. G, Neutrophils ($CD11b^+Ly6G^+$) from lungs of *Mtb*-infected mice were enumerated on day 14 and day 25. Combined results of two independent infections. All animals except B6 were bred in-house (A-E); all animals were bred in-house (F-G). Error bars are SEM. Analyzed with two-ended Mann-Whitney test (A-G). Asterisk, $p \leq 0.05$; two asterisks, $p \leq 0.01$; three asterisks, $p \leq 0.001$.

We reasoned that the high levels of IL-1α/β in B6.*Sst1*^{S} mice may be a consequence of the higher bacterial burdens in these mice, or alternatively, may be causing increased bacterial replication via induction of a pro-bacterial inflammatory milieu, as previously proposed[109,110]. To distinguish these possibilities, we inhibited IL-1 signaling *in vivo* using an anti-IL-1R1 blocking antibody[111], beginning 12 days post-infection (Figure 2.5C, 2.6A). Both B6 and B6.*Sst1*^{S} mice treated with IL-1R1 blocking antibody exhibited increased bacterial burdens compared to mice treated with an isotype control antibody. These results confirm prior evidence that IL-1 plays a protective role in

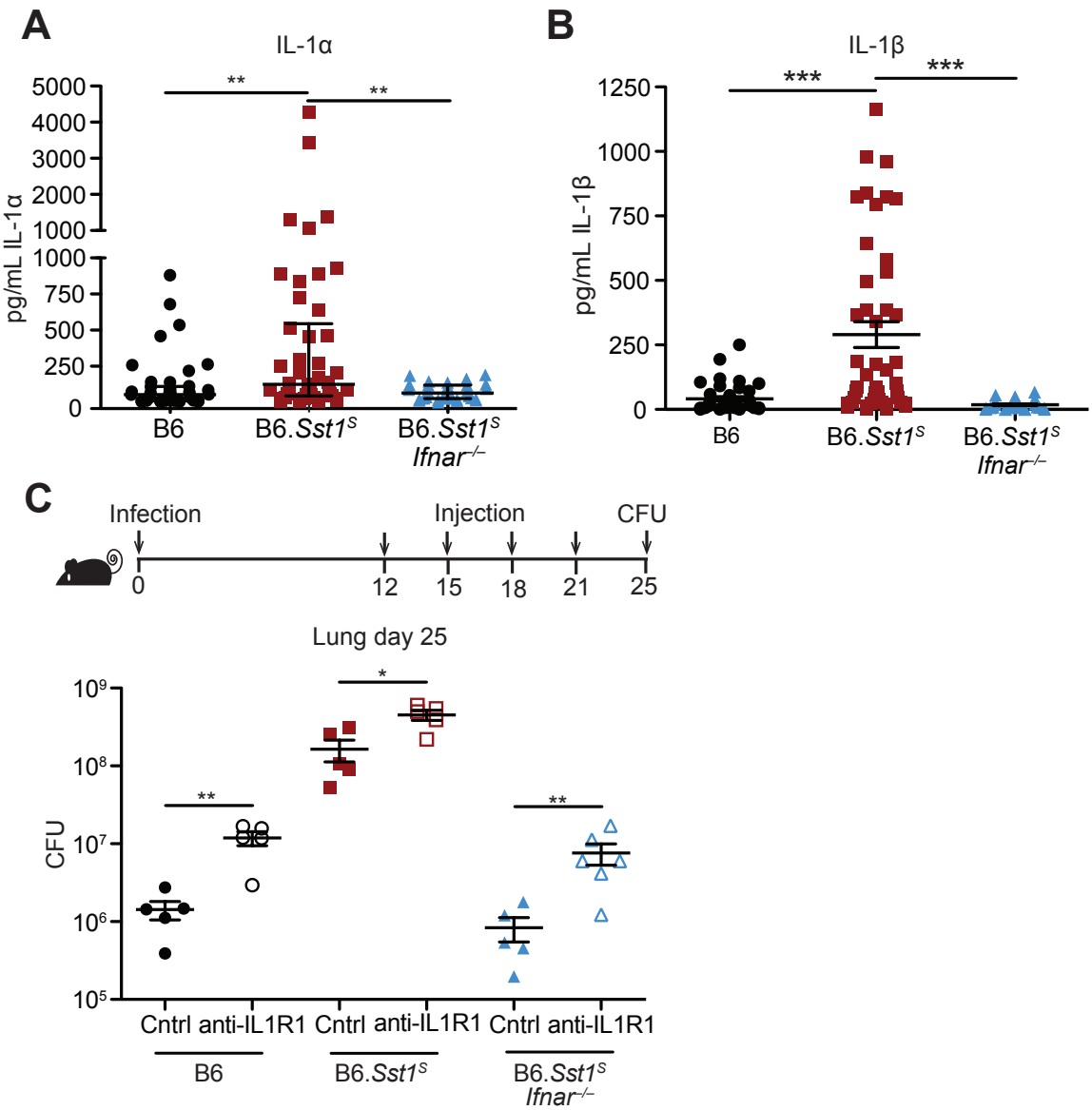

Figure 2.5 | IFNAR signaling results in high but non-pathological IL-1 protein levels in B6.*Sst1*^{S} mice. A-B, Protein levels of IL-1α (A) and IL-1β (B) were measured in the lungs of *Mtb*-infected mice by ELISA at day 25. Combined results of four independent experiments. C, Lung bacterial burdens at day 25 from *Mtb*-infected mice treated with anti-IL1R1 or isotype control antibody. All animals except B6 were bred in-house (A-C). Error bars are SEM. Analyzed with two-ended Mann-Whitney test (A-C). Asterisk, $p \leq 0.05$; two asterisks, $p \leq 0.01$; three asterisks, $p \leq 0.001$.

B6 mice[69–72,74,75,112], and extend this observation to B6.*Sst1*^{S} mice as well. Thus, elevated IL-1 levels do not explain the exacerbated infections of B6.*Sst1*^{S} mice.

Type I IFNs induce the expression of hundreds of target genes. However, given that IL-1 signaling is essential for resistance to *Mtb*[69–72,74,75,112], we were particularly interested in *Il1rn*, which encodes the secreted IL-1 receptor antagonist (IL-1Ra)[113]. IL-1Ra binds to IL-1R1 without generating a signal and blocks binding of both IL-1α and IL-1β[73] (Figure 2.7A). *Il1rn* is known to be induced during *Mtb* infection[65] and by type I IFN signaling[114,115], and as expected, B6.*Sst1*^{S} BMMs strongly upregulated *Il1rn* in an *Ifnar*-dependent manner when stimulated with TNF (Figure 2.7B). Similarly, B6.*Sst1*^{S} mice infected with *M. tuberculosis* had higher levels of IL-1Ra protein in their lungs, as compared to infected B6 or B6.*Sst1*^{S}*Ifnar*$^{-/-}$ mice (Figure 2.6B, 2.7C). These results raised the possibility that the high IL-1 protein levels in B6.*Sst1*^{S} mice are inadequate to

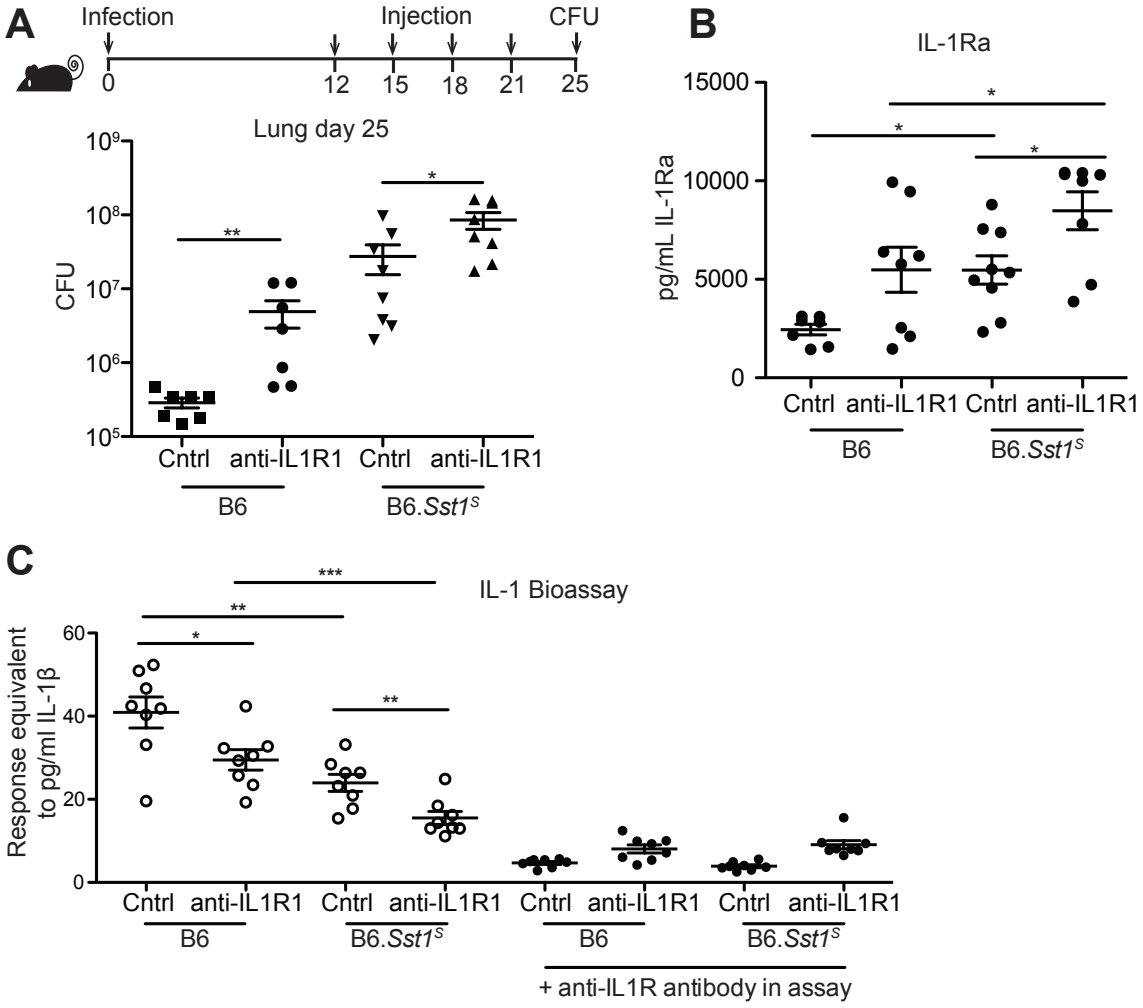

Figure 2.6 | IL-1 blockade increases susceptibility in both B6 and B6.*Sst1*^{S} mice. A-C, *Mtb*-infected mice were treated with anti-IL1R or isotype control antibodies, and on day 25 the lungs were measured for bacterial burden (A), IL-1Ra protein levels (B), and IL-1 bioactivity (C). All animals except B6 were bred in-house (A-C). Error bars are SEM. Analyzed with two-ended Mann-Whitney test (A-C). Asterisk, $p \leq 0.05$; two asterisks, $p \leq 0.01$; three asterisks, $p \leq 0.001$.

protect against infection because of a block in IL-1 signaling. To test this possibility, we examined the amount of functional IL-1 signaling in lung homogenates from infected mice using HEK-Blue-IL-1R™ reporter cells (Invivogen). Despite higher levels of IL-1 proteins, lung homogenates from infected B6.*Sst1*^{S} mice had less functional IL-1 signaling capacity as compared with B6 mice (Figure 2.6C, 2.7D). The reporter appeared to be a reliable indicator of functional IL-1 as responses were blocked by anti-IL-1R1 antibody (Figure 2.6C). The lower levels of IL-1 signaling seen in B6.*Sst1*^{S} mice was reversed in B6.*Sst1*^{S}*Ifnar*$^{-/-}$ mice. Interestingly, the reduced IL-1 bioactivity in B6.*Sst1*^{S} mice compared to B6 and B6.*Sst1*^{S}*Ifnar*$^{-/-}$ mice is only observed early during *Mtb* infection (Figure 2.8). As disease progresses, functional IL-1 signaling in B6.*Sst1*^{S} mice increases to levels similar to that of B6 mice, though this does not appear to be protective as all B6.*Sst1*^{S} mice eventually succumb to the infection. These data underline the importance of distinguishing IL-1 protein levels from signaling capacity, and suggest that B6.*Sst1*^{S} mice may be susceptible to *Mtb* because of reduced functional IL-1 signaling

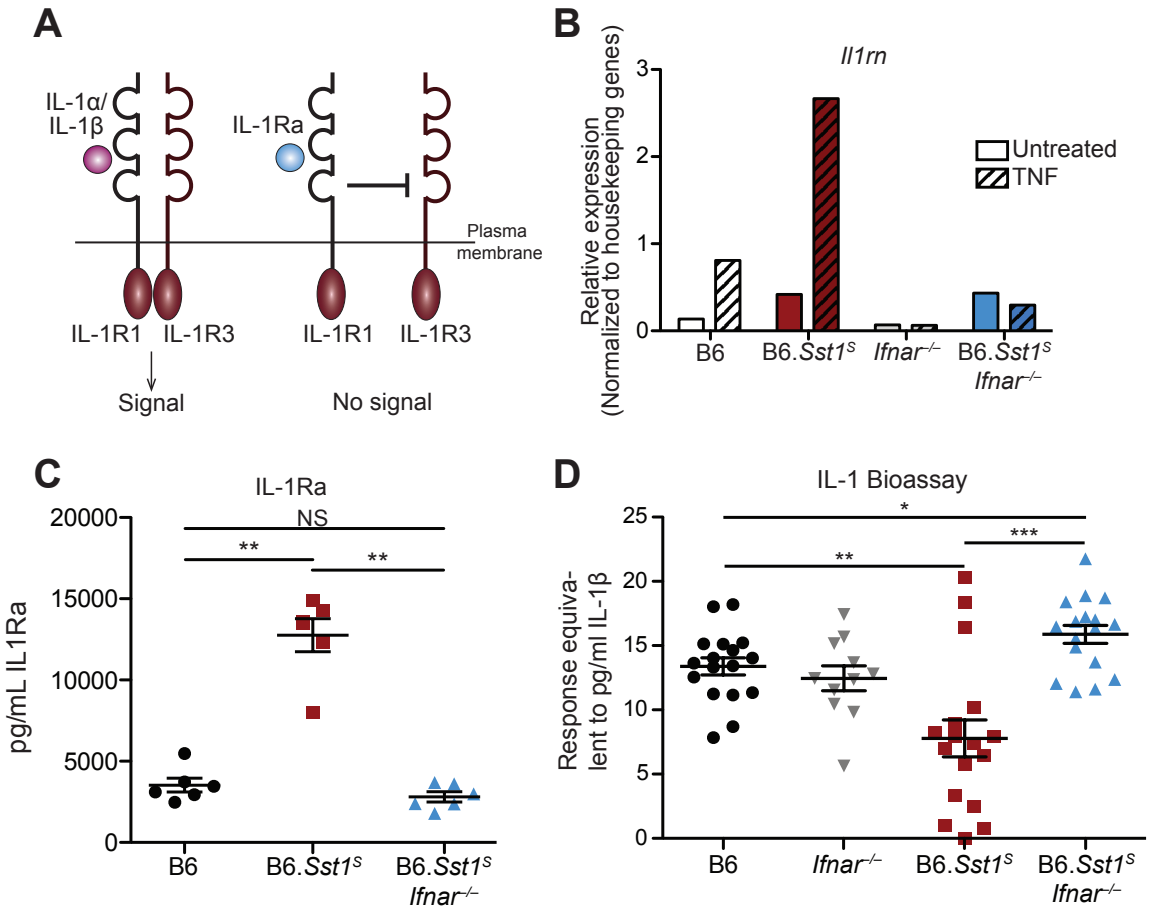

Figure 2.7 | Elevated IL-1Ra and decreased functional IL-1 signaling in *Mtb*-infected B6.*Sst1*^{S} mice. A, Schematic of IL-1R signaling. B, *Il1rn* expression in BMMs treated with 10ng/ml TNFα for 24 hours. C, IL-1Ra protein levels and D, IL-1 reporter assay measuring functional IL-1 bioactivity in lungs of *Mtb*-infected mice at day 25. Combined results of three independent infections (D) or representative of at least two independent experiments (B, C). All animals except B6 were bred in-house (B-D). Error bars are SEM. Analyzed with two-ended Mann-Whitney test (C, D). Asterisk, $p \leq 0.05$; two asterisks, $p \leq 0.01$; three asterisks, $p \leq 0.001$.

early during infection, despite increased IL-1 protein levels. Consistent with these observations, some data suggest IL-1Ra is associated with exacerbated TB in humans[116–119].

To test whether excessive type I IFN signaling neutralizes IL-1 signaling via IL-1Ra, we sought to reduce IL-1Ra levels in B6.*Sst1*^{S} mice during *Mtb* infection. To do this, we first crossed B6.*Sst1*^{S} to *Il1rn*$^{-/-}$ mice[120]. Since uninfected homozygous *Il1rn*$^{-/-}$ mice exhibit signs of inflammatory disease due to dysregulated IL-1 signaling[73,120,121], and because heterozygous *Il1rn*$^{+/-}$ mice have a partial decrease in IL-1Ra levels[120], we generated both heterozygous B6.*Sst1*^{S}*Il1rn*$^{+/-}$ and homozygous B6.*Sst1*^{S}*Il1rn*$^{-/-}$ mice. Both heterozygous and homozygous *Il1rn* deficiency protected B6.*Sst1*^{S} mice from *Mtb*. In fact, bacterial burdens in B6.*Sst1*^{S}*Il1rn*$^{-/-}$ mice were even lower than those found in 'resistant' B6 mice (Figure 2.9A). Notably, a partial reduction in IL-1Ra levels due to heterozygous deficiency of *Il1rn* was sufficient to almost entirely reverse the enhanced IFN-driven susceptibility of *Sst1*^{S} mice (Figure 2.9B). Interestingly, B6.*Sst1*^{S}*Il1rn*$^{-/-}$ mice succumbed faster than their heterozygote littermates, though this may be due to the reduced lifespan independent of infection previously reported for *Il1rn*$^{-/-}$ mice[121]. Histological samples of infected lungs showed significant reduction in lesion sizes in both B6.*Sst1*^{S}*Il1rn*$^{+/-}$ and B6.*Sst1*^{S}*Il1rn*$^{-/-}$ mice as compared to B6.*Sst1*^{S} (Figure 2.9C). Despite concerns that enhanced IL-1 signaling may cause immunopathology, both B6.*Sst1*^{S}*Il1rn*$^{+/-}$ and B6.*Sst1*^{S}*Il1Rn*$^{-/-}$ mice retained more body weight and exhibited increased survival as compared to infected B6.*Sst1*^{S} mice (Figure 2.10A-B). Despite

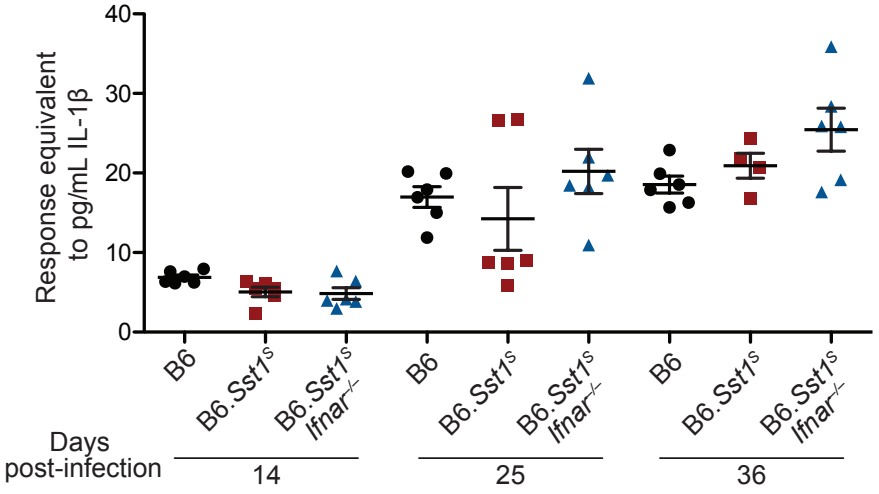

Figure 2.8 | IL-1 bioactivity changes as infections progress. Mice were infected with *Mtb* and input dose was verified a day later using 5 mice (25-43CFU/mouse). IL-1 bioactivity was measured in lung samples collect- ed on the indicated days, using an IL-1R reporter cell line. B6.*Sst1*^{S} and B6.*Sst1*^{S}*Ifnar*$^{-/-}$ mice were bred in-house.

decreased bacteria burdens, B6.*Sst1*^{S}*Il1rn*$^{+/-}$ mice had similar levels of *Ifnb* transcript as B6.*Sst1*^{S} mice (Figure 2.10C). We observed a similar trend with other ISGs such as *Ch25h* (Figure 2.10D). These results suggest IL-1Ra acts downstream of type I IFN signaling, and do not contribute to reducing *Ifnb* levels other than by reducing overall bacteria burden. And expected, infected B6.*Sst1*^{S}*Il1rn*$^{+/-}$ mice had greater IL-1 bioactivity than B6.*Sst1* (Figure 2.11A). Although we have repeatedly observed reduced IL-1 bioactivity in the lungs of infected B6.*Sst1*^{S} mice as compared to wild-type B6 mice,

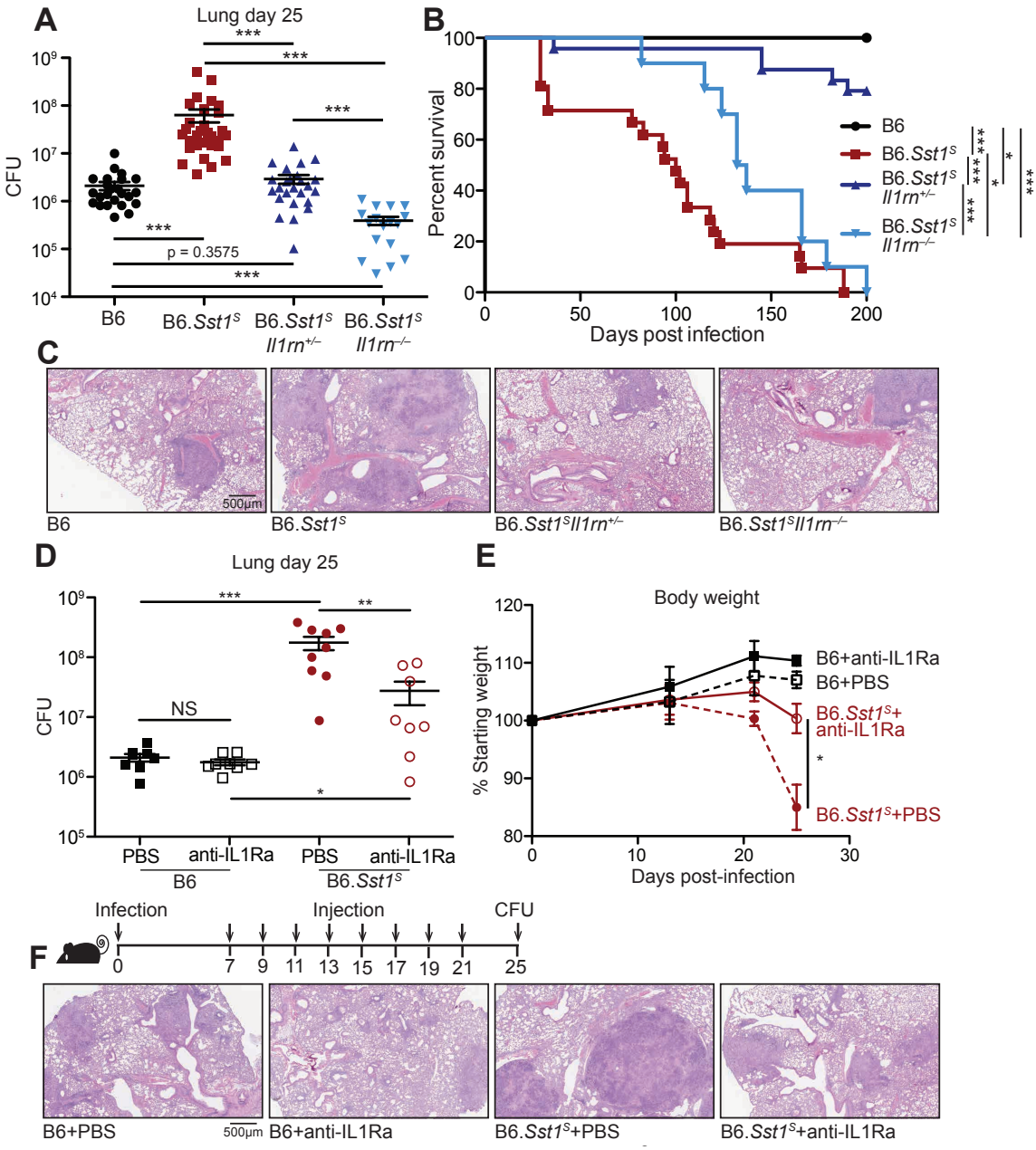

Figure 2.9 | Inhibition of IL-1Ra rescues the susceptibility of B6.*Sst1*^{S} mice. A-C, *Mtb*-infected mice were measured for (A) bacterial burdens in the lungs at day 25, (B) survival, or (C) lung sections were stained with hematoxylin and eosin (H&E) for histology. D-F, *Mtb*-infected mice were treated with anti-IL1Ra antibody or PBS and (D) lung bacterial burdens were measured at day 25, or (F) day 25 lung sections were stained with H&E, or (E) body weights were recorded over time. Combined results of four (A) or two independent experiments (B). C, D-F, representative results of two experiments. For B, B6, n = 17; B6.*Sst1*^{S}, n = 21; B6.*Sst1*^{S}*Il1rn*$^{+/-}$, n = 24; B6.*Sst1*^{S}*Il1rn*$^{-/-}$, n = 10. All were bred in-house, and all except B6 and B6.*Sst1*^{S} were littermates (A-C); B6.*Sst1*^{S} were bred in-house (D-F). Error bars are SEM. Analyzed with two-ended Mann-Whitney test (A, D, E) or Log-rank (Mantel-Cox) test (B). Asterisk, $p \leq 0.05$; two asterisks, $p \leq 0.01$;

this observation appears to be very sensitive to input dose. Our time course data (Figure 2.8) suggest there may be a limited window for observing reduced IL-1 bioactivity, such

that when sampled too early, the sensitivity of the IL-1 reporter cells is insufficient to detect a signal above background. Nevertheless, low levels of IL-1 may provide important functional protection. However, when we sample later, after CFU increases drive higher and detectable IL-1 levels, the infection often appears to have progressed too far to observe the phenotype. It is also difficult to consistently infect mice by aerosol route to be within a narrow range (11-35 CFU/mouse), and because *Mtb* grows so slowly we cannot determine the input dose early enough to adjust the endpoint accordingly. Importantly, we are able to consistently and completely block the responses observed in the IL-1 bioassay with anti-IL-1R antibody (for example see Figure 2.6C). Thus, we believe that the enhanced response of the bioassay is truly reflective of IL-1 activity in

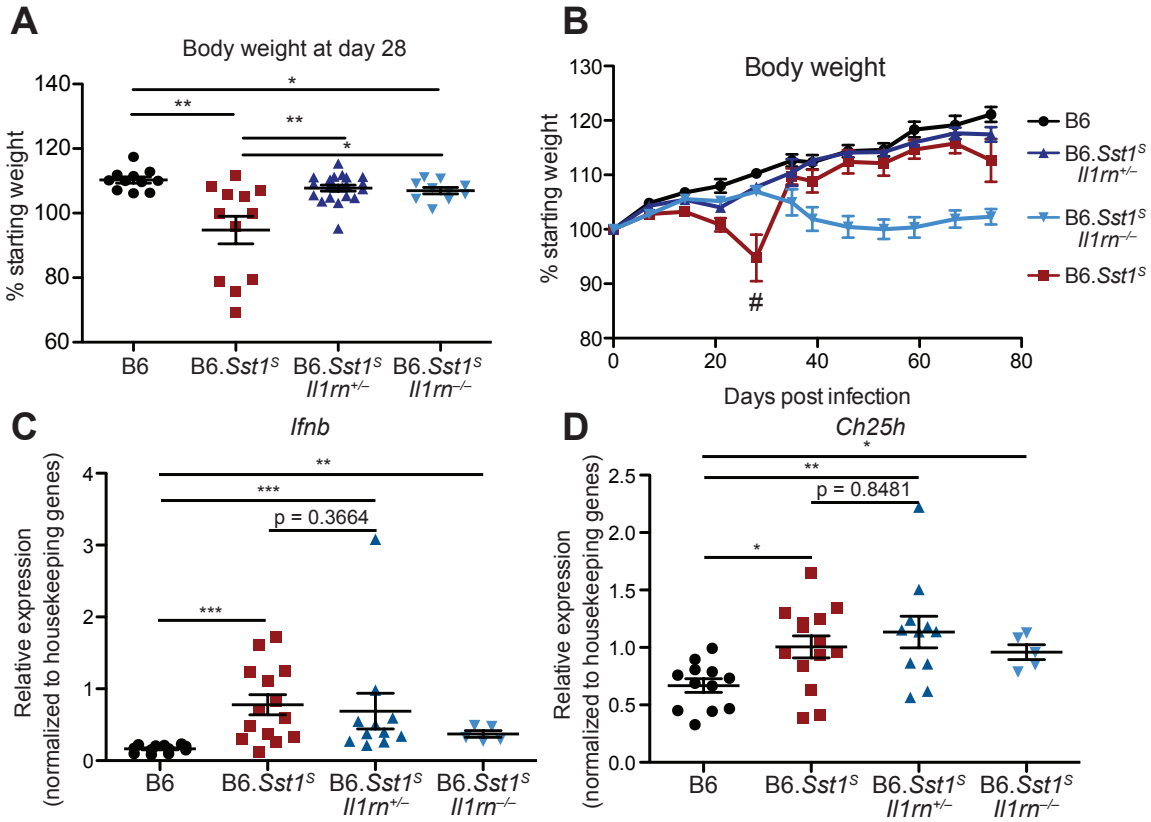

Figure 2.10 | B6.*Sst1*^{S} mice with homozygous or heterozygous *Il1rn* deletion are more resistant than B6.*Sst1*^{S} mice downstream of type I IFN signaling. A-B, Body weights on day 28 (A) or monitored over time (B). # indicates where 4 mice succumbed to the disease. C-D, RTqPCR measuring the amount of *Ifnb* (C) and *Ch25h* (D) in lungs of *Mtb*-infected mice sampled at 25 days post-infection. A, C-D, combined results from 2 independent experiments. B, representative result from 2 independent experiments. All were bred in-house and all except B6 and B6.*Sst1*^{S} were littermates (A-D). Error bars are SEM. Analyzed with two-ended Mann-Whitney test. Asterisk, $p \leq 0.05$; two asterisks, $p \leq 0.01$; three asterisks, $p \leq 0.001$.

the lung. Furthermore, our findings for the role for excess IL-1Ra (and thus decreased IL-1) in the susceptibility of B6.*Sst1*^{S} mice is supported by multiple other lines of evidence, including genetic deletion and antibody-based neutralization of IL-1Ra. Nevertheless, it is formally possible that the type I IFN signaling-dependent susceptibility in the B6.*Sst1*^{S} mice are not the direct result of reduced IL-1 signaling, but enhanced IL-1 signaling through the loss of *Il1rn* in this context provides dominant protection. We think our observations — while not straightforward — are actually very important and help reveal

some of the complexities of the IL-1 response. In fact, we believe that understanding why high levels of bioactive IL-1 are not always protective is a key question for future investigation. To examine whether deletion of IL-1Ra can rescue susceptibility in other models of type I IFN-driven disease, we injected mice with ADU-S100, a STING agonist[122]. Wild-type mice treated with ADU-S100 exhibited significantly greater bacteria burden in their lungs compared to those that received vehicle control (Figure 2.11B), but *Il1rn*$^{+/-}$ had similar increase in bacteria burden. It is not clear why *Il1rn* deficiency does not protect against ADU-S100 treatment, but it may be that ADU-S100 treatment induced excessive type I IFN response that overwhelmed whatever protection heterozygous deletion of *Il1rn* may have offered. Further optimization may reveal protective effects of IL-1Ra in the ADU-S100 model as well.

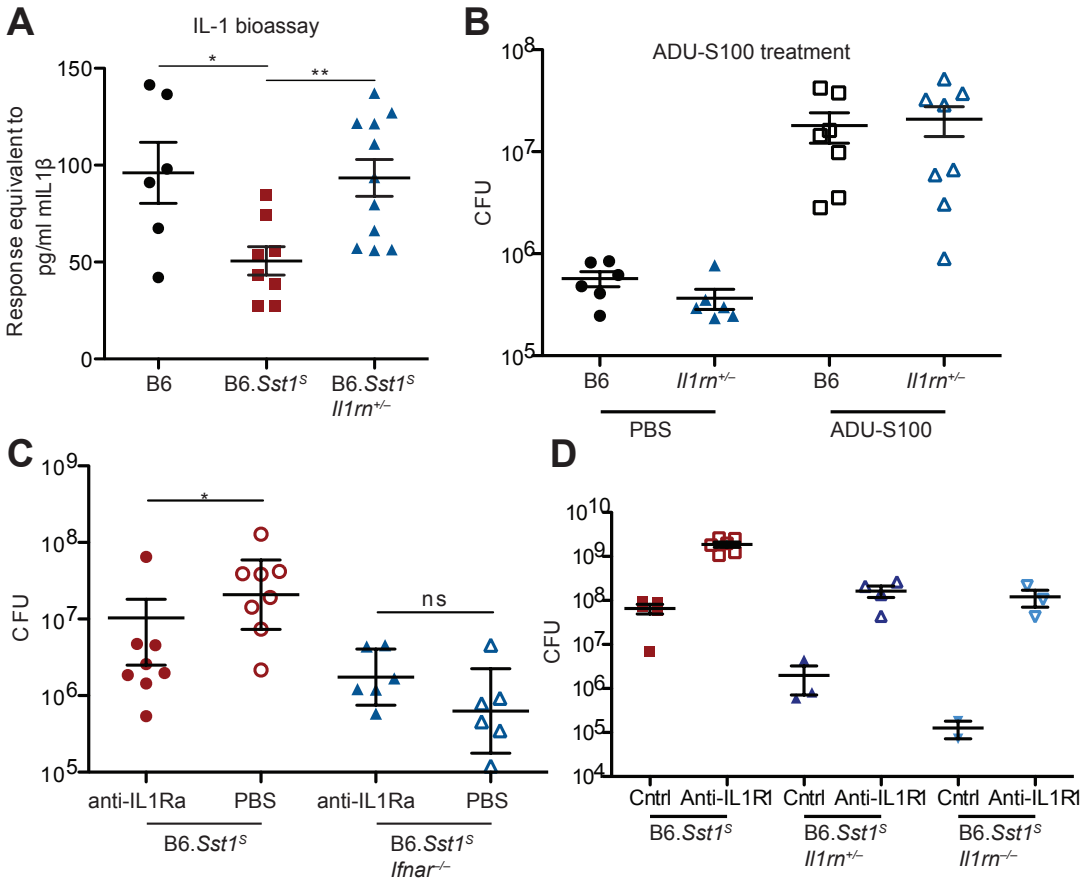

Figure 2.11 | Deletion of *Il1rn* protects B6.*Sst1*^{S} mice downstream of type I IFN signaling, by increasing IL-1 bioactivity. A, IL-1 bioactivity in lung lysates of mice infected with *Mtb* was measured using reporter cells. Samples were collected at 21 days-post infection. B, Mice infected with *Mtb* were treated with ADU-S100 intraperitoneally (50μg/mouse, every 2 days for 8 injections) starting 1st day post-infection. At 25 days post-infections the lungs were collected for CFU. C, Mice infected with *Mtb* were treated with anti-IL1Ra antibody or PBS starting 3 days post-infection. Mice received 500μg each every 2 days (11 injections total). At 25 days post-infection lungs were harvested for measuring bacterial burden. D, Mice infected with *Mtb* were treated with anti-IL1R1 antibody or isotype control starting 7 days post-infection, 200μg/mouse every 3 days. At 25 days post-infection lungs were harvested for measuring bacterial burden. B–D, All mice were bred in-house. B6.*Sst1*^{S}*Il1rn*$^{+/-}$ and B6.*Sst1*^{S}*Il1rn*$^{-/-}$ mice in (A) and (C), and B6 and *Il1rn*$^{+/-}$ in (B) were all littermates. B6 mice in (A) were purchased. Error bars are SEM. Analyzed with two-ended Mann-Whitney test. Asterisk, $p \leq 0.05$; two asterisks, $p \leq 0.01$; three asterisks, $p \leq 0.001$.

The dramatic protective effects of even partial reductions in IL-1Ra in B6.*Sst1*^{S} mice suggested that IL-1Ra might be a suitable target for host-directed therapy during *Mtb* infection. To test this idea, we treated infected B6.*Sst1*^{S} mice with an anti-IL-1Ra antibody[123] to block IL-1Ra and restore IL-1 signaling (Figure 2.9D). B6.*Sst1*^{S} mice that received the antibody for two weeks had significantly lower bacterial burdens in their lungs as compared to those receiving a control injection of PBS. In addition, mice treated with anti-IL-1Ra antibody retained significantly more body weight than their control counterparts (Figure 2.9E), and exhibited reduced lung lesions (Figure 2.9F), suggesting that the treatment did not cause detrimental inflammation. Type I IFN-signaling drives expression of hundreds of genes[10]. To show that IL-1Ra acts downstream of type I IFN-signaling we neutralized IL-1Ra in B6.*Sst1*^{S}*Ifnar*$^{-/-}$ mice (Figure 2.11C). As expected, bacteria burden was similar between B6.*Sst1*^{S}*Ifnar*$^{-/-}$ mice treated with the anti-IL1Ra antibody and control, whereas antibody-treated B6.*Sst1*^{S} mice exhibited reduced CFU. Control of the infection in *Il1rn*-deficient mice depended on IL-1R signaling, as mice treated with an anti-IL1R1 antibody exhibited higher bacterial burden than *Il1rn*-deficient mice that did not (Figure 2.11D). Although these data strongly imply that protection afforded by the loss of IL-1Ra in B6.*Sst1*^{S} mice are mediated by enhanced IL-1 signaling, we acknowledge the unlikely but formal possibilities that loss of IL-1Ra protects the B6.*Sst1*^{S} mice via a mechanism unrelated to IL-1 and that neutralization of IL-1 signaling dominantly overcomes this protection. Overall these data indicate that genetic or antibody-mediated reduction of IL-1Ra rescues the type I IFN-driven susceptibility in B6.*Sst1*^{S} mice without overt detrimental immunopathology.

2.4 Discussion

There is increasing interest in developing host-directed therapeutics for *Mtb*[101]. Although such therapeutics have not yet proven to be curative, and may thus be unlikely to replace antibiotics, host-directed therapies may offer some advantages in specific scenarios. For example, host-directed therapy could serve as an adjunct to antibiotic regimens in multidrug-resistant or extensively-drug resistant tuberculosis, where mortality is at 20%[124,125]. It may also be more difficult for *Mtb* strains to evolve resistance to a host-directed therapy, an important consideration given the increasing prevalence of multi-drug resistant *Mtb* strains. In addition, our results, along with those of others[96,97], suggest a strategy in which latently infected individuals could be screened for the type I IFN signature known to be a strong predictor of progression to active TB. If the type I IFN signature in these individuals could then be reset or reversed by a host-directed therapy targeting IL-1Ra, or other host factors[22], then it might be possible to prevent progression to active TB — the transmissible form of the disease — without the prolonged (6-month) antibiotic treatments that are associated with poor compliance and emergence of drug-resistant strains. This therapeutic strategy, though only presented here as a proof-of-concept in animals, may help focus treatments on those who are likely to transmit among the billions of latently infected persons. The success of such a strategy would not necessarily require microbiological cure, but would depend on identification of highly potent master-regulators of interferon-driven TB disease that can be readily targeted clinically in TB endemic areas. Identification of such regulators and development of therapies appropriate for resource-limited settings will require better animal models of interferon-driven TB disease *in vivo*. Our results show that the B6.*Sst1*^{S}

mouse may represent a useful model of IFN-driven TB disease in humans and suggest that therapeutic targeting of IL-1Ra may be a potent strategy for reversing type I IFN-driven susceptibility *in vivo*.

Chapter 3: Identifying and Validating the Causative Gene within the *Sst1* Locus

3.1 Introduction

Mycobacterium tuberculosis remains the worldwide leading cause of death from a single pathogen, resulting in the death of 1.6 million people in 2017 alone[1]. Infection by *Mtb* in most immunocompetent individuals are asymptomatic; however, 10% of infected individuals can progress to active and transmissible tuberculosis (TB) disease[6]. Like many human diseases, complex host genetics contribute to disease outcomes during *Mtb* infection[7]. Recently there has been significant interest in the role of type I IFNs during *Mtb* infections (extensively reviewed elsewhere[13,15]). Multiple publications have reported that type I IFN expression signature correlates with active TB disease[98,99] or progression to active disease in human patients[13,15,96,97]. To better understand the mechanisms of susceptibility mediated by type I IFN signaling, many groups have used the mouse model of *Mtb* infection (summarized in[13]). However, the most commonly used mouse strain, C57BL/6 (B6), exhibits low type I IFN responses and resistance to many bacterial infections, including *Mtb*. By contrast, B6 mice carrying the susceptible allele of the *Super susceptibility to tuberculosis 1* locus ($Sst1^S$) exhibit enhanced susceptibility to *Mtb* infection[2,3,92], and we have previously reported that this susceptibility is driven by type I IFN signaling. B6.$Sst1^S$ mice are also susceptible to other bacterial pathogens such as *Listeria monocytogenes* and *Chlamydia pneumoniae*[92,104]. While the robust susceptibility of B6.$Sst1^S$ mice makes them an attractive model for studying type I IFN responses during *Mtb* infection, the exact mechanism of how *Sst1* locus controls type I IFN signaling is unknown. It is therefore unclear whether other pathways contribute to the susceptibility in these congenic mice.

The *Sst1* locus in B6.$Sst1^S$ encompasses about 10M base pairs of chromosome 1, a region that contains ~50 genes. Pan *et al* identified the gene *Ipr1* (also known as *Sp110*) as the candidate gene responsible for the susceptibility of $Sst1^S$ mice by comparing the expression levels of genes in the *Sst1* interval in resistant (B6) versus susceptible (C3H) mice[2]. Mice carrying the $Sst1^S$ allele lack expression of *Sp110* at both the transcript and protein levels. Targeted mutation of *Sp110* in B6 mice was not performed, however transgenic expression of *Sp110* in $Sst1^S$ mice partially reversed susceptibility of the mice to *Mtb* and *L. monocytogenes*. Null mutations of human SP110 are associated with VODI (hepatic veno-occlusive disease with immunodeficiency syndrome, OMIM 235550), but not mycobacterial diseases[126–129]. GWAS studies have associated SNPs of SP110 with susceptibility to TB, though not consistently so across different ethnic groups and there are no known mechanisms for these SNPs[130–136].

SP110 is a part of the Speckled Protein (SP) family of nuclear proteins, consisting of SP100, SP110 and SP140 (and SP140L in humans only)[137]. All SP genes are linked in a cluster in both mouse and human genomes. All members of the SP100 family in both mouse and human have an N-terminal SP100 domain which is related to CARD domains involved in protein-protein interactions, as well as a DNA-binding SAND domain[138]. These features are also shared with AIRE, a well-known transcription regulator. All human full length SP family proteins and mouse SP140 also include a plant homeobox domain (PHD) and a bromodomain (BRD)[137], whereas mouse SP100 only has a BRD and the most abundant isoform of human SP110 (SP110B) and mouse SP110 are truncated

after the SAND[139]. All SP family proteins are inducible by interferons in a variety of cell lines, and co-localize with PML within the ND10/PML-nuclear bodies (PML-NBs)[95,137,140,141]. PML-NBs have been implicated in a variety of cell processes such as apoptosis, cell cycle, DNA damage response, senescence, and cell-intrinsic antiviral responses[94]. Based on their domain structures and association with the PML-NBs, the SP family members are thought to also be transcriptional regulators. Full-length human SP110C can act as a coactivator of retinoic acid receptor-mediated transcription[137] whereas the truncated SP110B instead acts as an inhibitor of RARα signaling[139]. Viruses also target SP family members to alter expression of host and viral genes. Hepatitis C Virus core protein sequesters SP110B from the nucleus, which promotes RARα-dependent signaling in response to ATRA[139]. Epstein-Barr Virus SM protein interacts with SP110B to accumulate mRNA and lytic phase proteins[142]. Hepatitis B Virus HBx protein binds to full-length SP110C to separate it from PML-NBs[143]. HBx-SP110C complex alters expression of a large number of host genes by recruiting p300 or HDAC1 to their promoters[143]. Interestingly, Sengupta *et al* found that siRNA-mediated depletion of SP110 led to upregulation of type I IFN-stimulated genes (ISGs) and a concurrent ISGF3-dependent decrease in viral replication, reminiscent of our previous results with B6.*Sst1*^{S} mice (see Chapter 2). Overexpression of SP110B in human macrophage cell lines is reported to protect against IFNγ-induced apoptosis by limiting TNFα production[144,145], but overexpression of mouse SP110 appears to result in resistance against an attenuated strain of *Mtb* via increased apoptosis, ER stress, and altered mRNA and miRNA expression profiles[140,146,147]. Clearly there is a need for better understanding of the complex and apparently pleiotropic role of Sp110 using an animal model.

Mouse *Sp110* is adjacent to a highly repetitive homogenous staining region of chromosome 1 that remains poorly assembled in the most recent genome assembly due to the presence of numerous near-identical repeats of SP110-like sequences[148]. While all these repeated Sp110-like sequences appear to be pseudogenes and are not translated[2,148], their presence has complicated the generation of specific *Sp110*-gene targeted mice using conventional targeting vectors. Therefore, the hypothesis that the susceptibility phenotype in *Sst1*^{S} is due to the loss of Sp110 has not been fully tested. Using CRISPR/Cas9 we were able to generate *Sp110*$^{-/-}$ mice on the B6 background. Surprisingly we found that *Sp110*$^{-/-}$ mice did not phenocopy the susceptibility of *Sst1*^{S} mice to *Mtb* infection *in vivo*. Instead, we found that B6.*Sst1*^{S} also lack expression of *Sp140*, a homolog of Sp110. To test whether loss of *Sp140* might account for the susceptibility of *Sst1*^{S} mice to bacterial infection, we generated *Sp140*$^{-/-}$ mice. We found these mice were similarly susceptible as B6.*Sst1*^{S} mice to *Mtb, L. monocytogenes* and another intracellular pathogen *Legionella pneumophila*. Similar to our previous findings with B6.*Sst1*^{S} mice (see Chapter 2), the susceptibility of *Sp140*$^{-/-}$ mice to *Mtb* and *Lp* was dependent on type I IFN signaling. Our results suggest that loss of *Sp140* explains the susceptibility associated with the *Sst1*^{S} allele. These data further indicate that *Sp140* may be a novel negative regulator of type I IFN responses during intracellular bacterial infections.

3.2 *Sp110*$^{-/-}$ mice are not susceptible to *Mycobacterium tuberculosis*

Previous work proposed that *Sp110* is the causative gene within the *Sst1* locus that accounts for the effect of this locus on susceptibility to bacterial infections[2]. Bone marrow-derived macrophages (BMMs) from B6. *Sst1*^{S} mice lack expression of *Sp110* transcripts and proteins as previously described (Figure 3.1A, B). Using CRISPR/Cas9

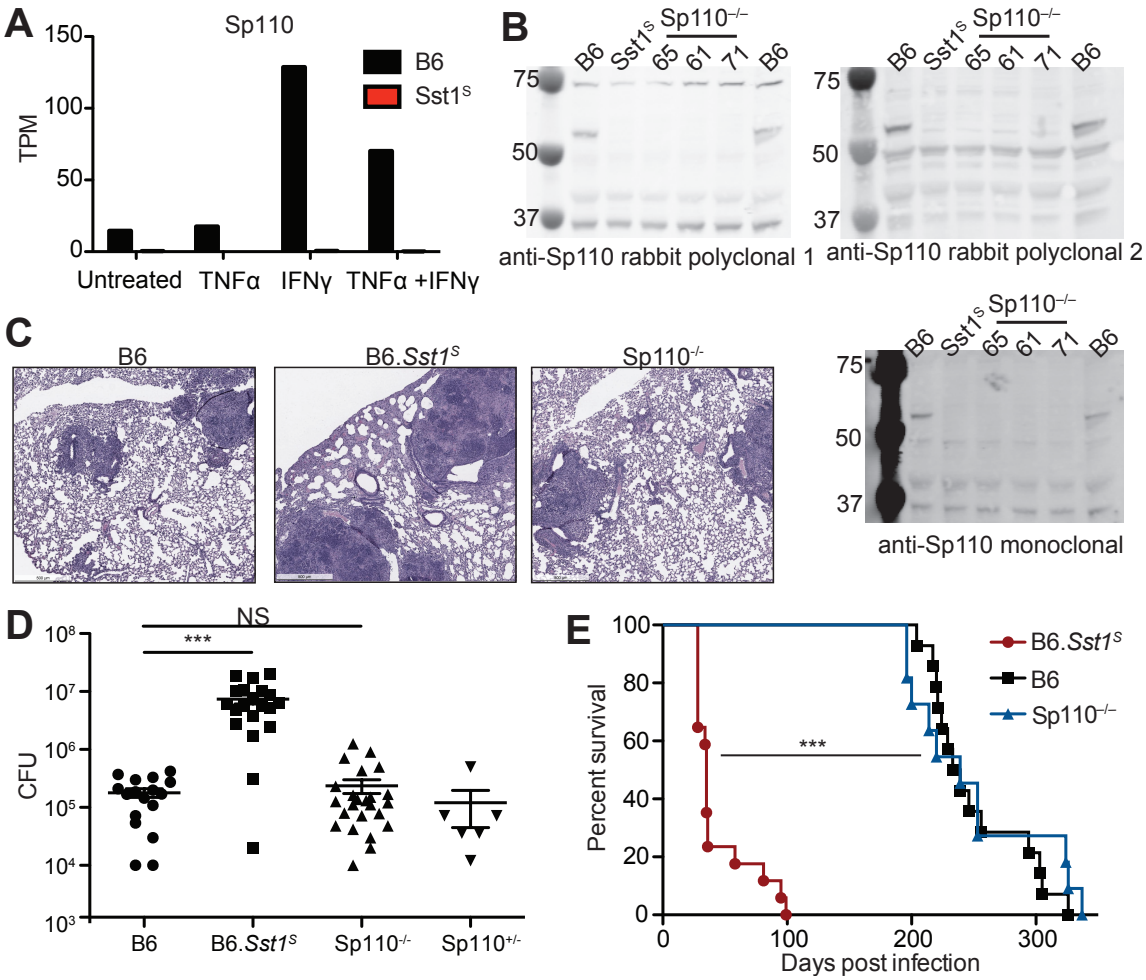

Figure 3.1 | *Sp110*$^{-/-}$ mice are not susceptible to *Mtb* infections. A, BMDMs were treated with the stimuli as indicated for 24hours and processed for RNAseq. TPM, transcripts per million. B, BMDMs were treated with 10U/ml of IFNγ for 24hours and cells were lysed with RIPA buffer. 5μg of total protein was loaded on each lane, and immunoblot was performed with different antibodies as shown. Individual membranes were imaged separately. C-D, Lung of mice infected with *Mtb* were stained with hematoxylin and eosin (H&E) for histology (C) and measured for lung CFU (D). E, Mice infected with *Mtb* were monitored for survival. All but B6 were bred in-house, and *Sp110*$^{-/-}$ and *Sp110*$^{+/-}$ in (D) were littermates. Error bars are SEM. Analyzed with two-ended Mann-Whitney test (D) or Log-rank (Mantel-Cox) test (E). Asterisk, $p \leq 0.05$; two asterisks, $p \leq 0.01$; three asterisks, $p \leq 0.001$.

we targeted exon 3 of *Sp110* to generate *Sp110*$^{-/-}$ mice on the B6 background (Figure 3.2). As expected, the three independent founders of *Sp110*$^{-/-}$ all lacked expression of *Sp110*, verified using three different antibodies (Figure 3.1B). *Sp110*$^{-/-}$ mice are viable, and are born at normal Mendelian ratios and litter sizes. Surprisingly, when aerosol infected with a low-dose of *Mtb*, *Sp110*$^{-/-}$ mice did not phenocopy the susceptibility

observed in B6.*Sst1*^{S} mice (Figure 3.1A–C). At day 25 post-infection, *Sp110*$^{-/-}$ lungs resembled those of B6 mice (Figure 3.1C) and had lower bacterial burdens than the B6.*Sst1*^{S} mice, similar to both the B6 and *Sp110*$^{+/-}$ littermates (Figure 3.1D). Likewise, *Sp110*$^{-/-}$ mice survived to a similar time point as the B6 mice, and both were significantly more resistant than the B6.*Sst1*^{S} mice (Figure 3.1E). Thus, contrary to what has been previously proposed[2], our result indicate that the loss of *Sp110* is not sufficient to replicate the susceptibility associated the *Sst1* locus.

The guide sequence used to target exon 3 of *Sp110* also targets an unknown number of pseudogene copies of *Sp110*-like genes located within the unassembled adjacent HSR region of mouse chromosome 1. Thus we expect that additional off-target

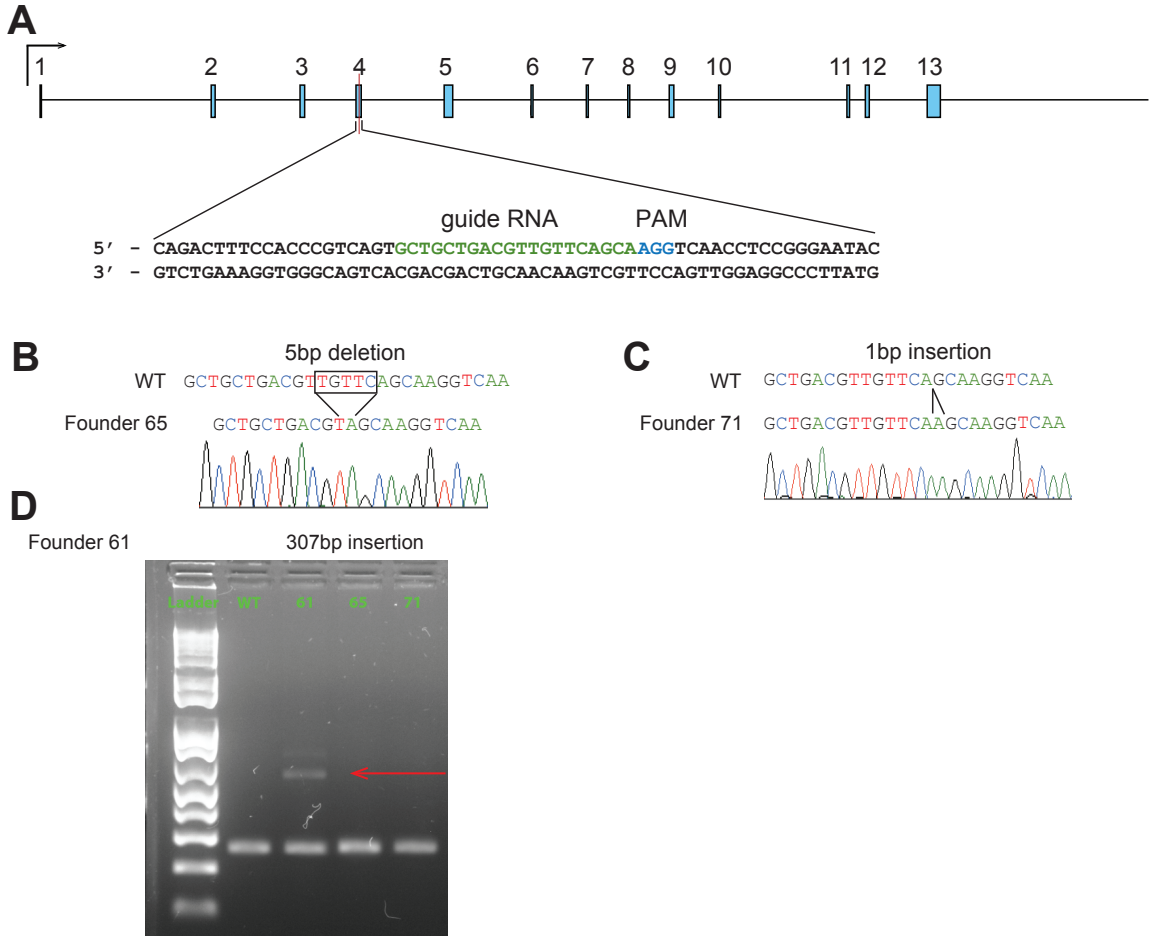

Figure 3.2 | CRISPR/Cas9 targeting strategy for *Sp110*$^{-/-}$ mice. A, Mouse *Sp110* gene. Guide RNA sequence for CRISPR/Cas9 targeting and protospacer-adjascent motif (PAM) are indicated. B-D, The *Sp110* locus in wildtype (WT) and three independent lines. B-C, showing homozygotes identified by sequencing, D, showing a heterozygote by PCR products separated on an agarose gel. Arrow indicates the mutant band.

mutations were also present in our mutant mice. However, these off-target mutations should differ among the three founder mice. In addition, since all the founders at a minimum lack *Sp110*, additional mutations should not affect our conclusion that *Sp110* is not required for resistance to *Mtb*.

3.3 B6.*Sst1*^{S} mice also lack expression of *Sp140*

Since Sp110 deficiency does not seem to account for the *Sst1*^{S} phenotype, we examined genes found within the *Sst1* locus looking for any differences in expression between B6 and B6.*Sst1*^{S} cells. Interestingly, *Sp140*, a homolog of *Sp110*, also has

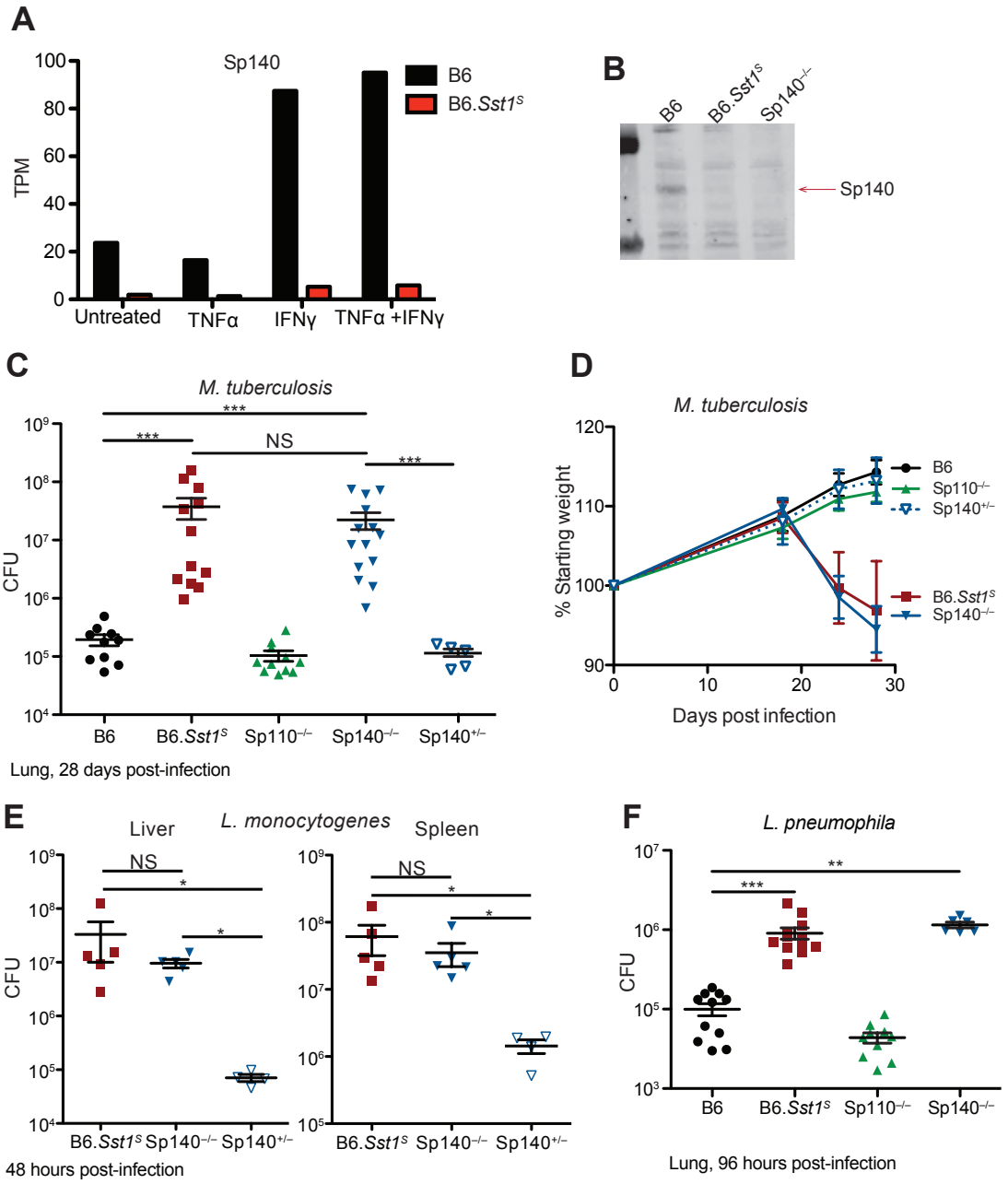

Figure 3.3 | *Sp140*$^{-/-}$ mice are susceptible to bacterial pathogens. A, BMDMs were treated with stimuli as indicated for 24 hours, then processed for RNAseq. TPM, transcript per million. B, BMDMs of indicated genotypes were lysed for protein, and equal amounts were loaded for immunoblot. C-D, Mice were infected with *Mtb* and measured for lung CFU at 28 days post-infection (C) or body weight over the course of infection (D). E, Mice were infected with *L. monocytogenes* and tissues were measured for CFU at 48 hours post-infection. F, Mice were infected with *L. pneumophila* and lungs were measured for CFU at 96 hours post-infection. All mice were bred in-house. Analyzed with two-ended Mann-Whitney test (C-F). Asterisk, $p \leq 0.05$; two asterisks, $p \leq 0.01$; three asterisks, $p \leq 0.001$.

reduced expression in B6.*Sst1*^{S} cells compared to B6 cells (Figure 3.3A). Mouse SP140 includes SP100, SAND, PHD and BRD, and is reported to regulate transcription[149]. It also localizes to the PML-NB, and has been implicated in antiviral responses[95,150]. Human SP140 is associated with chronic lymphocytic leukemia (CLL), Crohn's disease and multiple sclerosis (MS)[151–155]. As previously reported, we observed that expression of *Sp140* is inducible by IFNγ treatment[149]. Immunoblot confirms that B6.*Sst1*^{S} cells do not express Sp140 protein (Figure 3.3B). We generated *Sp140*$^{-/-}$ mice by CRISPR/Cas9 on the B6 background (Figure 3.4A-B). These mice lack the expression of Sp140 protein (Figure 3.2B) but retain the expression of Sp110 protein (Figure 3.4C). Like *Sp110*$^{-/-}$ mice, *Sp140*$^{-/-}$ mice are viable, fertile and born at the expected Mendelian ratios. When infected with *Mtb*, *Sp140*$^{-/-}$ mice exhibited high bacterial burdens in their lungs, similar to B6.*Sst1*^{S} mice but significantly greater than B6, *Sp110*$^{-/-}$ and *Sp140*$^{+/-}$ mice at day 28 post-infection (Figure 3.3C). The increased susceptibility of *Sp140*$^{-/-}$ mice was

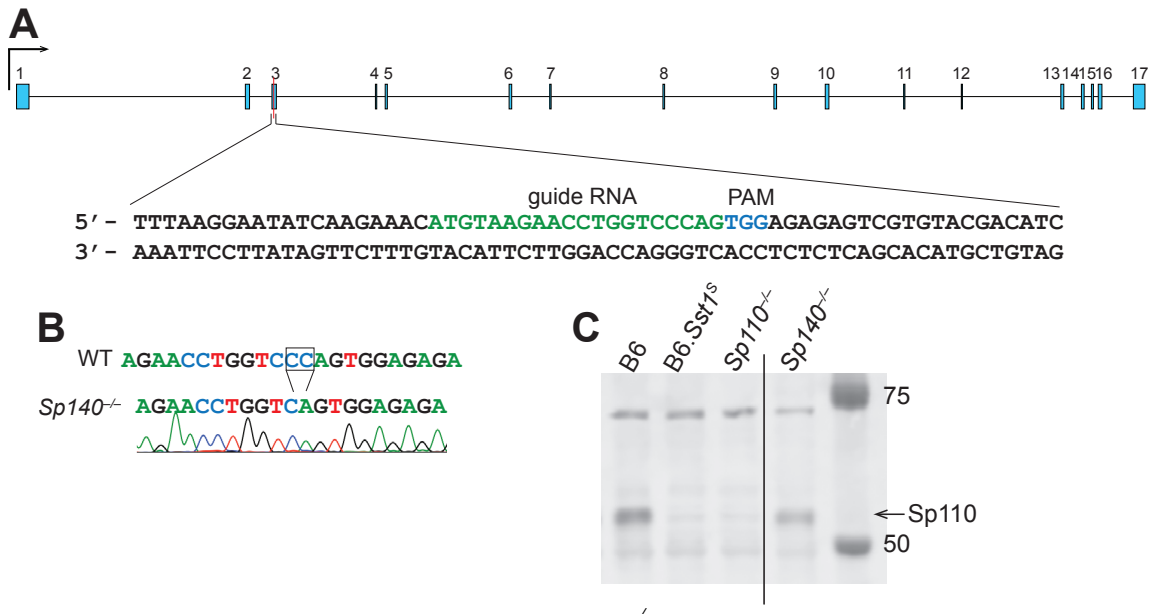

Figure 3.4 CRISPR/Cas9 targeting strategy for *Sp140*$^{-/-}$ and validation of founder. a) Mouse *Sp140* gene. Guide RNA sequence for CRISPR/Cas9 targeting and protospacer-adjascent motif (PAM) are indicated. b) The *Sp140* locus in wildtype (WT) and *Sp140*$^{-/-}$. c) Immunoblot for Sp110 using BMDMs from mice of the indicated genotypes. Intervening lanes have been removed for clarity (indicated by line in the image).

accompanied by significant weight loss, again phenocoping the B6.*Sst1*^{S} mice (Figure 3.3D). Previous reports have shown that in addition to *Mtb,* the *Sst1* locus also controls immune response against other intracellular bacterial pathogens such as *L. monocytogenes* and *C. pneumoniae* [92,104,156]. Therefore we infected Sp140$^{-/-}$ and B6.*Sst1*^{S} mice with *L. monocytogenes.* As previously reported[92,156], B6.*Sst1*^{S} mice were more susceptible to *L. monocytogenes,* and *Sp140*$^{-/-}$ mice had similarly increased bacterial burden in their liver and spleen as compared to the *Sp140*$^{+/-}$ control mice (Figure 3.3E). We also found that both B6.*Sst1*^{S} and *Sp140*$^{-/-}$ mice were more susceptible to the intracellular Gram-negative bacterium *Legionella pneumophila*, as compared to the B6 and Sp110$^{-/-}$ mice (Figure 3.3F). Collectively our results demonstrate that B6.*Sst1*^{S} mice lack expression of Sp140, and that the loss of Sp140 appears necessary and sufficient to

phenocopy the broad susceptibility of *Sst1*^{S} mice to mycobacterial, Gram-positive, and Gram-negative bacterial infections.

3.4 *Sp140*$^{-/-}$ mice have elevated *Ifnb* and ISG transcripts similar to B6.*Sst1*^{S}

B6.*Sst1*^{S} BMMs expressed elevated levels of *Ifnb* and other ISG transcripts when stimulated with TNFα (see Figure 2.2). Compared to B6 or *Sp110*$^{-/-}$ macrophages, *Sp140*$^{-/-}$ macrophages also exhibit enhanced induction of *Ifnb* and ISGs (e.g., *Ifit3*, *Gbp4*, *Gbp5*) when treated with TNFα (Fig. 3.5A). Like previously described for B6.*Sst1*^{S} mice, we also observed elevated *Ifnb* and *Il1rn* transcripts in the lungs of *Mtb*-infected *Sp140*$^{-/-}$ but not *Sp110*$^{-/-}$ mice (Fig. 3.5B). Our results suggest that similar to the B6.*Sst1*^{S} mice, *Sp140*$^{-/-}$ mice overproduce type I IFNs upon stimulation.

3.5 Susceptibility to *Mycobacterium tuberculosis* infections in *Sp140*$^{-/-}$ mice is dependent on type I IFN signaling.

The susceptibility of B6.*Sst1*^{S} mice to *Mtb* is dependent on type I IFN signaling, as described in Chapter 2. To test whether this is also true of *Sp140*$^{-/-}$ mice, we treated

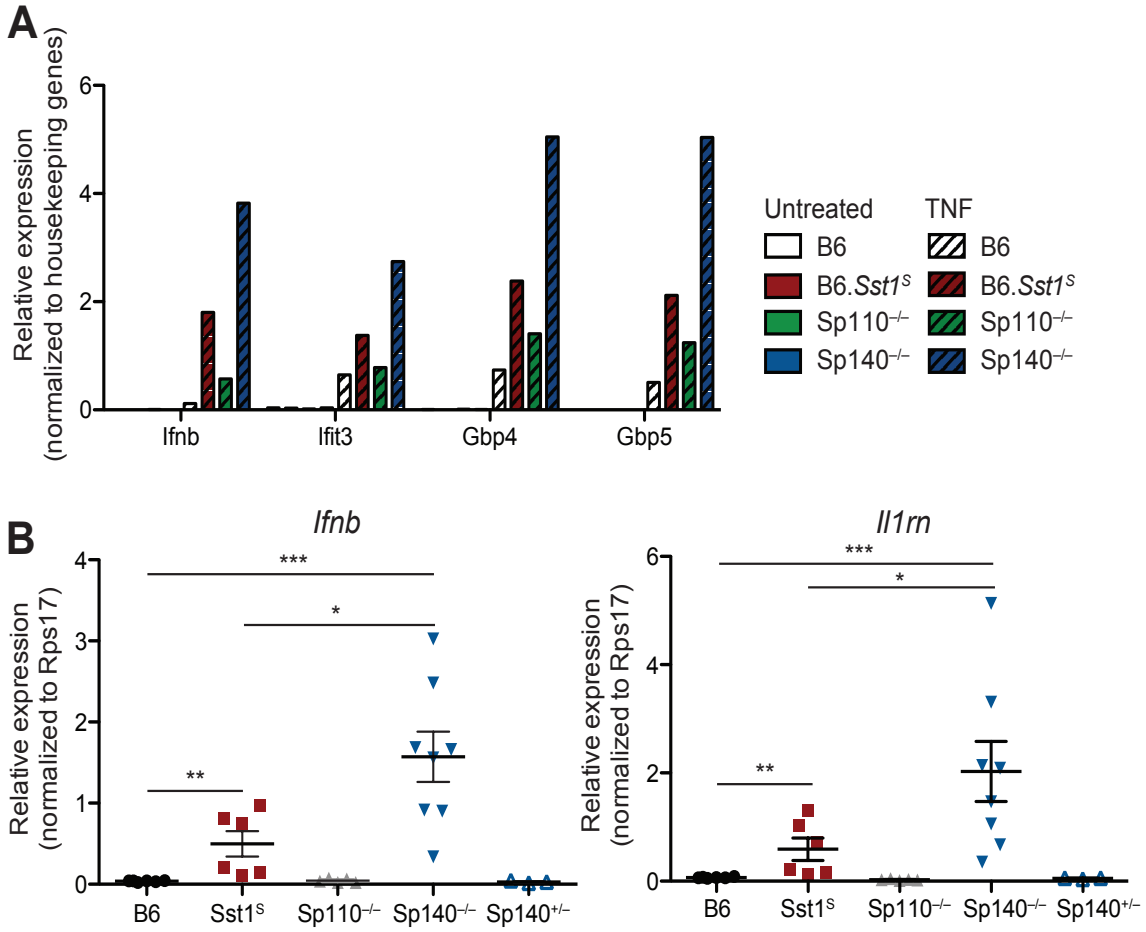

Figure 3.5 | *Sp140*$^{-/-}$ macrophages and mice have elevated transcripts of *Ifnb* and ISGs. A, BMDMs were left untreated or TNFα for 24 hours, total RNA were used for RT-qPCR. B, Mice were infected with *Mtb* and at 28 days post-infection lungs were processed for total RNA, which were used for RT-qPCR. Analyzed with two-ended Mann-Whitney test (C-F). Asterisk, $p \leq 0.05$; two asterisks, $p \leq 0.01$; three asterisks, $p \leq 0.001$.

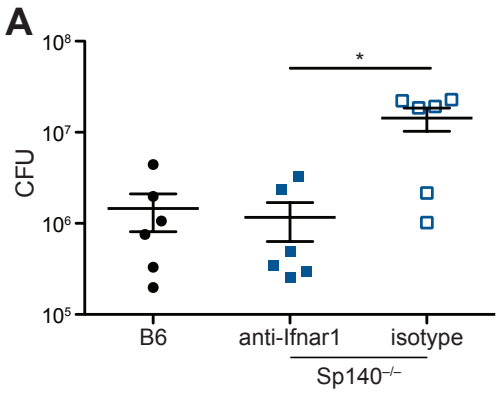

Figure 3.6 | Susceptibility of *Sp140*$^{-/-}$ mice to *Mtb* is dependent on type I IFN signaling. A, Mice were infected with *Mtb* and treated with either IFNAR1-blocking antibody or isotype control starting 7 days post-infection as illustrated. At 25 days post-infection lungs were harvested to enumerate CFU. All mice were bred in-house. Analyzed with two-ended Mann-Whitney test. Asterisk, $p \leq 0.05$; two asterisks, $p \leq 0.01$; three asterisks, $p \leq 0.001$.

Sp140$^{-/-}$ mice infected with *Mtb* with a blocking antibody against IFNAR1. Compared to those that only received isotype control, *Sp140*$^{-/-}$ mice that received the anti-IFNAR1 antibody had reduced bacterial burdens in their lungs (Figure 3.6A). These results suggest that loss of Sp140 is sufficient to cause the type I IFN-driven susceptibility to *Mtb* infection as observed in B6.*Sst1*^{S} mice. We are currently breeding *Sp140*$^{-/-}$*Ifnar*$^{-/-}$ mice to confirm these results in *Mtb, L. monocytogenes* and *L. pneumophila* infections.

3.6 Discussion

Here I report the generation and characterization of the first *Sp110*$^{-/-}$ and *Sp140*$^{-/-}$ mice on the B6 background, and show that contrary to expectations, *Sp110*$^{-/-}$ mice are not susceptible to *Mtb* infections. I further show that B6.*Sst1*^{S} mice also lack the expression of *Sp140*, a homolog of Sp110. By generation of *Sp140*$^{-/-}$ mice, I show that loss of *Sp140* is sufficient to phenocopy the susceptibility of B6.*Sst1*^{S} mice to various intracellular bacterial pathogens, including *Mtb.* Similar to B6.*Sst1*^{S} mice, the susceptibility of *Sp140*$^{-/-}$ mice appears to be driven by exacerbated type I IFN signaling.

It was previously reported that transgenic expression of *Sp110* can enhance the susceptibility of *Sst1*^{S} mice. This result is likely due to some overlap in function between *Sp110* and *Sp140*, such that transgenic overexpression of Sp110 can partially compensate for the loss of *Sp140*. Human SP110 appears to require SP140 expression to localize correctly to PML-NBs in certain cell lines, which might explain the more dominant phenotype of *Sp140*$^{-/-}$[137]. Involvement of human SP140 may also account for some of the previous inconsistencies in correlating human SP110 SNPs and TB disease[130–136]. Polymorphisms in SP140 may explain some of the disparities between studies of different populations. Our results merit a renewed investigation of the roles of human SP110 and SP140 in susceptibility to TB and perhaps other bacterial infections.

An important caveat of my work is that the genetic locus encoding SP100 family members remains incompletely assembled in the mouse genome and thus the entire complement of SP100-family genes remains unknown. Our *Sp140*$^{-/-}$ mice may have off-target mutations within the incompletely assembled region that is actually responsible for the observed susceptibility. *In vitro* complementation is currently ongoing to verify the role of Sp140.

These data suggest Sp140 is a novel negative regulator of type I IFN responses. However the mechanism by which it acts remains unknown. When stimulated with IFNγ, human SP140 co-localized with some, but not all the PML-NBs, suggesting that function of SP140 was location-specific within the nucleus[95]. Like many other proteins in the

PML-NB, Sp140 is SUMOylated, though the effect of this on Sp140 function is unknown[157]. The PHD-BRD cassette of SP140 specifically recognizes unmodified histone 3 tail (H3K4me0)[158], and the PHD also binds to Pin1, another member of the PML-NB that has been shown to control type I IFN-signaling through IRF3 and IRF7[159–161]. Overexpression of SP140 fused with the DNA-binding domain of Gal4 was able to activate expression[149], though siRNA knockdown of SP140 in lymphoblastoid cell lines led to de-repression of many inflammatory cytokines, suggesting that in this context SP140 is a repressor[155]. Sp140 may interact directly with promoter regions and transcription factors as suggested by Mehta *et al*[162], and as proposed for human SP110[144,145] and SP100[163]; or it may indirectly control transcription by modifying chromatin structure, as has been suggested also for SP100[164]. It is possible that Sp140 can function through multiple mechanisms in response to different stimuli. Previous work has also mostly relied on overexpression or siRNA-mediated knockdowns in immortalized cell lines and MEFs. Behavior of Sp140 may differ significantly in primary cells, as well as between cell types that express it *in vivo*. Thus, the *Sp140*$^{-/-}$ mice will hopefully be a valuable tool for better understanding of the function of Sp140 *in vivo* and *ex vivo.*

My results differ from previously published work from Mehta *et al* that proposed Sp140 controls macrophage differentiation and lineage specification[162]. In the *Sp140*$^{-/-}$ macrophages, I see elevated expression of ISGs, instead of generally decreased cytokine responses. These differences may be explained in part by the divergent methodology. Mehta *et al* rely on shRNA and siRNA-based knockdowns throughout their paper, including their mouse model, which may account for many of the differences between the results. As Sp140 may be regulating antiviral responses[150], directly or through association with PML-NB[94], RNAi-based methods that potentially stimulate antiviral sensors may confound the results[165,166].

Here I report that Sp140 is the dominant causal gene within the *Sst1* locus, and demonstrate that *Sp140*$^{-/-}$ mice are susceptible to a variety of bacterial pathogens through a type I IFN-driven mechanism. These mice may be useful in several areas of studies, such as elucidating the role of Sp140 *in vivo*, both at steady state and during pathologies such as CLL, MS and Crohn's disease; and as a model for dissecting the effects of inappropriate type I IFN responses during bacterial infections.

Chapter 4: Questions and Thoughts for the Future

In the following section I will discuss some of the unanswered questions resulting from our findings previous chapters, and potential experiments or approaches that may help address those questions.

4.1 Of mouse models, mechanisms and consistency in TB

To better understand the mechanism of how type I IFNs promote TB disease, many groups have turned to the mouse model with highly variable results. Some groups have found that type I IFN is protective or makes little difference, whereas other groups have identified a host-detrimental function for type I IFN (summarized by [13,15]). As described in Chapter 1 (Introduction), genetic backgrounds of the mice likely contribute significantly to this. B6 mice are a popular background for many knockout strains. However they do not have a strong, detrimental type I IFN response in the lung during *Mtb* infection[29]. Researchers have tried to circumvent this by 1) using the 129 strain of mice (for which fewer genetic tools and knockouts were available in the pre-CRISPR era [footnote[5]]), 2) using a knockout that happens to have a type I IFN-driven disease (our B6.*Sst1*^{S} and *Sp140*$^{-/-}$ mice or the *Tlp2*$^{-/-}$[63]) or 3) inducing an artificial type I IFN response in B6 mice. Intranasal instillation of polyICLC has been one approach to artificially induce type I IFN that has been used in several studies[29,66], though its mechanism of action and relevance to a natural *Mtb* infection remains unknown. In addition to the elevated type I IFN response, there are likely other immunological differences in 129, B6.*Sst1*^{S} and *Sp140*$^{-/-}$ mice. This raises the question whether any of the type I IFN-dependent mechanisms discovered using one of these models would easily translate to another, and whether any of this will have relevance to the human disease. For example, Mayer-Barber *et al* demonstrated that lipid mediators are an important negative regulator of type I IFN responses downstream of IL-1 signaling using the polyICLC-B6 model[65]. However, interventions that worked in this model did not work in the susceptible C3H/HeJ mice[65] (from which the susceptible *Sst1*^{S} allele derives from), and we did not observe a decrease in PGE2 levels in the B6.*Sst1*^{S} mice downstream of the reduced IL-1 signaling. Deletion of *Il1rn* is protective in B6.*Sst1*^{S} mice, though not in B6 mice stimulated with a STING-agonist (Figure 2.11B). While negative data can be difficult to interpret, it raises the question of which mouse model is the best representation of the type I IFN-driven TB disease that appears to occur in humans.

There may not be a perfect mouse model for studying *Mtb* and type I IFN responses. Better understanding of the models, and the underlying reasons for their susceptibility, will at least clarify to what extent the models recapitulate human disease. In this respect, our *Sp140*$^{-/-}$ mice are better defined than the B6.*Sst1*^{S} mice, which carry a complex and variable 10Mb region in chromosome 1 from the C3H/HeJ mice. While *Sp110* and *Sp140* were the only genes that were differentially transcribed, there may be

[5] Although CRISPR greatly facilitates generation of gene-targeted mouse strains, it is still costly and labor-intensive to generate every knockout strain *de novo* in the post-CRISPR era

other unknown polymorphisms in the *Sst1* interval that affect infection outcomes. Understanding the mechanisms of SP140 will also better define the *Sp140*$^{-/-}$ mouse model. For example, further investigation will hopefully answer such questions as why B6.*Sst1*^{S}*Ifnar*$^{-/-}$ mice (and presumably *Sp140*$^{-/-}$*Ifnar*$^{-/-}$ mice) still succumb to *Mtb* infection faster than the control B6 mice.

A more unbiased approach is to profile the peripheral blood expression in various mouse models and compare them to available datasets from humans and non-human primate models[167]. Some labs have begun to do so to identify correlates of immunity in mouse models[168], and the same technique should be employed to better characterize or develop a mouse model that closely resembles the observed immune responses in human. This may also help highlight any facility or vendor-specific effects (likely acting through the microbiota) that lead to contradictory or inconsistent results.

Though my studies have been exclusively with the Erdman strain of *Mtb*, it may be of interest to test other common strains of *Mtb* to see if inhibition of IL-1Ra mediates protection in all cases. As mentioned before, Erdman strain induces less IL-10 than H37Rv, another commonly used laboratory strain[84]; this may explain why we did not observe a particularly strong induction of IL-10 in our susceptible mice. Other *Mtb* strains induce different immune responses: CDC1551 seems to be defective in IL-1 induction[62]; virulent clinical isolates such as HN878, BTB02-1771 and the newly described W_7642 strongly induce type I IFN responses[31,33,34]. The very strong type I IFN response induced by W_7642 strain may even be suppressing the IL-1 response such that there is no CFU difference between the control and *Il1r*$^{-/-}$ mice[34]. If this is the case, it may be interesting to determine if the virulence of W_7642 in B6 mice could be reversed with anti-IL-1Ra therapy. Regardless, the differences between bacterial strains should be taken into consideration when designing and interpreting results.

Mtb is a human-specific pathogen. While mouse models are informative and fascinating, it is important to be aware that they are model systems and, like all model systems, may not fully recapitulate all aspects of human disease.

4.2 Of IL-1 and how it regulates *Mycobacterium tuberculosis* replication

The results presented in Chapter 2 are in line with previous works by Mayer-Barber and colleagues, demonstrating that type I IFNs suppress IL-1 activity during *Mtb* infection. While previous studies have measured levels of IL-1Ra *in vivo* and noted that with *Mtb* infection and/or treatments such as polyICLC there is an increase[65], we are the first to report that IL-1Ra is functionally important during *Mtb* infection *in vivo*. Our results highlight the reciprocal, finely tuned interaction between IL-1 and type I IFN signaling; and the complexities of IL-1 signaling where protein levels do not necessarily equate functional activity.

Is suppressing IL-1 signaling the dominant mechanism of action for type I IFNs? In the B6.*Sst1*^{S} model it appears so. Increasing the amount of IL-1 activity through IL-1Ra deletion restored bacterial burden to B6 level and increased survival (Chapter 2) on the B6.*Sst1*^{S} background. I would be curious to see if this is also the case in other models, such as polyICLC treatment where there is also an increase in IL-1Ra levels.

What is the function of IL-1? IL-1 is required on either hematopoietic and non-hematopoietic cell types, but not necessarily both[75]. IL-1R signaling in bystander cells is apparently sufficient, regardless whether they are hematopoietic cells or not. This

suggests that whatever protective pathways are downstream of IL-1R, signaling can be activated by both hematopoietic and non-hematopoietic cells. Comparing transcriptomes of IL-1R^{+} and IL-1R^{-} hematopoietic cells and non-hematopoietic cells may generate some shared candidate pathways. The results may be more informative if one can isolate cells that have specifically turned on IL-1 signaling, possibly using a reporter system. *Il1rn*-deficient mice should be capable of greater dynamic range of IL-1 signaling as they lack the competitive inhibitor of IL-1R. Greater dynamic range of IL-1 signaling should result in improved signal-to-noise ratio of any IL-1 signaling-dependent effects, and reduced likelihood of a false hit.

While we (as a field) have identified many immune signaling pathways required for protection, the bacteriostatic or bactericidal effector functions downstream of these immune pathways are not as elucidated. To complete its lifecycle, *Mtb* must have pathways essential to surviving these stressors. In other words, the bacterium may not care about how much IL-1 protein there are (as far as we can tell IL-1 is not directly antibacterial), but it will respond to the downstream effector functions, which could nutrient depletion, antimicrobial peptides, reactive oxygen species or other unknown mechanisms. By analyzing how the bacterium responds to a particular immune pathway, such as IL-1 signaling, we may be able to identify the relevant antibacterial effector functions downstream of the immune pathway of interest. Screening for essential bacterial pathways using mutant library is a well-established technique, and I think IL-1 signaling would be an important pathway to investigate using this method. This screen should preferably be performed *in vivo*, with all the relevant cell types and immune pathways that function *in trans* between different cell types. It is important that the library be introduced via the aerosol route, as others have shown that different responses are required in the lung compared to systemic sites like the spleen[169]. By comparing how the mutant library respond to different levels of IL-1 signaling (utilizing the various mouse models available) and whether any genes that are not essential in the absence of IL-1 but become essential in the presence of elevated IL-1 we may gain some insights to how the pathogen cope, and consequently how the immune system attempted to control *Mtb*. I am curious to see whether the presence of IL-1R only on the hematopoietic versus non-hematopoietic compartment exerts similar pressure on *Mtb* (suggesting different cell types converge on the same set of effector functions against *Mtb*), or there are diverse effector functions that both result in control of *Mtb* growth. It may also be interesting to compare the changes to the *Mtb* mutant library in the permissive alveolar macrophages and restrictive interstitial macrophages[170]. Despite the technical challenges it is important to do these screen *in vivo*, as the effects of bystander cells and overall inflammatory cannot be accurately replicated *in vitro*[75].

4.3 Of Sp140, Sp110 and the regulation of innate immune pathways

What does Sp140 do? While our experiments focused mainly on its effects on type I IFN responses (Chapter 3), previous work on the *Sst1* locus suggest it may also have a role in regulating ER stress and apoptosis[103]. It is unclear whether or how potential effects on ER stress or apoptosis relate to the effects of SP140 on type I IFN responses we observe. The structural resemblance to AIRE and interaction with the PML-NB further suggest Sp140 may regulate many genes, not necessarily just type I IFN responses. However, we are currently limited by the lack of a good anti-Sp140 antibody

to perform direct ChIPseq or immunoprecipitation and mass spectrometry. Complementation of *Sp140*$^{-/-}$ cells with a tagged version is ongoing and may allow us to use ChIPseq to identify candidate loci directly targeted by SP140. These results can be compared to the results of ongoing ATACseq and histone marker ChIPseq experiments in *Sp140*$^{+/+}$ and *Sp140*$^{-/-}$ cells. To eliminate indirect effects on chromatin due to autocrine IFNAR signaling, these experiments should be done using an *Ifnar*$^{-/-}$ background. Using *Sp140*$^{-/-}$*Cas9*$^{+}$ mice we can perform CRISPR-knockout screens in BMDMs. By looking for cells that lose the elevated type I IFN response (by flow for example) we can identify binding partners or pathways involved in Sp140 function. These candidate genes/pathways may in turn suggest more conditions where Sp140 may function.

Sp100 is the only member of the Sp100 family proteins that has been shown to repress gene expression, via interaction with HP1 and recruiting chromatin silencing complexes[164]. Sp140 does not have the corresponding HP1-binding domain, though it could interact with Sp100 through the Sp100 domain. Sp140 may act as an adaptor protein between different transcription factors or histone markers and Sp100, which then mediates gene silencing. Formation of heterodimers between Sp140, Sp100 or Sp110 has never been specifically shown, though it is reported that human SP110 requires SP140 to localize to PML-NBs[137]. If this is true, it would suggest that *Sp100*$^{-/-}$ mice/macrophages would behave similarly as *Sp140*$^{-/-}$, and have elevated type I IFN responses. The same applies for PML-NB, which has already been suggested to act as a platform for recruiting other proteins[94]. Infecting *Pml*$^{-/-}$ or *Sp100*$^{-/-}$ mice with *L. pneumophila* and examining them for elevated type I IFN responses may help determine whether they also contribute to control during bacterial infections. Of note, current research on how the Sp100 family members function is mostly based on overexpression in cell lines. Because overexpression can often lead to unintended artifacts, proposed mechanisms based on overexpression alone may not recapitulate in primary cells.

Sp140$^{-/-}$ and B6.*Sst1*^{S} mice produce more type I IFNs during bacterial infections. Do they also produce more type I IFNs during viral infections? If so, one might predict that *Sp140*$^{-/-}$ and B6.*Sst1*^{S} mice might be resistant to viral infections. SP100 is known to have cell-intrinsic antiviral effector functions[171], and both SP140 and SP110 have been shown to interact with viral proteins (see Chapter 3), though their role in cell intrinsic immune response is less understood. Thus, *Sp140*$^{-/-}$ may be susceptible to viral infections *in vitro* due to loss of potential intrinsic antiviral functions but be more protected *in vivo* through increased production of type I IFNs. Certain viruses may also target SP140 for sequestration or degradation, as ICP0 targets SP100 for degradation[172]. This suggests an interesting model in which SP140 might function in a novel pathway for induction of type I IFNs in response to viruses. In this model, if/when SP140 is targeted for degradation, cells will de-repress type I IFNs, which would then be upregulated as a response. It is as if the cell is using SP140 to set a trap for viruses that antagonize cell-intrinsic responses. Of course, there is currently no data suggesting that any viral proteins target SP140 for degradation to support this hypothesis, although SP140 is reported to interact with HIV Vif[150]. It may be interesting to investigate whether viral proteins known to target SP100 or other PML-NB proteins may also target SP140 in a recombinant system. Screening different viruses against *Sp140*$^{+/+}$ and *Sp140*$^{-/-}$ cells on an *Ifnar*$^{-/-}$ background to identify potential cell-intrinsic functions of Sp140 would also provide leads.

Finally, does Sp110 have a function in mice? Sp110 is not necessary to repress type I IFNs during *Mtb* and *Legionella* infections, but it is possible that it is required in other contexts. *Sp110*$^{-/-}$ macrophages treated with TNFα induced some type I IFN responses though not to the same magnitude as B6.*Sst1*^{S} and *Sp140*$^{-/-}$ mice. *Sp110*$^{-/-}$ mice may be more resistant to certain viruses or treatment with virus mimetic polyIC *in vivo*.

4.4 Concluding remarks

In this thesis I have presented results that further our understanding of how type I IFN signaling 1) acts to suppress anti-bacterial immune responses during *Mtb* infections and 2) can be controlled by a putative transcription regulator. In Chapter 2 I present evidence that type I IFNs induce the inhibitor IL-1Ra to suppress IL-1 signaling without affecting IL-1 protein levels. Using B6.*Sst1*^{S}*Il1rn*$^{+/-}$ mice we showed that even a heterozygous deletion that partially decreased IL-1Ra levels can rescue the susceptible B6.*Sst1*^{S} background, suggesting that control of *Mtb* infection is finely tuned by different cytokine signaling pathways. We also demonstrated for the first time the susceptibility of the *Sst1*^{S} locus is driven by type I IFN signaling.

In Chapter 3 I presented evidence that loss of *Sp140* leads to upregulation of type I IFN responses that drives susceptibility to infection by several intracellular bacteria. We identify Sp140 as a potential novel negative regulator of type I IFN responses. The investigations into the molecular mechanisms of SP140 are ongoing. These results also identify the gene responsible for the phenotypes associated with the *Sst1* locus, a longstanding question in the TB field.

Finally, I wanted to end with some musings on the system that we study: *Mtb*. *Mtb* is a fascinating pathogen. Without an environmental reservoir it must, without fail, persist and replicate within a hostile host, then facilitate its transmission to a new host. It causes disease in only a fraction of the infected and the incubation period is long, potentially reactivating decades later (though the importance of long latency during most TB transmission is contested[173]). As a bacterium, it causes infections like a virus, though it does not require host machinery or even the cytosol to replicate. Through it we discovered the delicate balance between type I IFNs and the importance of Sp140. And TB has exerted evolutionary pressure on humans for possibly hundreds of thousands of years, suggesting that there may be many other *Mtb*-specific adaptations to be discovered[4]. There is a sort of tragic elegance, that as we study it in search of ways to eradicate it, *Mtb* is helping us to discover ourselves.

Materials and Methods

Chapter 2

Mice. All mice were specific pathogen-free, maintained under a 12-hr light-dark cycle (7AM to 7PM), and given a standard chow diet (Harlan irradiated laboratory animal diet) *ad libitum*. Within each experiment mice of all genotypes were sex and age-matched at 6-10 weeks old at the beginning of infections. Same number of each sex was used in all genotypes as much as possible. C57BL/6J (B6), B6.129S-*Il1rn*^{tm1Dih}/J (*Il1rn*$^{-/-}$), B6(Cg)-*Ifnar1*$^{tm1.2Ees}$/J (*Ifnar*$^{-/-}$) and B6.129S6-^{Ch25htm1Rus}/J (*Ch25h*$^{-/-}$) were originally purchased from Jackson Laboratories and subsequently bred at UC Berkeley. B6J.C3-*Sst1*$^{C3HeB/FeJKrmn}$ mice (referred to as B6.*Sst1*^{S} throughout) were from the colony of I. Kramnik at Boston University and then transferred to UC Berkeley. *Sting*$^{gt/gt}$ mice were previously described[61]. All animals used in experiments were bred in-house unless otherwise noted in the figure legends. All animal experiments complied with the regulatory standards of, and were approved by, the University of California Berkeley Institutional Animal Care and Use Committee.

***Mycobacterium tuberculosis* infections.** *Mtb* strain Erdman (gift of S.A. Stanley) was used for all infections. Frozen stocks of this wild-type strain were made from a single culture and used for all experiments. Cultures for infection were grown in Middlebrook 7H9 liquid medium supplemented with 10% albumin-dextrose-saline, 0.4% glycerol and 0.05% Tween-80 for five days at 37°C. Mice were aerosol infected using an inhalation exposure system (Glas-Col, Terre Haute, IN). A total of 9ml of culture was loaded into the nebulizer calibrated to deliver ~20 to 50 bacteria per mouse as measured by colony forming units (CFUs) in the lungs 1 day following infection (data not shown). Mice were sacrificed at various days post-infection as indicated in the figure legends to measure CFUs and/or cytokines. All but 1 lung lobe was homogenized in PBS plus 0.05% Tween-80 or processed for cytokines (see below), and serial dilutions were plated on 7H11 plates supplemented with 10% oleic acid, albumin, dextrose, catalase (OADC) and 0.5% glycerol. CFUs were counted 21-25 days after plating. The remaining lobe was used for histology or for RNA extraction. For histology the sample was fixed in 10% formalin for at least 48 hours then stored in 70% ethanol. Samples were sent to Histowiz Inc for embedding in wax, sectioning and staining.

Cytokine measurements. Cell-free lung homogenates were generated as previously described[72]. Briefly, lungs were crushed through 100µm Falcon cell strainers in sterile PBS with 1% FBS and Pierce Protease Inhibitor (Thermo Fisher). An aliquot was removed for measuring CFU by plating as described above. Cells and debris were then removed by low-speed centrifugation (300×*g*) and the resulting cell-free homogenate was filtered twice with 0.2µm filters to remove all *Mtb* for work outside of BSL3. All homogenates were aliquoted, flash-frozen in liquid nitrogen and stored at –80°C. Each aliquot was thawed a maximum of twice to avoid potential artifacts due to repeated freeze-thaw cycles. All cytokines except IL-10 and

IL-1Ra was measured using Cytometric Bead Assay (BD Biosciences) according to manufacturer protocols. Results were collected using BD LSRFortessa (BD Biosciences) and analyzed using FCAP Array v3.0. IL-10 levels were measured using Mouse IL-10 ELISA Ready-SET-Go! (2^{nd} Generation, eBioscience). IL-1Ra levels were measured by ELISA using Mouse IL-1ra/IL-1F3 Quantikine ELISA Kit (R&D Systems) according to manufacturer protocols.

IL-1 bioactivity reporter assay. Mice were infected with ~25-35 bacteria per mouse and sacrificed at 25 days-post infection to prepare cell-free lung homogenates. Assays were performed using HEK-Blue™ IL-1R cells (InvivoGen) with minor modifications. Cells were cultured under antibiotic-selection according to manufacturer protocols. Cells were plated at 3.75×10^4 cells/well in 100µl in 96-well plates (~80% confluent), and allowed to adhere overnight in DMEM supplemented with 10% FBS, 2mM glutamine, 100 U/ml streptomycin and 100 µg/ml penicillin in a humidified incubator (37°C, 5% CO_2). 50µl cell-free lung homogenates or standard curve made from recombinant mouse IL-1β (R&D systems 401-ML-005) were mixed with 50ul of fresh media. Media from the cells were removed and replaced with lung lysate/media mixture and incubated overnight in a humidified incubator. Assays were developed using QUANTI-Blue (InvivoGen) according to manufacturer protocols. Experiments in which the initial CFU was either too high or too low produced inconsistent results in this assay. Reporter cells should be less than 80% confluent when plating into 96-wells or results will be inconsistent.

Flow cytometry. Lungs were perfused with 10 ml of cold PBS and strained through 40µm cell strainers. Aliquots were removed for quantifying CFU. Cells were washed and stained with fixable viability dye (Thermo Fisher 65-0865-14). An aliquot of cells from each sample were removed and mixed with counting beads (Thermo Fisher C36950) for later enumeration. The rest of the cells were incubated with anti-mouse CD16/CD32 monoclonal antibody to block Fc receptors (Thermo Fisher 14-0161-81), then with antibodies for surface staining. The following antigens were stained for: CD45 (30-F11, Biolegend 103107), CD11b (M1/70, Thermo Fisher 48-0112-82), CD11c (N418, Biolegend 117335), Ly6G (1A8, BD Biosciences 740554), Ly6C (HK1.4, Thermo Fisher 17-5932-80), CD24 (M1/69, BD Bioscience 564664), MHC II (M5/114.15.2, Biolegend 107625), SiglecF (E50-2440, BD Biosciences 562680). Cells were fixed with fixation buffer (BD Biosciences 554714) for at least 1 hour at room temperature and stored in PBS with 1% FBS and 2mM EDTA overnight at 4°C in the dark. Data were acquired on a BD Fortessa X-20 flow cytometer and analyzed with FlowJo v10.

Bone marrow-derived macrophages (BMMs) and TNF-treatment. Bone marrow was harvested from mouse femurs and tibias, and cells were differentiated by culture on non-tissue culture-treated plates in RPMI supplemented with supernatant from 3T3-MCSF cells (gift of B. Beutler), 10% fetal bovine serum (FBS), 2mM glutamine, 100 U/ml streptomycin and 100 µg/ml penicillin in a humidified incubator (37°C, 5%CO_2). BMMs were harvested six days after plating and frozen in

95% FBS and 5% DMSO. For *in vitro* experiments, BMMs were thawed into media as described above for 4 hours in a humidified 37°C incubator. Adherent cells were washed with PBS, counted and replated at $1.2x10^6 \sim 1.5x10^6$ cells/well in a TC-treated 6-well plate. Cells were treated with 10 ng/ml recombinant mouse TNFα (410-TRNC-010, R&D systems) diluted in the media as described above.

Quantitative RT-PCR. Total RNA from BMMs was extract using RNeasy total RNA kit (Qiagen) according to manufacturer specifications. Total RNA from infected tissues was extracted by homogenizing in TRIzol reagent (Life technologies) then mixing thoroughly with chloroform, both done under BSL3 conditions. Samples were then removed from the BSL3 facility and transferred to fresh tubes under BSL2 conditions. Aqueous phase was separated by centrifugation and RNA was further purified using an RNeasy total RNA kit (Qiagen). Equal amounts of RNA from each sample were treated with DNase (RQ1, Promega) and cDNA was made using Superscript III (Invitrogen). Complementary cDNA reactions were primed with poly(dT) for the measurement of mature transcripts. For experiments with multiple time points, samples were frozen in the RLT buffer (Qiagen) or RNA*later*™ solution (Invitrogen). Quantitative PCR was performed using QuantiStudio 5 Real-Time PCR System (Applied Biosystems) with Power Sybr Green PCR Master Mix (Thermo Fisher Scientific) according manufacturer specifications. Transcript levels were normalized to housekeeping genes *Rps17, Actb and Oaz1* unless otherwise specified. The following primers were used in this study. *Rps17* sense: CGCCATTATCCC CAGCAAG; *Rps17* antisense: TGTCGGGATCCACCTCAATG; *Oaz1* sense: GTG GTG GCC TCT ACA TCG AG; *Oaz1* antisense: AGC AGA TGA AAA CGT GGT CAG; *Actb* sense: CGC AGC CAC TGT CGA GTC; *Actb* antisense: CCT TCT GAC CCA TTC CCA CC; *Ifnb* sense: GTCCTCAACTGCTCTCCACT; *Ifnb* antisense: CCTGCAACCACCACTCATTC; *Il1rn* sense: CGCCCTTCTGGGAAAAGACC, *Il1rn* antisense: CCGTGGATGCCCAAGAACAC; *Irf1* sense: TGAGGAAGGGAAGATAGCCG; *Irf1* antisense: TGTATGCCTATCCCAATGTCCC; *Irgm1* sense: AAAACCAGAGAGCCTCACCA; *Irgm1* antisense: ATGTTGGGGAGTAGTGGAGC; *Gbp4* sense: TGAGTACCTGGAGAATGCCCT; *Gbp4* antisense: TGGCCGAATTGGATGCTTGG; *Gbp5* sense: TGTTCTTACTGGCCCCTGCT; *Gbp5* antisense: CCAATGAGGCACAAGGGTTC; *Ifit3* sense: AGCCCACACCCAGCTTTT; *Ifit3* antisense: CAGAGATTCCCGGTTGACCT; *Stat1* sense: CAGAAAAACGCTGGGAACAGA; *Stat1* antisense: CAAGCCTGGCTGGCAC; *Gbp7* sense: AGCAAGCCCAAGTTCACACT; *Gbp7* antisense: TCCGCTCTGTCAGTTCTGTG.

Antibody-mediated neutralization. For all antibody treatments, the schedules are indicated in the figures. All treatments were delivered by intraperitoneal injection. Mouse anti-mouse IFNAR1 (MAR1-5A3) and isotype control (GIR208, mouse anti-human IFNGR-α chain) were purchased from Leinco Technologies Inc. Each mouse was given 500μg per injection. Hamster anti-IL1R1 antibody (mIL1R-M147) was obtained from Amgen. Isotype control was Ultra-LEAF Purified Armenian Hamster IgG Isotype Antibody from Biolegend (400940). Each mouse was given 200μg per injection. Armenian hamster anti-IL1Ra antibody was produced in-house using a previously published hybridoma line[123]. Cells were grown in Wheaton CELLine Bioreactor Flasks (Fisher Scientific) according to manufacturer instructions. Media

in the cell compartment used ultra-low IgG FBS (ThermoFisher 16250078) to minimize bovine IgG contamination during purification. Cell-free supernatant from the cell compartment was purified using protein G resin (GenScript). IgG was eluted using 0.1M acetic acid, then 10% of total volume of 1M Tris pH8 and 0.5M NaCl was added to neutralize. Size exclusion and buffer exchange to PBS was performed using Amicon Ultra-4 Centrifugal Filter Units (EMD Millipore). The final product was filter sterilized and stored at –80°C. For injections antibody stocks were diluted in sterile PBS and each mouse received 500μg per injection.

ADU-S100 injection. ADU-S100 was purchased from Chemietek (CAS number 1638241-89-0 for the free acid) and resuspended in sterile PBS at 500μg/ml. Mice were given 50μg (in 100μl) each every other day for 8 injections, intraperitoneally, starting 1 day post-infection.

PGE_2 measurement. Eicosanoids were isolated as previously described, with modifications for BSL3 conditions[174]. Lungs were collected and 1 lobe was kept in PBS and 0.05% Tween-80 for enumeration of CFU (as described above). Rest of the samples were homogenized immediately in 1ml 100% methanol and kept cold during transfer out of the BSL3 containment. Samples were transferred to new tubes under BSL2 conditions, then centrifuged at 3000x*g* for 10 minutes at 4°C to remove precipitated proteins. The supernatants were processed as previously described. PGE_2 levels were measured using the Prostaglandin E_2 ELISA Kit from Cayman Chemical (514010) according to manufacturer specifications.

Statistical analysis. All survival data were analyzed with Log-rank (Mantel-Cox) Test. All other data were analyzed with two-ended Mann-Whitney test unless otherwise noted. Both tests were run using GraphPad Prism 5. Asterisk, $p \leq 0.05$; two asterisks, $p \leq 0.01$; three asterisks, $p \leq 0.001$. All error bars are SEM and all center bars indicate means.

Chapter 3

Mice. All mice were specific pathogen-free, maintained under a 12-hr light-dark cycle (7AM to 7PM), and given a standard chow diet (Harlan irradiated laboratory animal diet) *ad libitum*. All mice were sex and age-matched at 6-10 weeks old at the beginning of infections. C57BL/6J (B6) and B6(Cg)-*Ifnar1*$^{tm1.2Ees}$/J (*Ifnar*$^{-/-}$) were originally purchased from Jackson Laboratories and subsequently bred at UC Berkeley. B6J.C3-*Sst1*$^{C3HeB/FeJKrmn}$ mice (referred to as B6.*Sst1*^{S} throughout) were from the colony of I. Kramnik at Boston University and then transferred to UC Berkeley. CRISPR/Cas9 targeting was performed by pronuclear injection of Cas9 mRNA and sgRNA into fertilized zygotes from colony-born C57BL/6J mice, essentially as described previously[175]. Founder mice were genotyped as described in Genotyping of *Sp140* alleles, and founders carrying *Sp140* mutations were bred one generation to C57BL/6J to separate modified *Sp140* haplotypes. Homozygous lines were generated by interbreeding heterozygotes carrying matched *Sp140* haplotypes. *Sp140*$^{-/-}$*Ifnar*$^{-/-}$ were generated by crossing the *Sp140*$^{-/-}$ and *Ifnar*$^{-/-}$ mice in-house. All animals used in experiments were bred in-house unless otherwise noted in the figure legends. All animal experiments complied with the regulatory standards of, and were approved by, the University of California Berkeley Institutional Animal Care and Use Committee.

Genotyping of *Sp140* alleles. Exon 3 and the surrounding intronic regions were amplified by bracket PCR using the following primers (all 5′ to 3′): Sp140-1 fwd, ACGAATAGCAAGCAGGAATGCT, and rev, GGTTCCGGCTGAGCACTTAT. The PCR products are diluted at 1:10 and 2ul are used as template for the second PCR using the following primers: Sp140-2 fwd, TGA GGA CAG AAC TCA GGG AG, and rev, ACA CGC CTT TAA TCC CAG CAT TT. The primer combinations distinguish Sp140 from other Sp140-like genes. Primers were used at 200 nM in each 20ul reaction with 1x Dreamtaq Green PCR Master Mix (Thermo Fisher Scientific). Cleaned PCR products were diluted at 1:10 and sequenced using Sanger sequencing (Elim Biopharm).

***Mycobacterium tuberculosis* infections.** *Mtb* strain Erdman (gift of S.A. Stanley) was used for all infections. Frozen stocks of this wild-type strain were made from a single culture and used for all experiments. Cultures for infection were grown in Middlebrook 7H9 liquid medium supplemented with 10% albumin-dextrose-saline, 0.4% glycerol and 0.05% Tween-80 for five days at 37°C. Mice were aerosol infected using an inhalation exposure system (Glas-Col, Terre Haute, IN). A total of 9ml of culture was loaded into the nebulizer calibrated to deliver ~20 to 50 bacteria per mouse as measured by colony forming units (CFUs) in the lungs 1 day following infection (data not shown). Mice were sacrificed at various days post-infection (as described in figure legends) to measure CFUs and/or cytokines. All but 1 lung lobe was homogenized in PBS plus 0.05% Tween-80 or processed for cytokines (see below), and serial dilutions were plated on 7H11 plates supplemented with 10% oleic acid, albumin, dextrose, catalase (OADC) and 0.5% glycerol. CFUs were counted 21 days after plating. The remaining lobe was used for histology or for RNA extraction. For histology the sample was fixed in 10% formalin for at least 48 hours then stored in 70% ethanol. Samples were sent to Histowiz Inc for embedding in wax, sectioning and staining with hematoxylin and eosin. For survival experiments mice where monitored for weight loss and were euthanized when they

reached a humane endpoint as determined by the University of California Berkeley Institutional Animal Care and Use Committee.

***Legionella pneumophila* infections.** Infections were performed using *L. pneumophila* strain JR32 Δ*flaA* (gift of D.S. Zamboni) as previously described[176]. Briefly, frozen cultures were streaked out on to CYE plates to obtain single colonies. A single colony was chosen and streaked on to a new CYE plate to obtain a 1cm by 1cm square, and incubated for 2 days at 37°C. The patch was solubilized in sterilized MilliQ water and the optical density was measured at 600nm. Culture was diluted to 2.5 x10^6 bacteria/mL in sterile PBS. The mice were first anesthetized with ketamine and xylazine (90 mg/kg and 5 mg/kg, respectively) by intraperitoneal injection then infected intranasally with 40 μL with PBS containing a final dilution of 1×10^5 bacteria per mouse. For enumerating of colony-forming units (CFU), the lungs were harvested and homogenized in 5 mL of sterile water for 30 seconds, using a tissue homogenizer. Lung homogenates were diluted in sterile water and plated on CYE agar plates. CFU was enumerated after plates were incubated for 4 days at 37°C.

***Listeria monocytogenes* infections.** For in vivo infections, bacterial cultures were grown overnight in BHI, diluted 1:5 in BHI and grown at 37°C for 1.5 h until they reached an optical density at 600 nm of 0.5. Mice were injected with 10^4 wildtype (10403S) bacteria intravenously by the tail vein. At 48 h post-infection, the spleens and livers were harvested, homogenized, and plated in serial dilutions to enumerate CFU as previously described[61].

Cytokine measurements. Cell-free lung homogenates were generated as previously described[72]. Briefly, lungs were crushed through 100μm Falcon cell strainers in sterile PBS with 1% FBS and Pierce Protease Inhibitor (Thermo Fisher). An aliquot was removed for measuring CFU by plating as described above. Cells were then removed by low-speed centrifugation (300×*g*). Debris was removed by high-speed centrifugation (1000x*g*) and the resulting cell-free homogenate was filtered twice with 0.2μm filters to remove all *Mtb* for work outside of BSL3. All homogenates were aliquoted, flash-frozen in liquid nitrogen and stored at –80°C. Each aliquot was thawed a maximum of twice to avoid potential artifacts due to repeated freeze-thaw cycles. All cytokines except IL-1Ra was measured using Cytometric Bead Assay (BD Biosciences) according to manufacturer protocols. Results were collected using BD LSRFortessa (BD Biosciences) and analyzed using FCAP Array v3.0. IL-1Ra levels were measured by ELISA using Mouse IL-1ra/IL-1F3 DuoSet ELISA Kit (R&D Systems) according to manufacturer protocols.

Bone marrow-derived macrophages (BMMs) and TNF-treatment. Bone marrow was harvested from mouse femurs and tibias, and cells were differentiated by culture on non-tissue culture-treated plates in RPMI supplemented with supernatant from 3T3-MCSF cells (gift of B. Beutler), 10% fetal bovine serum (FBS), 2mM glutamine, 100 U/ml streptomycin and 100 μg/ml penicillin in a humidified incubator (37°C, 5%CO_2). BMMs were harvested six days after plating and frozen in 95% FBS and 5% DMSO. For *in vitro* experiments, BMMs were thawed into media as described above for 4 hours in a humidified 37°C incubator. Adherent cells were washed with PBS, counted and replated

at $1.2x10^6$ ~ $1.5x10^6$ cells/well in a TC-treated 6-well plate. Cells were treated with 10ng/ml recombinant mouse TNFα (410-TRNC-010, R&D systems) diluted in the media as described above.

Quantitative RT-PCR. Total RNA from BMMs was extract using E.Z.N.A. Total RNA Kit I (Omega Bio-tek) according to manufacturer specifications. Total RNA from infected tissues was extracted by homogenizing in TRIzol reagent (Life technologies) then mixing thoroughly with chloroform, both done under BSL3 conditions. Samples were then removed from the BSL3 facility and transferred to fresh tubes under BSL2 conditions. Aqueous phase was separated by centrifugation and RNA was further purified using the E.Z.N.A. Total RNA Kit I (Omega Bio-tek). Equal amounts of RNA from each sample were treated with DNase (RQ1, Promega) and cDNA was made using Superscript III (Invitrogen). Complementary cDNA reactions were primed with poly(dT) for the measurement of mature transcripts. For experiments with multiple time points, macrophage samples were frozen in the RLT buffer (Qiagen) and infected tissue samples in RNA*later*™ solution (Invitrogen) and processed to RNA at the same time. Quantitative PCR was performed using QuantiStudio 5 Real-Time PCR System (Applied Biosystems) with Power Sybr Green PCR Master Mix (Thermo Fisher Scientific) according manufacturer specifications. Transcript levels were normalized to housekeeping genes *Rps17, Actb and Oaz1* unless otherwise specified. The following primers were used in this study. *Rps17* sense: CGCCATTATCCC CAGCAAG; *Rps17* antisense: TGTCGGGATCCACCTCAATG; *Oaz1* sense: GTG GTG GCC TCT ACA TCG AG; *Oaz1* antisense: AGC AGA TGA AAA CGT GGT CAG; *Actb* sense: CGC AGC CAC TGT CGA GTC; *Actb* antisense: CCT TCT GAC CCA TTC CCA CC; *Ifnb* sense: GTCCTCAACTGCTCTCCACT; *Ifnb* antisense: CCTGCAACCACCACTCATTC; *Il1rn* sense: CGCCCTTCTGGGAAAAGACC, *Il1rn* antisense: CCGTGGATGCCCAAGAACAC; *Gbp4* sense: TGAGTACCTGGAGAATGCCCT; *Gbp4* antisense: TGGCCGAATTGGATGCTTGG; *Gbp5* sense: TGTTCTTACTGGCCCCTGCT; *Gbp5* antisense: CCAATGAGGCACAAGGGTTC; *Ifit3* sense: AGCCCACACCCAGCTTTT; *Ifit3* antisense: CAGAGATTCCCGGTTGACCT.

Immunoblot. Samples were lysed in RIPA buffer as previously described to obtain total protein lysate and were clarified by spinning at ~16,000×g for 30 min at 4°C. Clarified lysates were analyzed with Pierce BCA protein assay kit (Thermo Fisher Scientific) according to manufacturer specification and diluted to the same concentration and denatured with SDS-loading buffer. Samples were separated on NuPAGE Bis–Tris 4% to 12% gradient gels (Thermo Fisher Scientific) following the manufacturer's protocol. Gels were transferred onto ImmobilonFL PVDF membranes at 35 V for 90 min and blocked with Odyssey blocking buffer (Li-Cor). Proteins were detected on a Li-Cor Odyssey Blot Imager using the following primary and secondary antibodies. Rabbit anti-Sp110 or Sp140 serums were used at 1:1000 dilution. Alexa Fluor 680- conjugated secondary antibodies (Invitrogen) were used at 0.4 mg/ml.

RNA sequencing and analysis. Total RNA was isolated as described above. Illumina-compatible libraries were generated by the University of California, Berkeley, QB3

Vincent J. Coates Genomics Sequencing Laboratory. The libraries were multiplexed and sequenced using one flow cell on HiSeq4000 (Illumina) as 100bp single-end reads. The data were aligned using Sleuth and analyzed using Kallisto.

Antibody-mediated neutralization. For all antibody treatments, the schedules are indicated in the figures. All treatments were delivered by intraperitoneal injection. Mouse anti-mouse IFNAR1 (MAR1-5A3) and isotype control (GIR208, mouse anti-human IFNGR-α chain) were purchased from Leinco Technologies Inc. For injections antibody stocks were diluted in sterile PBS and each mouse received 500μg per injection.

Statistical analysis. All survival data were analyzed with Log-rank (Mantel-Cox) Test. All other data were analyzed with Mann-Whitney test unless otherwise noted. Both tests were run using GraphPad Prism 5. Asterisk, $p \leq 0.05$; two asterisks, $p \leq 0.01$; three asterisks, $p \leq 0.001$. All error bars are s.e.

References

1. World Health Organization. Global Tuberculosis Report 2018. 2018.

2. Pan H, Yan B-S, Rojas M, et al. Ipr1 gene mediates innate immunity to tuberculosis. *Nature*. 2005;434(7034):767-772. doi:10.1038/nature03419.

3. Kramnik I, Dietrich WF, Demant P, Bloom BR. Genetic control of resistance to experimental infection with virulent *Mycobacterium tuberculosis*. *Proc Natl Acad Sci*. 2002;97(15):8560-8565. doi:10.1073/pnas.150227197.

4. Brites D, Gagneux S. The Nature and Evolution of Genomic Diversity in the *Mycobacterium tuberculosis* Complex. In: Gagneux S, ed. *Strain Variation in the Mycobacterium Tuberculosis Complex: Its Role in Biology, Epidemiology and Control*. Cham: Springer International Publishing; 2017:1-26. doi:10.1007/978-3-319-64371-7_1.

5. Simmons JD, Stein CM, Seshadri C, et al. Immunological mechanisms of human resistance to persistent *Mycobacterium tuberculosis infection*. *Nat Rev Immunol*. 2018;18(9):575-589. doi:10.1038/s41577-018-0025-3.

6. Guinn KM, Rubin EJ. Tuberculosis: Just the FAQs. *MBio*. 2017;8(6):1-14. doi:10.1128/mBio.01910-17.

7. Abel L, Fellay J, Haas DW, et al. Genetics of human susceptibility to active and latent tuberculosis: present knowledge and future perspectives. *Lancet Infect Dis*. 2018;18(3):e64-e75. doi:10.1016/S1473-3099(17)30623-0.

8. Vilcek J. Fifty Years of Interferon Research: Aiming at a Moving Target. *Immunity*. 2006;25(3):343-348. doi:10.1016/j.immuni.2006.08.008.

9. McNab F, Mayer-Barber K, Sher A, Wack A, O'Garra A. Type I interferons in infectious disease. *Nat Rev Immunol*. 2015;15(2):87-103. doi:10.1038/nri3787.

10. González-Navajas JM, Lee J, David M, Raz E. Immunomodulatory functions of type I interferons. *Nat Rev Immunol*. 2012;12(2):125-135. doi:10.1038/nri3133.

11. Jaitin DA, Roisman LC, Jaks E, et al. Inquiring into the differential action of interferons (IFNs): an IFN-alpha2 mutant with enhanced affinity to IFNAR1 is functionally similar to IFN-beta. *Mol Cell Biol*. 2006;26(5):1888-1897. doi:10.1128/MCB.26.5.1888-1897.2006.

12. Boxx GM, Cheng G. The Roles of Type I Interferon in Bacterial Infection. *Cell Host Microbe*. 2016;19(6):760-769. doi:10.1016/j.chom.2016.05.016.

13. Moreira-Teixeira L, Mayer-Barber K, Sher A, O'Garra A. Type I interferons in tuberculosis: Foe and occasionally friend. *J Exp Med*. 2018;215(5):1273-1285. doi:10.1084/jem.20180325.

14. Cliff JM, Kaufmann SHE, McShane H, van Helden P, O'Garra A. The human immune response to tuberculosis and its treatment: a view from the blood. *Immunol Rev*. 2015;264(1):88-102. doi:10.1111/imr.12269.

15. Donovan ML, Schultz TE, Duke TJ, Blumenthal A. Type I interferons in the pathogenesis of tuberculosis: Molecular drivers and immunological consequences. *Front Immunol*. 2017;8(NOV). doi:10.3389/fimmu.2017.01633.

16. Bogunovic D, Byun M, Durfee LA, et al. Mycobacterial disease and impaired IFN-γ immunity in humans with inherited ISG15 deficiency. *Science*. 2012;337(6102):1684-1688. doi:10.1126/science.1224026.

17. Zhang X, Bogunovic D, Payelle-Brogard B, et al. Human intracellular ISG15 prevents interferon-α/β over-amplification and auto-inflammation. *Nature*. 2015;517(7532):89-93. doi:10.1038/nature13801.

18. Zhang G, DeWeerd NA, Stifter SA, et al. A proline deletion in IFNAR1 impairs IFN-signaling and underlies increased resistance to tuberculosis in humans. *Nat Commun*. 2018;9(1):85. doi:10.1038/s41467-017-02611-z.

19. Sabbatani S, Manfredi R, Marinacci G, Pavoni M, Cristoni L, Chiodo F. Reactivation of severe, acute pulmonary tuberculosis during treatment with pegylated interferon-alpha and ribavirin for chronic HCV hepatitis. *Scand J Infect Dis*. 2006;38(3):205-208. doi:10.1080/00365540500263268.

20. Farah R, Awad J. The association of interferon with the development of pulmonary tuberculosis. *Int J Clin Pharmacol Ther*. 2007;45(11):598-600. http://www.ncbi.nlm.nih.gov/pubmed/18077924.

21. Matsuoka S, Fujikawa H, Hasegawa H, Ochiai T, Watanabe Y, Moriyama M. Onset of Tuberculosis from a Pulmonary Latent Tuberculosis Infection during Antiviral Triple Therapy for Chronic Hepatitis C. *Intern Med*. 2016;55(15):2011-2017. doi:10.2169/internalmedicine.55.6448.

22. de Oliveira Uehara SN, Emori CT, Perez RM, et al. High incidence of tuberculosis in patients treated for hepatitis C chronic infection. *Brazilian J Infect Dis*. 2016;20(2):205-209. doi:10.1016/j.bjid.2015.12.003.

23. Telesca C, Angelico M, Piccolo P, et al. Interferon-alpha treatment of hepatitis C induces tuberculosis exacerbation in an immigrant. *J Infect*. 2007;54(4):e223-6. doi:10.1016/j.jinf.2006.12.009.

24. Grebenciucova E, Pruitt A. Infections in Patients Receiving Multiple Sclerosis Disease-Modifying Therapies. *Curr Neurol Neurosci Rep*. 2017;17(11). doi:10.1007/s11910-017-0800-8.

25. Ward CM, Jyonouchi H, Kotenko S V., et al. Adjunctive treatment of disseminated *Mycobacterium avium* complex infection with interferon alpha-2b in a patient with complete interferon-gamma receptor R1 deficiency. *Eur J Pediatr*.

2007;166(9):981-985. doi:10.1007/s00431-006-0339-1.

26. Bax HI, Freeman AF, Ding L, et al. Interferon alpha treatment of patients with impaired interferon gamma signaling. *J Clin Immunol*. 2013;33(5):991-1001. doi:10.1007/s10875-013-9882-5.

27. Novikov A, Cardone M, Thompson R, et al. *Mycobacterium tuberculosis* triggers host type I IFN signaling to regulate IL-1β production in human macrophages. *J Immunol*. 2011;187(5):2540-2547. doi:10.4049/jimmunol.1100926.

28. McNab FW, Ewbank J, Howes A, et al. Type I IFN induces IL-10 production in an IL-27-independent manner and blocks responsiveness to IFN-γ for production of IL-12 and bacterial killing in *Mycobacterium tuberculosis*-infected macrophages. *J Immunol*. 2014;193(7):3600-3612. doi:10.4049/jimmunol.1401088.

29. Antonelli LR V, Gigliotti Rothfuchs A, Gonçalves R, et al. Intranasal Poly-IC treatment exacerbates tuberculosis in mice through the pulmonary recruitment of a pathogen-permissive monocyte/macrophage population. *J Clin Invest*. 2010;120(5):1674-1682. doi:10.1172/JCI40817.

30. Stanley SA, Johndrow JE, Manzanillo P, Cox JS. The Type I IFN response to infection with *Mycobacterium tuberculosis* requires ESX-1-mediated secretion and contributes to pathogenesis. *J Immunol*. 2007;178(5):3143-3152. doi:10.4049/jimmunol.178.5.3143.

31. Manca C, Tsenova L, Bergtold A, et al. Virulence of a *Mycobacterium tuberculosis* clinical isolate in mice is determined by failure to induce Th1 type immunity and is associated with induction of IFN-alpha /beta. *Proc Natl Acad Sci*. 2001;98(10):5752-5757. doi:10.1073/pnas.091096998.

32. Manca C, Tsenova L, Freeman S, et al. Hypervirulent *M. tuberculosis* W/Beijing strains upregulate type I IFNs and increase expression of negative regulators of the Jak-Stat pathway. *J Interferon Cytokine Res*. 2005;25(11):694-701. doi:10.1089/jir.2005.25.694.

33. Carmona J, Cruz A, Moreira-Teixeira L, et al. *Mycobacterium tuberculosis* Strains Are Differentially Recognized by TLRs with an Impact on the Immune Response. *PLoS One*. 2013;8(6):1-10. doi:10.1371/journal.pone.0067277.

34. Howard NC, Marin ND, Ahmed M, et al. *Mycobacterium tuberculosis* carrying a rifampicin drug resistance mutation reprograms macrophage metabolism through cell wall lipid changes. *Nat Microbiol*. 2018;3(10):1099-1108. doi:10.1038/s41564-018-0245-0.

35. Stamm CE, Collins AC, Shiloh MU. Sensing of *Mycobacterium tuberculosis* and consequences to both host and bacillus. *Immunol Rev*. 2015;264(1):204-219. doi:10.1111/imr.12263.

36. Bulut Y, Michelsen KS, Hayrapetian L, et al. *Mycobacterium tuberculosis* heat

shock proteins use diverse toll-like receptor pathways to activate pro-inflammatory signals. *J Biol Chem*. 2005;280(22):20961-20967. doi:10.1074/jbc.M411379200.

37. Cehovin A, Coates ARM, Hu Y, et al. Comparison of the moonlighting actions of the two highly homologous chaperonin 60 proteins of *Mycobacterium tuberculosis*. *Infect Immun*. 2010;78(7):3196-3206. doi:10.1128/IAI.01379-09.

38. Kim K, Sohn H, Kim JS, et al. *Mycobacterium tuberculosis* Rv0652 stimulates production of tumour necrosis factor and monocytes chemoattractant protein-1 in macrophages through the Toll-like receptor 4 pathway. *Immunology*. 2012;136(2):231-240. doi:10.1111/j.1365-2567.2012.03575.x.

39. Jung S-B, Yang C-S, Lee J-S, et al. The mycobacterial 38-kilodalton glycolipoprotein antigen activates the mitogen-activated protein kinase pathway and release of proinflammatory cytokines through Toll-like receptors 2 and 4 in human monocytes. *Infect Immun*. 2006;74(5):2686-2696. doi:10.1128/IAI.74.5.2686-2696.2006.

40. Choi HG, Choi S, Back YW, et al. *Mycobacterium tuberculosis* Rv2882c protein induces activation of macrophages through TLR4 and exhibits vaccine potential. *PLoS One*. 2016;11(10):1-21. doi:10.1371/journal.pone.0164458.

41. Doz E, Rose S, Nigou J, et al. Acylation determines the toll-like receptor (TLR)-dependent positive versus TLR2-, mannose receptor-, and SIGNR1-independent negative regulation of pro-inflammatory cytokines by mycobacterial lipomannan. *J Biol Chem*. 2007;282(36):26014-26025. doi:10.1074/jbc.M702690200.

42. Kim WS, Jung ID, Kim J-S, et al. *Mycobacterium tuberculosis* GrpE, A Heat-Shock Stress Responsive Chaperone, Promotes Th1-Biased T Cell Immune Response via TLR4-Mediated Activation of Dendritic Cells. *Front Cell Infect Microbiol*. 2018;8(March):1-15. doi:10.3389/fcimb.2018.00095.

43. Jang AR, Choi JH, Shin SJ, Park JH. *Mycobacterium tuberculosis* ESAT6 induces IFN-β gene expression in Macrophages via TLRs-mediated signaling. *Cytokine*. 2018;104(September 2017):104-109. doi:10.1016/j.cyto.2017.10.006.

44. Moreira-Teixeira L, Sousa J, McNab FW, et al. Type I IFN Inhibits Alternative Macrophage Activation during *Mycobacterium tuberculosis* Infection and Leads to Enhanced Protection in the Absence of IFN-γ Signaling. *J Immunol*. 2016;197(12):4714-4726. doi:10.4049/jimmunol.1600584.

45. Reiling N, Hölscher C, Fehrenbach A, et al. Cutting edge: Toll-like receptor TLR2- and TLR4-mediated pathogen recognition in resistance to airborne infection with *Mycobacterium tuberculosis*. *J Immunol*. 2002;169(7):3480-3484. doi:10.4049/jimmunol.169.7.3480.

46. Abel B, Thieblemont N, Quesniaux VJF, et al. Toll-like receptor 4 expression is required to control chronic *Mycobacterium tuberculosis* infection in mice. *J Immunol*. 2002;169(6):3155-3162. doi:10.4049/jimmunol.169.6.3155.

47. Shim TS, Turner OC, Orme IM. Toll-like receptor 4 plays no role in susceptibility of mice to *Mycobacterium tuberculosis* infection. *Tuberculosis*. 2003;83(6):367-371. doi:10.1016/S1472-9792(03)00071-4.

48. Bénard A, Sakwa I, Schierloh P, et al. B Cells Producing Type I IFN Modulate Macrophage Polarization in Tuberculosis. *Am J Respir Crit Care Med*. 2017;197(6):801-813. doi:10.1164/rccm.201707-1475OC.

49. Heitmann L, Schoenen H, Ehlers S, Lang R, Hölscher C. Mincle is not essential for controlling *Mycobacterium tuberculosis* infection. *Immunobiology*. 2013;218(4):506-516. doi:10.1016/j.imbio.2012.06.005.

50. Behler F, Steinwede K, Balboa L, et al. Role of Mincle in Alveolar Macrophage-Dependent Innate Immunity against Mycobacterial Infections in Mice. *J Immunol*. 2012;189(6):3121-3129. doi:10.4049/jimmunol.1201399.

51. Manzanillo PS, Shiloh MU, Portnoy DA, Cox JS. *Mycobacterium tuberculosis* activates the DNA-dependent cytosolic surveillance pathway within macrophages. *Cell Host Microbe*. 2012;11(5):469-480. doi:10.1016/j.chom.2012.03.007.

52. Watson RO, Bell SL, MacDuff DA, et al. The Cytosolic Sensor cGAS Detects *Mycobacterium tuberculosis* DNA to Induce Type I Interferons and Activate Autophagy. *Cell Host Microbe*. 2015;17(6):811-819. doi:10.1016/j.chom.2015.05.004.

53. Watson RO, Manzanillo PS, Cox JS. Extracellular *M. tuberculosis* DNA targets bacteria for autophagy by activating the host DNA-sensing pathway. *Cell*. 2012;150(4):803-815. doi:10.1016/j.cell.2012.06.040.

54. Collins AC, Cai H, Li T, et al. Cyclic GMP-AMP Synthase Is an Innate Immune DNA Sensor for *Mycobacterium tuberculosis*. *Cell Host Microbe*. 2015;17(6):820-828. doi:10.1016/j.chom.2015.05.005.

55. Wassermann R, Gulen MF, Sala C, et al. *Mycobacterium tuberculosis* Differentially Activates cGAS- and Inflammasome-Dependent Intracellular Immune Responses through ESX-1. *Cell Host Microbe*. 2015;17(6):799-810. doi:10.1016/j.chom.2015.05.003.

56. Sun L, Wu J, Du F, Chen X, Chen ZJ. Cyclic GMP-AMP synthase is a cytosolic DNA sensor that activates the type I interferon pathway. *Science*. 2013;339(6121):786-791. doi:10.1126/science.1232458.

57. Wu J, Sun L, Chen X, et al. Cyclic GMP-AMP is an endogenous second messenger in innate immune signaling by cytosolic DNA. *Science*. 2013;339(6121):826-830. doi:10.1126/science.1229963.

58. Chen Q, Sun L, Chen ZJ. Regulation and function of the cGAS-STING pathway of cytosolic DNA sensing. *Nat Immunol*. 2016;17(10):1142-1149. doi:10.1038/ni.3558.

59. Dey B, Dey RJ, Cheung LS, et al. A bacterial cyclic dinucleotide activates the cytosolic surveillance pathway and mediates innate resistance to tuberculosis. *Nat Med*. 2015;21(4):401-408. doi:10.1038/nm.3813.

60. Van Dis E, Sogi KM, Rae CS, et al. STING-Activating Adjuvants Elicit a Th17 Immune Response and Protect against *Mycobacterium tuberculosis* Infection. *Cell Rep*. 2018;23(5):1435-1447. doi:10.1016/j.celrep.2018.04.003.

61. Sauer J-D, Sotelo-Troha K, von Moltke J, et al. The N-ethyl-N-nitrosourea-induced Goldenticket mouse mutant reveals an essential function of Sting in the *in vivo* interferon response to *Listeria monocytogenes* and cyclic dinucleotides. *Infect Immun*. 2011;79(2):688-694. doi:10.1128/IAI.00999-10.

62. Cheng Y, Schorey JS. *Mycobacterium tuberculosis*–induced IFN-β production requires cytosolic DNA and RNA sensing pathways . *J Exp Med*. 2018;215(11):2919-2935. doi:10.1084/jem.20180508.

63. McNab FW, Ewbank J, Rajsbaum R, et al. TPL-2-ERK1/2 signaling promotes host resistance against intracellular bacterial infection by negative regulation of type I IFN production. *J Immunol*. 2013;191(4):1732-1743. doi:10.4049/jimmunol.1300146.

64. Mayer-Barber KD, Andrade BB, Barber DL, et al. Innate and Adaptive Interferons Suppress IL-1α and IL-1β Production by Distinct Pulmonary Myeloid Subsets during *Mycobacterium tuberculosis* Infection. *Immunity*. 2011;35(6):1023-1034. doi:10.1016/j.immuni.2011.12.002.

65. Mayer-Barber KD, Andrade BB, Oland SD, et al. Host-directed therapy of tuberculosis based on interleukin-1 and type I interferon crosstalk. *Nature*. 2014;511(7507):99-103. doi:10.1038/nature13489.

66. Redford PS, Mayer-Barber KD, McNab FW, et al. Influenza A virus impairs control of mycobacterium tuberculosis coinfection through a type i interferon receptor-dependent pathway. *J Infect Dis*. 2014;209(2):270-274. doi:10.1093/infdis/jit424.

67. Kimmey JM, Campbell JA, Weiss LA, Monte KJ, Lenschow DJ, Stallings CL. The impact of ISGylation during *Mycobacterium tuberculosis* infection in mice. *Microbes Infect*. 2017;19(4-5):249-258. doi:10.1016/j.micinf.2016.12.006.

68. Dorhoi A, Yeremeev V, Nouailles G, et al. Type I IFN signaling triggers immunopathology in tuberculosis-susceptible mice by modulating lung phagocyte dynamics. *Eur J Immunol*. 2014;44(8):2380-2393. doi:10.1002/eji.201344219.

69. Yamada H, Mizumo S, Horai R, Iwakura Y, Sugawara I. Protective role of interleukin-1 in mycobacterial infection in IL-1 alpha/beta double-knockout mice. *Lab Invest*. 2000;80(5):759-767. http://www.ncbi.nlm.nih.gov/pubmed/10830786.

70. Juffermans NP, Florquin S, Camoglio L, et al. Interleukin-1 Signaling Is Essential

for Host Defense during Murine Pulmonary Tuberculosis. *J Infect Dis*. 2002;182(3):902-908. doi:10.1086/315771.

71. Fremond CM, Togbe D, Doz E, et al. IL-1 receptor-mediated signal is an essential component of MyD88-dependent innate response to *Mycobacterium tuberculosis* infection. *J Immunol*. 2007;179(2):1178-1189. doi:10.4049/jimmunol.179.2.1178.

72. Mayer-Barber KD, Barber DL, Shenderov K, et al. Caspase-1 independent IL-1beta production is critical for host resistance to *Mycobacterium tuberculosis* and does not require TLR signaling in vivo. *J Immunol*. 2010;184(7):3326-3330. doi:10.4049/jimmunol.0904189.

73. Dinarello CA. Overview of the IL-1 family in innate inflammation and acquired immunity. *Immunol Rev*. 2018;281(1):8-27. doi:10.1111/imr.12621.

74. Di Paolo NC, Shafiani S, Day T, et al. Interdependence between Interleukin-1 and Tumor Necrosis Factor Regulates TNF-Dependent Control of *Mycobacterium tuberculosis* Infection. *Immunity*. 2015;43(6):1125-1136. doi:10.1016/j.immuni.2015.11.016.

75. Bohrer AC, Tocheny C, Assmann M, Ganusov V V., Mayer-Barber KD. Cutting Edge: IL-1R1 Mediates Host Resistance to *Mycobacterium tuberculosis* by Trans-Protection of Infected Cells. *J Immunol*. 2018;201(6):1645-1650. doi:10.4049/jimmunol.1800438.

76. Cohen SB, Gern BH, Delahaye JL, et al. Alveolar Macrophages Provide an Early *Mycobacterium tuberculosis* Niche and Initiate Dissemination. *Cell Host Microbe*. 2018;24(3):439-446.e4. doi:10.1016/j.chom.2018.08.001.

77. Deyerle KL, Sims JE, Dower SK, Bothwell MA. Pattern of IL-1 receptor gene expression suggests role in noninflammatory processes. *J Immunol*. 1992;149(5):1657-1665. http://www.ncbi.nlm.nih.gov/pubmed/1387148.

78. Redford PS, Murray PJ, O'Garra A. The role of IL-10 in immune regulation during *M. tuberculosis* infection. *Mucosal Immunol*. 2011;4(3):261-270. doi:10.1038/mi.2011.7.

79. Moreira-Teixeira L, Redford PS, Stavropoulos E, et al. T Cell-Derived IL-10 Impairs Host Resistance to *Mycobacterium tuberculosis* Infection. *J Immunol*. 2017;199(2):613-623. doi:10.4049/jimmunol.1601340.

80. Demangel C, Bertolino P, Britton WJ. Autocrine IL-10 impairs dendritic cell (DC)-derived immune responses to mycobacterial infection by suppressing DC trafficking to draining lymph nodes and local IL-12 production. *Eur J Immunol*. 2002;32(4):994-1002. doi:10.1002/1521-4141(200204)32:4<994::AID-IMMU994>3.0.CO;2-6.

81. Redford PS, Boonstra A, Read S, et al. Enhanced protection to *Mycobacterium tuberculosis* infection in IL-10-deficient mice is accompanied by early and

enhanced Th1 responses in the lung. *Eur J Immunol*. 2010;40(8):2200-2210. doi:10.1002/eji.201040433.

82. Beamer GL, Flaherty DK, Assogba BD, et al. Interleukin-10 promotes *Mycobacterium tuberculosis* disease progression in CBA/J mice. *J Immunol*. 2008;181(8):5545-5550. doi:10.4049/jimmunol.181.8.5545.

83. Turner J, Gonzalez-Juarrero M, Ellis DL, et al. In vivo IL-10 production reactivates chronic pulmonary tuberculosis in C57BL/6 mice. *J Immunol*. 2002;169(11):6343-6351. doi:10.4049/jimmunol.169.11.6343.

84. Ordway D, Henao-Tamayo M, Harton M, et al. The hypervirulent *Mycobacterium tuberculosis* strain HN878 induces a potent TH1 response followed by rapid down-regulation. *J Immunol*. 2007;179(1):522-531. doi:10.4049/jimmunol.179.1.522.

85. Eshleman EM, Delgado C, Kearney SJ, Friedman RS, Lenz LL. Down regulation of macrophage IFNGR1 exacerbates systemic *L. monocytogenes* infection. *PLoS Pathog*. 2017;13(5):1-22. doi:10.1371/journal.ppat.1006388.

86. Rayamajhi M, Humann J, Penheiter K, Andreasen K, Lenz LL. Induction of IFN-alphabeta enables *Listeria monocytogenes* to suppress macrophage activation by IFN-gamma. *J Exp Med*. 2010;207(2):327-337. doi:10.1084/jem.20091746.

87. de Paus RA, van Wengen A, Schmidt I, et al. Inhibition of the type I immune responses of human monocytes by IFN-α and IFN-β. *Cytokine*. 2013;61(2):645-655. doi:10.1016/j.cyto.2012.12.005.

88. Desvignes L, Wolf AJ, Ernst JD. Dynamic Roles of Type I and Type II IFNs in Early Infection with *Mycobacterium tuberculosis*. *J Immunol*. 2012;188(12):6205-6215. doi:10.4049/jimmunol.1200255.

89. Gautier G, Humbert M, Deauvieau F, et al. A type I interferon autocrine–paracrine loop is involved in Toll-like receptor-induced interleukin-12p70 secretion by dendritic cells. *J Exp Med*. 2005;201(9):1435-1446. doi:10.1084/jem.20041964.

90. Ruangkiattikul N, Nerlich A, Abdissa K, et al. cGAS-STING-TBK1-IRF3/7 induced interferon-β contributes to the clearing of non tuberculous mycobacterial infection in mice. *Virulence*. 2017;8(7):1303-1315. doi:10.1080/21505594.2017.1321191.

91. Kuchtey J, Fulton SA, Reba SM, Harding C V., Boom WH. Interferon-αβ mediates partial control of early pulmonary *Mycobacterium bovis* bacillus Calmette-Guérin infection. *Immunology*. 2006;118(1):39-49. doi:10.1111/j.1365-2567.2006.02337.x.

92. Pichugin A V., Yan BS, Sloutsky A, Kobzik L, Kramnik I. Dominant role of the sst1 locus in pathogenesis of necrotizing lung granulomas during chronic tuberculosis infection and reactivation in genetically resistant hosts. *Am J Pathol*. 2009;174(6):2190-2201. doi:10.2353/ajpath.2009.081075.

93. Mathis D, Benoist C. Aire. *Annu Rev Immunol*. 2009;27(1):287-312. doi:10.1146/annurev.immunol.25.022106.141532.

94. Scherer M, Stamminger T. Emerging Role of PML Nuclear Bodies in Innate Immune Signaling. *J Virol*. 2016;90(13):5850-5854. doi:10.1128/jvi.01979-15.

95. Bloch DB, Chiche JD, Orth D, de la Monte SM, Rosenzweig A, Bloch KD. Structural and functional heterogeneity of nuclear bodies. *Mol Cell Biol*. 1999;19(6):4423-4430. doi:10.1128/mcb.19.6.4423.

96. Zak DE, Penn-Nicholson A, Scriba TJ, et al. A blood RNA signature for tuberculosis disease risk: a prospective cohort study. *Lancet*. 2016;387(10035):2312-2322. doi:10.1016/S0140-6736(15)01316-1.

97. Scriba TJ, Penn-Nicholson A, Shankar S, et al. Sequential inflammatory processes define human progression from *M. tuberculosis* infection to tuberculosis disease. *PLoS Pathog*. 2017;13(11):1-24. doi:10.1371/journal.ppat.1006687.

98. Berry MPR, Graham CM, McNab FW, et al. An interferon-inducible neutrophil-driven blood transcriptional signature in human tuberculosis. *Nature*. 2010;466(7309):973-977. doi:10.1038/nature09247.

99. Singhania A, Verma R, Graham CM, et al. A modular transcriptional signature identifies phenotypic heterogeneity of human tuberculosis infection. *Nat Commun*. 2018;9(1):2308. doi:10.1038/s41467-018-04579-w.

100. Nunes-Alves C, Jayaraman P, Booty MG, Carpenter SM, Behar SM, Rothchild AC. In search of a new paradigm for protective immunity to TB. *Nat Rev Microbiol*. 2014;12(4):289-299. doi:10.1038/nrmicro3230.

101. Hawn TR, Shah JA, Kalman D. New tricks for old dogs: Countering antibiotic resistance in tuberculosis with host-directed therapeutics. *Immunol Rev*. 2015;264(1):344-362. doi:10.1111/imr.12255.

102. Teles RMB, Graeber TG, Krutzik SR, et al. Type I interferon suppresses type II interferon-triggered human anti-mycobacterial responses. *Science*. 2013;339(6126):1448-1453. doi:10.1126/science.1233665.

103. Bhattacharya B, Chatterjee S, Berland R, et al. Increased susceptibility to intracellular bacteria and necrotic inflammation driven by a dysregulated macrophage response to TNF. *bioRxiv*. 2018. http://biorxiv.org/content/early/2018/03/15/238873.abstract.

104. Ingalls RR, Christensen TG, He X, et al. The sst1 Resistance Locus Regulates Evasion of Type I Interferon Signaling by *Chlamydia pneumoniae* as a Disease Tolerance Mechanism. *PLoS Pathog*. 2013;9(8):e1003569. doi:10.1371/journal.ppat.1003569.

105. Dunn GP, Bruce AT, Sheehan KCF, et al. A critical function for type I interferons in cancer immunoediting. *Nat Immunol*. 2005;6(7):722-729. doi:10.1038/ni1213.

106. Wiens KE, Ernst JD. The Mechanism for Type I Interferon Induction by *Mycobacterium tuberculosis* is Bacterial Strain-Dependent. *PLoS Pathog*. 2016;12(8):1-20. doi:10.1371/journal.ppat.1005809.

107. Reboldi A, Dang E V, McDonald JG, Liang G, Russell DW, Cyster JG. 25-Hydroxycholesterol suppresses interleukin-1-driven inflammation downstream of type I interferon. *Science*. 2014;345(6197):679-684. doi:10.1126/science.1254790.

108. Mayer-Barber KD, Yan B. Clash of the Cytokine Titans: Counter-regulation of interleukin-1 and type I interferon-mediated inflammatory responses. *Cell Mol Immunol*. 2017;14(1):22-35. doi:10.1038/cmi.2016.25.

109. Mishra BB, Rathinam VAK, Martens GW, et al. Nitric oxide controls the immunopathology of tuberculosis by inhibiting NLRP3 inflammasome-dependent processing of IL-1β. *Nat Immunol*. 2013;14(1):52-60. doi:10.1038/ni.2474.

110. Mishra BB, Lovewell RR, Olive AJ, et al. Nitric oxide prevents a pathogen-permissive granulocytic inflammation during tuberculosis. *Nat Microbiol*. 2017;2(May):17072. doi:10.1038/nmicrobiol.2017.72.

111. Nichols RD, Von Moltke J, Vance RE. NAIP/NLRC4 inflammasome activation in MRP8+ cells is sufficient to cause systemic inflammatory disease. *Nat Commun*. 2017;8(1). doi:10.1038/s41467-017-02266-w.

112. Sugawara I, Yamada H, Hua S, Mizuno S. Role of interleukin (IL)-1 type 1 receptor in mycobacterial infection. *Microbiol Immunol*. 2001;45(11):743-750. doi:10.1111/j.1348-0421.2001.tb01310.x.

113. Eisenberg SP, Evans RJ, Arend WP, et al. Primary structure and functional expression from complementary DNA of a human interleukin-1 receptor antagonist. *Nature*. 1990;343(6256):341-346. doi:10.1038/343341a0.

114. Molnarfi N, Hyka-Nouspikel N, Gruaz L, Dayer J-M, Burger D. The production of IL-1 receptor antagonist in IFN-beta-stimulated human monocytes depends on the activation of phosphatidylinositol 3-kinase but not of STAT1. *J Immunol*. 2005;174(5):2974-2980. doi:10.4049/jimmunol.174.5.2974.

115. Corr M, Boyle DL, Ronacher LM, et al. Interleukin 1 receptor antagonist mediates the beneficial effects of systemic interferon beta in mice: Implications for rheumatoid arthritis. *Ann Rheum Dis*. 2011;70(5):858-863. doi:10.1136/ard.2010.141077.

116. Janson RW, Hance KR, Arend WP. Production of IL-1 receptor antagonist by human in vitro-derived macrophages. Effects of lipopolysaccharide and granulocyte-macrophage colony-stimulating factor. *J Immunol*. 1991;147(12):4218-4223. http://www.ncbi.nlm.nih.gov/pubmed/1836481.

117. Settas LD, Tsimirikas G, Vosvotekas G, Triantafyllidou E, Nicolaides P. Reactivation of pulmonary tuberculosis in a patient with rheumatoid arthritis

during treatment with IL-1 receptor antagonists (anakinra). *J Clin Rheumatol*. 2007;13(4):219-220. doi:10.1097/RHU.0b013e31812e00a1.

118. He D, Bai F, Zhang S, et al. High incidence of tuberculosis infection in rheumatic diseases and impact for chemoprophylactic prevention of tuberculosis activation during biologics therapy. *Clin Vaccine Immunol*. 2013;20(6):842-847. doi:10.1128/CVI.00049-13.

119. Brassard P, Kezouh A, Suissa S. Antirheumatic drugs and the risk of tuberculosis. *Clin Infect Dis*. 2006;43(6):717-722. doi:10.1086/506935.

120. Hirsch E, Irikura VM, Paul SM, Hirsh D. Functions of interleukin 1 receptor antagonist in gene knockout and overproducing mice. *Proc Natl Acad Sci*. 2002;93(20):11008-11013. doi:10.1073/pnas.93.20.11008.

121. Nicklin MJH, Hughes DE, Barton JL, Ure JM, Duff GW. Arterial inflammation in mice lacking the interleukin 1 receptor antagonist gene. *J Exp Med*. 2000;191(2):303-312. doi:10.1084/jem.191.2.303.

122. Sivick KE, Desbien AL, Glickman LH, et al. Magnitude of Therapeutic STING Activation Determines CD8+ T Cell-Mediated Anti-tumor Immunity. *Cell Rep*. 2018;25(11):3074-3085.e5. doi:10.1016/j.celrep.2018.11.047.

123. Fujioka N, Mukaida N, Harada A, et al. Preparation of specific antibodies against murine IL-1ra and the establishment of IL-1ra as an endogenous regulator of bacteria-induced fulminant hepatitis in mice. *J Leukoc Biol*. 1995;58(1):90-98. doi:10.1002/jlb.58.1.90.

124. Mitnick CD, Franke MF, Rich ML, et al. Aggressive regimens for multidrug-resistant tuberculosis decrease all-cause mortality. *PLoS One*. 2013;8(3):e58664. doi:10.1371/journal.pone.0058664.

125. Chung-Delgado K, Guillen-Bravo S, Revilla-Montag A, Bernabe-Ortiz A. Mortality among MDR-TB cases: comparison with drug-susceptible tuberculosis and associated factors. *PLoS One*. 2015;10(3):e0119332. doi:10.1371/journal.pone.0119332.

126. Roscioli T, Cliffe ST, Bloch DB, et al. Mutations in the gene encoding the PML nuclear body protein Sp110 are associated with immunodeficiency and hepatic veno-occlusive disease. *Nat Genet*. 2006;38(6):620-622. doi:10.1038/ng1780.

127. Cliffe ST, Wong M, Taylor PJ, et al. The first prenatal diagnosis for veno-occlusive disease and immunodeficiency syndrome, an autosomal recessive condition associated with mutations in SP110. *Prenat Diagn*. 2007;27(7):674-676. doi:10.1002/pd.1759.

128. Wang T, Ong P, Roscioli T, Cliffe ST, Church JA. Hepatic veno-occlusive disease with immunodeficiency (VODI): First reported case in the U.S. and identification of a unique mutation in Sp110. *Clin Immunol*. 2012;145(2):102-107.

doi:10.1016/j.clim.2012.07.016.

129. Buckley MF, Abinun M, Trizzino A, et al. Clinical, molecular, and cellular immunologic findings in patients with SP110-associated veno-occlusive disease with immunodeficiency syndrome. *J Allergy Clin Immunol*. 2012;130(3):735-742.e6. doi:10.1016/j.jaci.2012.02.054.

130. Tosh K, Campbell SJ, Fielding K, et al. Variants in the SP110 gene are associated with genetic susceptibility to tuberculosis in West Africa. *Proc Natl Acad Sci U S A*. 2006;103(27):10364-10368. doi:10.1073/pnas.0603340103.

131. Lei X, Zhu H, Zha L, Wang Y. SP110 gene polymorphisms and tuberculosis susceptibility: A systematic review and meta-analysis based on 10624 subjects. *Infect Genet Evol*. 2012;12(7):1473-1480. doi:10.1016/j.meegid.2012.05.011.

132. Fox GJ, Sy DN, Nhung NV, et al. Polymorphisms of SP110 are associated with both pulmonary and extra-pulmonary tuberculosis among the Vietnamese. *PLoS One*. 2014;9(7):e99496. doi:10.1371/journal.pone.0099496.

133. Png E, Alisjahbana B, Sahiratmadja E, et al. Polymorphisms in SP110 are not associated with pulmonary tuberculosis in Indonesians. *Infect Genet Evol*. 2012;12(6):1319-1323. doi:10.1016/j.meegid.2012.04.006.

134. Chang S-Y, Chen M-L, Lee M-R, et al. SP110 Polymorphisms Are Genetic Markers for Vulnerability to Latent and Active Tuberculosis Infection in Taiwan. *Dis Markers*. 2018;2018:4687380. doi:10.1155/2018/4687380.

135. Zhang S, Wang X Bin, Han Y Di, Wang C, Zhou Y, Zheng F. Certain Polymorphisms in SP110 Gene Confer Susceptibility to Tuberculosis: A Comprehensive Review and Updated Meta-Analysis. *Yonsei Med J*. 2017;58(1):165-173. doi:10.3349/ymj.2017.58.1.165.

136. Thye T. No associations of human pulmonary tuberculosis with Sp110 variants. *J Med Genet*. 2005;43(7):e32-e32. doi:10.1136/jmg.2005.037960.

137. Bloch DB, Nakajima A, Gulick T, et al. Sp110 localizes to the PML-Sp100 nuclear body and may function as a nuclear hormone receptor transcriptional coactivator. *Mol Cell Biol*. 2000;20(16):6138-6146. doi:10.1128/mcb.20.16.6138-6146.2000.

138. Bottomley MJ, Collard MW, Huggenvik JI, Liu Z, Gibson TJ, Sattler M. The SAND domain structure defines a novel DNA-binding fold in transcriptional regulation. *Nat Struct Biol*. 2001;8(7):626-633. doi:10.1038/89675.

139. Watashi K, Hijikata M, Tagawa A, Doi T, Marusawa H, Shimotohno K. Modulation of retinoid signaling by a cytoplasmic viral protein via sequestration of Sp110b, a potent transcriptional corepressor of retinoic acid receptor, from the nucleus. *Mol Cell Biol*. 2003;23(21):7498-7509. doi:10.1128/mcb.23.21.7498-7509.2003.

140. Yao K, Wu Y, Chen Q, Zhang Z, Chen X, Zhang Y. The arginine/lysine-richelement within the DNA-binding domain is essential for nuclear localization and function of the intracellular pathogen resistance 1. *PLoS One*. 2016;11(9):1-17. doi:10.1371/journal.pone.0162832.

141. Szostecki C, Guldner HH, Netter HJ, Will H. Isolation and characterization of cDNA encoding a human nuclear antigen predominantly recognized by autoantibodies from patients with primary biliary cirrhosis. *J Immunol*. 1990;145(12):4338-4347. http://www.ncbi.nlm.nih.gov/pubmed/2258622.

142. Nicewonger J, Suck G, Bloch D, Swaminathan S. Epstein-Barr Virus (EBV) SM Protein Induces and Recruits Cellular Sp110b To Stabilize mRNAs and Enhance EBV Lytic Gene Expression. *J Virol*. 2004;78(17):9412-9422. doi:10.1128/jvi.78.17.9412-9422.2004.

143. Sengupta I, Das D, Singh SP, Chakravarty R, Das C. Host transcription factor speckled 110 kDa (Sp110), a nuclear body protein, is hijacked by Hepatitis B virus protein X for viral persistence. *J Biol Chem*. 2017;292(50):20379-20393. doi:10.1074/jbc.M117.796839.

144. Leu JS, Chen ML, Chang SY, et al. SP110b controls host immunity and susceptibility to tuberculosis. *Am J Respir Crit Care Med*. 2017;195(3):369-382. doi:10.1164/rccm.201601-0103OC.

145. Leu JS, Chang SY, Mu CY, Chen ML, Yan BS. Functional domains of SP110 that modulate its transcriptional regulatory function and cellular translocation. *J Biomed Sci*. 2018;25(1):1-15. doi:10.1186/s12929-018-0434-4.

146. Wu Y, Guo Z, Yao K, et al. The Transcriptional Foundations of Sp110-mediated Macrophage (RAW264.7) Resistance to *Mycobacterium tuberculosis* H37Ra. *Sci Rep*. 2016;6(1):22041. doi:10.1038/srep22041.

147. Wu Y, Guo Z, Liu F, et al. Sp110 enhances macrophage resistance to *Mycobacterium tuberculosis* via inducing endoplasmic reticulum stress and inhibiting anti-apoptotic factors. *Oncotarget*. 2017;8(38):64050-64065. doi:10.18632/oncotarget.19300.

148. Weichenhan D, Kunze B, Winking H, et al. Source and component genes of a 6-200 Mb gene cluster in the house mouse. *Mamm Genome*. 2001;12(8):590-594. doi:10.1007/s00335-001-3015-9.

149. Bloch DB, de la Monte SM, Guigaouri P, Filippov A, Bloch KD. Identification and characterization of a leukocyte-specific component of the nuclear body. *J Biol Chem*. 1996;271(46):29198-29204. doi:10.1074/jbc.271.46.29198.

150. Madani N, Millette R, Platt EJ, et al. Implication of the Lymphocyte-Specific Nuclear Body Protein Sp140 in an Innate Response to Human Immunodeficiency Virus Type 1. *J Virol*. 2002;76(21):11133-11138. doi:10.1128/JVI.76.21.11133-11138.2002.

151. Jostins L, Ripke S, Weersma RK, et al. Host-microbe interactions have shaped the genetic architecture of inflammatory bowel disease. *Nature*. 2012;491(7422):119-124. doi:10.1038/nature11582.

152. Franke A, McGovern DPB, Barrett JC, et al. Genome-wide meta-analysis increases to 71 the number of confirmed Crohn's disease susceptibility loci. *Nat Genet*. 2010;42(12):1118-1125. http://dx.doi.org/10.1038/ng.717.

153. Slager SL, Caporaso NE, De Sanjose S, Goldin LR. Genetic susceptibility to chronic lymphocytic leukemia. *Semin Hematol*. 2013;50(4):296-302. doi:10.1053/j.seminhematol.2013.09.007.

154. Matesanz F, Potenciano V, Fedetz M, et al. A functional variant that affects exon-skipping and protein expression of SP140 as genetic mechanism predisposing to multiple sclerosis. *Hum Mol Genet*. 2015;24(19):5619-5627. doi:10.1093/hmg/ddv256.

155. Karaky M, Fedetz M, Potenciano V, et al. SP140 regulates the expression of immune-related genes associated with multiple sclerosis and other autoimmune diseases by NF-κB inhibition. *Hum Mol Genet*. 2018;27(23):4012-4023. doi:10.1093/hmg/ddy284.

156. Boyartchuk V, Rojas M, Yan B, et al. The Host Resistance Locus sst1 Controls Innate Immunity to *Listeria monocytogenes* Infection in Immunodeficient Mice. *J Immunol*. 2004;173(8):5112-5120. doi:10.4049/jimmunol.173.8.5112.

157. Zucchelli C, Tamburri S, Filosa G, et al. Sp140 is a multi-SUMO-1 target and its PHD finger promotes SUMOylation of the adjacent Bromodomain. *Biochim Biophys Acta - Gen Subj*. 2019;1863(2):456-465. doi:10.1016/j.bbagen.2018.11.011.

158. Zhang X, Zhao D, Xiong X, He Z, Li H. Multifaceted histone H3 methylation and phosphorylation readout by the plant homeodomain finger of human nuclear antigen Sp100C. *J Biol Chem*. 2016;291(24):12786-12798. doi:10.1074/jbc.M116.721159.

159. Lallemand-Breitenbach V, de Thé H. PML nuclear bodies: from architecture to function. *Curr Opin Cell Biol*. 2018;52:154-161. doi:10.1016/j.ceb.2018.03.011.

160. Tun-Kyi A, Finn G, Greenwood A, et al. Essential role for the prolyl isomerase Pin1 in Toll-like receptor signaling and type I interferon–mediated immunity. *Nat Immunol*. 2011;12(8):733-741. doi:10.1038/ni.2069.

161. Saitoh T, Tun-Kyi A, Ryo A, et al. Negative regulation of interferon-regulatory factor 3-dependent innate antiviral response by the prolyl isomerase Pin1. *Nat Immunol*. 2006;7(6):598-605. doi:10.1038/ni1347.

162. Mehta S, Cronkite DA, Basavappa M, et al. Maintenance of macrophage transcriptional programs and intestinal homeostasis by epigenetic reader SP140.

Sci Immunol. 2017;2(9):eaag3160. doi:10.1126/sciimmunol.aag3160.

163. Yordy JS, Li R, Sementchenko VI, Pei H, Muise-Helmericks RC, Watson DK. SP100 expression modulates ETS1 transcriptional activity and inhibits cell invasion. *Oncogene*. 2004;23(39):6654-6665. doi:10.1038/sj.onc.1207891.

164. Seeler JS, Marchio A, Sitterlin D, Transy C, Dejean A. Interaction of SP100 with HP1 proteins: a link between the promyelocytic leukemia-associated nuclear bodies and the chromatin compartment. *Proc Natl Acad Sci U S A*. 1998;95(13):7316-7321. doi:10.1073/pnas.95.13.7316.

165. Meng Z, Lu M. RNA interference-induced innate immunity, off-target effect, or immune adjuvant? *Front Immunol*. 2017;8(MAR):1-7. doi:10.3389/fimmu.2017.00331.

166. Judge A, MacLachlan I. Overcoming the Innate Immune Response to Small Interfering RNA. *Hum Gene Ther*. 2008;19(2):111-124. doi:10.1089/hum.2007.179.

167. Gideon HP, Skinner JA, Baldwin N, Flynn JL, Lin PL. Early Whole Blood Transcriptional Signatures Are Associated with Severity of Lung Inflammation in Cynomolgus Macaques with Mycobacterium tuberculosis Infection. *J Immunol*. 2016;197(12):4817-4828. doi:10.4049/jimmunol.1601138.

168. Gern B, Plumlee C, Gerner M, Urdahl K. Investigating Immune Correlates of Protection to Tuberculosis Using an Ultra-Low Dose Infection in a Mouse Model. In: *Open Forum Infectious Disease*.Vol 4.; 2017:S47-S48.

169. Sakai S, Kauffman KD, Sallin MA, et al. CD4 T Cell-Derived IFN-γ Plays a Minimal Role in Control of Pulmonary *Mycobacterium tuberculosis* Infection and Must Be Actively Repressed by PD-1 to Prevent Lethal Disease. *PLoS Pathog*. 2016;12(5):1-22. doi:10.1371/journal.ppat.1005667.

170. Huang L, Nazarova E V., Tan S, Liu Y, Russell DG. Growth of *Mycobacterium tuberculosis in vivo* segregates with host macrophage metabolism and ontogeny. *J Exp Med*. 2018;215(4):1135-1152. doi:10.1084/jem.20172020.

171. Tavalai N, Stamminger T. Interplay between herpesvirus infection and host defense by PML nuclear bodies. *Viruses*. 2009;1(3):1240-1264. doi:10.3390/v1031240.

172. Gu H, Roizman B. The degradation of promyelocytic leukemia and Sp100 proteins by herpes simplex virus 1 is mediated by the ubiquitin-conjugating enzyme UbcH5a. *Proc Natl Acad Sci*. 2003;100(15):8963-8968. doi:10.1073/pnas.1533420100.

173. Behr MA, Edelstein PH, Ramakrishnan L. Revisiting the timetable of tuberculosis. *BMJ*. 2018;362(August):1DUMMY. doi:10.1136/bmj.k2738.

174. Rauch I. Eicosanoid Isolation from Mouse Intestinal Tissue for ELISA. *Bio-*

protocol. 2018;8(21). doi:10.21769/BioProtoc.3066.

175. Wang H, Yang H, Shivalila CS, et al. One-step generation of mice carrying mutations in multiple genes by CRISPR/cas-mediated genome engineering. *Cell*. 2013;153(4):910-918. doi:10.1016/j.cell.2013.04.025.

176. Mascarenhas DPA, Pereira MSF, Manin GZ, Hori JI, Zamboni DS. Interleukin 1 receptor-driven neutrophil recruitment accounts to MyD88-dependent pulmonary clearance of legionella pneumophila infection in vivo. *J Infect Dis*. 2015;211(2):322-330. doi:10.1093/infdis/jiu430.

177. Dallow A. Mythbusters: Duct Tape Hour. 2009.